Structure and function of tomato disease resistance proteins

van Ooijen, G.

Publication date
2008
Document Version
Final published version

Structure and function of tomato disease resistance proteins

ACADEMISCH PROEFSCHRIFT

ter verkrijging van de graad van doctor
aan de Universiteit van Amsterdam
op gezag van de Rector Magnificus prof. dr. D.C. van den Boom
ten overstaan van een door het college voor promoties ingestelde
commissie, in het openbaar te verdedigen in de Aula der Universiteit

op woensdag 3 september 2008, te 14.00 uur

door
Gerben van Ooijen
geboren te Gorinchem

Promotiecommissie

Promotor	prof. dr. B.J.C. Cornelissen
Co-promotor	dr. ing. F.L.W. Takken
Commissieleden	prof. dr. ir. J. Bakker
	prof. dr. M.A. Haring
	prof. dr. A.J. van Tunen
	dr. M. Albrecht
	dr. ir. M.H.A.J. Joosten

Faculteit der Natuurwetenschappen, Wiskunde en Informatica

The research described in this thesis was carried out in the Swammerdam Institute for Life Sciences, Plant Pathology department, University of Amsterdam, Kruislaan 318, 1098 SM, Amsterdam, The Netherlands.

This research was financed by the Research Council for Earth and Life Sciences (ALW – Grant 813.06.005) with financial aid from the Netherlands Organization for Scientific Research (NWO). This project was supported by the Centre for BioSystems Genomics (CBSG) which is part of the Netherlands Genomics Initiative.

and I had some regrets,
but if I had to do it all again
well, that's something I'd like to do

Mark Oliver Everett

CONTENTS

Chapter 1

Introduction and outline

Like all higher organisms, plants are continually attacked by a large variety of potentially pathogenic organisms. Due to their immobile, and at first sight irresponsive nature, plants appear to be sitting ducks for malevolent pathogens. Nevertheless, plants are surprisingly effective in protecting themselves from invaders, and disease is a relatively rare occurrence. To reply to the broad range of pathogens lurking in the ecosystem, plants evolved a sophisticated defence system.

Introduction

Plants evolved a large number of proteins that trigger inducible defence responses upon pathogen perception (Jones and Dangl, 2006). These proteins include the Pathogen Recognition Receptors (PRRs), that sense Pathogen-Associated Molecular Patterns (PAMPs) that are often highly conserved molecules, shared between classes of pathogenic micro-organisms (Zipfel and Felix, 2005). The most well-studied group of proteins recognising potential pathogens are the Resistance (R) proteins that respond to microbial molecules that are generally not conserved between species or isolates of a species (Martin et al., 2003; van Ooijen et al., 2007). These pathogen-derived factors are referred to as Avirulence (AVR) proteins because their presence in a pathogen causes them to be avirulent on plants containing the cognate R protein. The reason that *AVR* genes withstood evolution is most likely that they contribute towards virulence on plants lacking the R protein (Grant et al., 2006; Kamoun, 2006; Bent and Mackey, 2007). Resistance mediated by R proteins is in most cases accompanied by programmed cell death at the infection site, a response aimed at limiting further pathogen proliferation. This localized cell death is called the Hypersensitive Response (HR).

Investigations into disease resistance started when in the 1840s a mysterious phenomenon wiped out most of Irelands primary food source potato; a period referred to as the “Irish potato famine”, or “great hunger”. Pioneer plant pathology research revealed that the devastating effect on the potato plants was the work of a member of the illustrious genus of oomycete plant pathogens *Phytophthora*. This genus is named after the Greek words *phyton* (plant) and *phthora* (destruction). Potato belongs to the plant family *Solanaceae*, in English called the nightshade family. To date, the solanaceous plant species potato and tomato are, together with thale cress (*Arabidopsis thaliana*), still leading model systems to study plant defense against possibly pathogenic organisms. Most of the R proteins that have been cloned over the past 15 years, originate from nightshade species (Chapter 2). The results presented in this thesis focus on the tomato R proteins I-2 and Mi-1. The *I-2* gene confers resistance to Avr2-containing isolates of the soil-borne fungal pathogen *Fusarium oxysporum* f.sp. *lycopersici*, that causes wilt disease on plants lacking *I-2* (Ori et al., 1997; Simons et al., 1998). *Mi-1* was identified as an *R* gene that confers resistance to several nematode species of the genus *Meloidogyne* (Milligan et al., 1998; Vos et al., 1998). Since these nematodes induce feeding structures in the tomato roots, that swell and produce galls, they are named root-knot nematodes (Williamson and Kumar, 2006). Later, this *R* gene was shown to be effective against infestations by the insect species whitefly (*Bemisia tabaci*) and potato aphid (*Macrosiphum euphorbiae*) as well (Vos et al., 1998; Nombela et al., 2003).

Outline of this thesis

In **chapter two**, a detailed description of our current knowledge of solanaceous R proteins and their modular domain structure is provided. Furthermore, this chapter deals with the intramolecular protein interactions required for R protein repression and activation. Another important aspect of R protein signalling that is discussed in this chapter, is the interaction with other proteins, in order to form large multi-protein complexes that are jointly able to induce immune responses to arrest pathogen proliferation.

Most R proteins contain a central NB-ARC domain and a C-terminal leucine-rich repeat (LRR) domain (Martin et al., 2003). The NB-ARC domain is a functional ATPase domain, and its nucleotide-binding state is proposed to regulate the activity of the R protein (Tameling et al., 2002; Tameling et al., 2006). A highly conserved methionine-histidine-aspartate (MHD) motif (Hammond-Kosack and Jones, 1997) is present at the carboxy-terminus of the NB-ARC domain. An extensive mutational analysis of this MHD motif is provided for R proteins I-2 and Mi-1 in the **chapter three**. Several novel autoactivating mutations were identified, indicating an important regulatory role for the MHD motif in the control of R protein activity. To explain this effect, a three-dimensional model of the NB-ARC domain of I-2 was built, based on the APAF-1 template structure (Riedl et al., 2005). The structural position of the MHD motif residues indicated that they coordinate the bound nucleotide and control subdomain interactions within the NB-ARC domain. The presented 3D model provides a framework for the formulation of hypotheses on how mutations in the NB-ARC exert their effects.

Since genetic experiments pointed towards dynamic interactions between the LRR domain and the N-terminus of Mi-1 (Hwang et al., 2000; Hwang and Williamson, 2003), we analysed the intramolecular interaction between these parts. In **chapter four**, we show that these domains do functionally transcomplement; known autoactivating LRR domain swaps were found to induce HR upon co-expression *in trans*. Likewise, some autoactivating mutants in the NB-ARC domain transcomplemented to induce HR, but others surprisingly did not, suggesting differences in the molecular mechanisms conferring autoactivity. Furthermore, we show that dissociation of the LRR is not required to release its negative regulation, as in all combinations of CC-NB-ARC and LRR domains tested a physical interaction was observed.

Not only intra- but also intermolecular interactions have been analysed, in order to determine the composition of R protein complexes. In **chapter five**, we focus on these interacting proteins, most of which are regarded to be R protein chaperones (Shirasu and Schulze-Lefert, 2003). Through yeast two-hybrid analyses we identified HSP17 as a member of the I-2 protein complex. Silencing of HSP17 was found to

disturb the ability of autoactivating R protein variants to induce HR, indicating the functional involvement of this protein in defence signalling. Furthermore, the effect of HSP17 on R protein expression levels was analysed.
Finally, the results presented in this thesis, and opportunities for future research are discussed in relation to current knowledge in **chapter six**.

References

Bent, A., and Mackey, D. (2007). Elicitors, Effectors, and R Genes: The New Paradigm and a Lifetime Supply of Questions. Annu Rev Phytopathol **45,** 399-436.

Grant, S.R., Fisher, E.J., Chang, J.H., Mole, B.M., and Dangl, J.L. (2006). Subterfuge and Manipulation: Type III Effector Proteins of Phytopathogenic Bacteria. Annu Rev Microbiol **60,** 425-449.

Hammond-Kosack, K.E., and Jones, J.D. (1997). Plant Disease Resistance Genes. Annu Rev Plant Physiol Plant Mol Biol **48,** 575-607.

Hwang, C.F., and Williamson, V.M. (2003). Leucine-rich repeat-mediated intramolecular interactions in nematode recognition and cell death signaling by the tomato resistance protein Mi. Plant J **34,** 585-593.

Hwang, C.F., Bhakta, A.V., Truesdell, G.M., Pudlo, W.M., and Williamson, V.M. (2000). Evidence for a role of the N terminus and leucine-rich repeat region of the *Mi* gene product in regulation of localized cell death. Plant Cell **12,** 1319-1329.

Kamoun, S. (2006). A catalogue of the effector secretome of plant pathogenic oomycetes. Annu Rev Phytopathol **44,** 41-60.

Martin, G.B., Bogdanove, A.J., and Sessa, G. (2003). Understanding the functions of plant disease resistance proteins. Annu Rev Plant Biol **54,** 23-61.

Milligan, S.B., Bodeau, J., Yaghoobi, J., Kaloshian, I., Zabel, P., and Williamson, V.M. (1998). The root knot nematode resistance gene *Mi* from tomato is a member of the leucine zipper, nucleotide binding, leucine-rich repeat family of plant genes. Plant Cell **10,** 1307-1319.

Nombela, G., Williamson, V.M., and Muniz, M. (2003). The root-knot nematode resistance gene Mi-1.2 of tomato is responsible for resistance against the whitefly *Bemisia tabaci*. Mol Plant Microbe Interact **16,** 645-649.

Ori, N., Eshed, Y., Paran, I., Presting, G., Aviv, D., Tanksley, S., Zamir, D., and Fluhr, R. (1997). The *I2C* family from the wilt disease resistance locus *I2* belongs to the nucleotide binding, leucine-rich repeat superfamily of plant resistance genes. Plant Cell **9,** 521-532.

Riedl, S.J., Li, W., Chao, Y., Schwarzenbacher, R., and Shi, Y. (2005). Structure of the apoptotic protease-activating factor 1 bound to ADP. Nature **434,** 926-933.

Shirasu, K., and Schulze-Lefert, P. (2003). Complex formation, promiscuity and multi-functionality: protein interactions in disease-resistance pathways. Trends Plant Sci **8,** 252-258.

Simons, G., Groenendijk, J., Wijbrandi, J., Reijans, M., Groenen, J., Diergaarde, P., Van der Lee, T., Bleeker, M., Onstenk, J., De Both, M., Haring, M., Mes, J., Cornelissen, B., Zabeau, M., and Vos, P. (1998). Dissection of the fusarium *I2* gene cluster in tomato reveals six homologs and one active gene copy. Plant Cell **10,** 1055-1068.

Tameling, W.I.L., Elzinga, S.D., Darmin, P.S., Vossen, J.H., Takken, F.L.W., Haring, M.A., and Cornelissen, B.J.C. (2002). The tomato *R* gene products I-2 and Mi-1 are functional ATP binding proteins with ATPase activity. Plant Cell **14,** 2929-2939.

Tameling, W.I.L., Vossen, J.H., Albrecht, M., Lengauer, T., Berden, J.A., Haring, M.A., Cornelissen, B.J.C., and Takken, F.L.W. (2006). Mutations in the NB-ARC domain of I-2 that impair ATP hydrolysis cause autoactivation. Plant Physiol **140,** 1233-1245.

Vos, P., Simons, G., Jesse, T., Wijbrandi, J., Heinen, L., Hogers, R., Frijters, A., Groenendijk, J., Diergaarde, P., Reijans, M., Fierens Onstenk, J., De Both, M., Peleman, J., Liharska, T., Hontelez, J., and Zabeau, M. (1998). The tomato *Mi-1* gene confers resistance to both root-knot nematodes and potato aphids. Nature Biotech **16,** 1365-1369.

Williamson, V.M., and Kumar, A. (2006). Nematode resistance in plants: the battle underground. Trends Genet **22,** 396-403.

Zipfel, C., and Felix, G. (2005). Plants and animals: a different taste for microbes? Curr Opin Plant Biol **8,** 353-360.

Chapter 2

Structure and function of resistance proteins in solanaceous plants

Gerben van Ooijen, Harrold A. van de Burg, Ben J.C. Cornelissen and Frank L.W. Takken

Adapted from: Annual Review of Phytopathology, 2007, Volume 45, 43-72

Gene-for-gene resistance in plants is based on the presence of a resistance (R) gene in the host and a matching Avirulence (Avr) gene in the pathogen. Many R genes have been cloned over the last two decades, mostly from the *Solanaceae*. The gene products, called R proteins, display modular domain structures. R protein function has recently been shown to require dynamic interactions between the various domains. In addition to these intramolecular interactions, R proteins interact with other proteins to form signalling complexes. These complexes are able to activate an innate immune response that arrests proliferation of the invading pathogen, thereby conferring disease resistance. In this review, we summarize current understanding of R protein structure and function, as well as the molecular mechanisms underlying the activation of defence signalling processes. Besides being a rich source for R genes, *Solanaceae* turn out to be a leading model system to study inter- and intramolecular interactions of R proteins.

Introduction

Solanaceae, a family of flowering dicot plants, likely derived the name from the Latin word *sol,* sun, because the flowers of the most prominent genus in this family, *Solanum*, resemble the sun and its rays. The family includes some prominent crops such as potato (*Solanum tuberosum)*, tomato (*S. lycopersicum)*, pepper (*Capsicum* spec.) and aubergine (*S. melongena)*. Like all other plants solanaceous plants are attacked by a wide range of pathogens including oomycetes, viruses, bacteria, fungi, nematodes and insects like white fly and aphids leading to significant crop losses (Strange and Scott, 2005). In response to these attackers, passive and active defence mechanisms have evolved. Active defence responses can be subdivided into adaptive and innate immunity. Adaptive immunity in plants appears to be restricted to antiviral defense responses depending on an RNAi like mechanism (Voinnet, 2005). The innate immune system is more general and responds to a wide variety of plant pathogens. Innate immunity relies on specialized receptors that can be roughly divided into two groups: the Pathogen or Pattern Recognition Receptors (PRRs) and the Resistance (R) proteins. PRRs recognize Microbe- or Pathogen-Associated Molecular Patterns (MAMPs/PAMPs) that are often a part of highly conserved molecules shared between microorganisms of the same class (Nürnberger et al., 2004; Zipfel and Felix, 2005). PRRs allow plants to recognize distinct invaders using a limited set of receptors (Zipfel and Felix, 2005; Chisholm et al., 2006). In contrast to PRRs, R proteins respond to molecules (called avirulence proteins or elicitors) that are generally not conserved between species or even between isolates of a given pathogen. Accordingly, R proteins are encoded by large gene families, numbering several hundreds of genes per genome (Meyers et al., 2003). Because of the one-to-one relationship between a plant *R* gene and the matching *avirulence (Avr)* gene in a pathogen, this type of immunity was called ‘gene-for-gene’ resistance (Flor, 1942). Resistance mediated by R proteins is often associated with the appearance of localized cell death at the infection site, a phenomenon called the hypersensitive response (HR). This is distinct from the resistance response mediated by PRR receptors, as these generally do not induce an HR response upon pathogen recognition (Jones and Dangl, 2006). In this review, we provide an overview of the R genes that have been cloned from the Solanaceae. We describe the encoded proteins and their predicted structures. Furthermore, we discuss the current data available on the intra- and intermolecular interactions of R proteins from Solanaceae in the context of other model systems. The interaction patterns together with the identified downstream signalling components provide new insights into R protein function and downstream signalling.

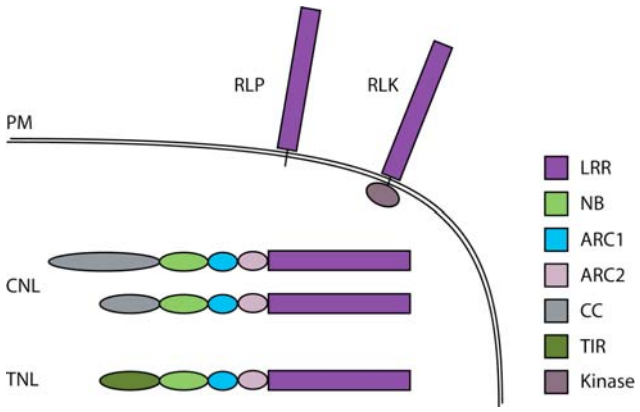

Figure 1

Schematic representation of typical members of the four R protein classes. Protein domains and putative cellular localization are indicated. The Receptor-Like Protein (RLP) and the Receptor-Like Kinase (RLK) classes of R proteins span the plasma membrane (PM) and contain an extracellular Leucine Rich Repeat (LRR) domain. The CNL and TNL classes of R proteins are located intracellularly (cytoplasmic, nuclear, or membrane-bound) and contain a central NB-ARC domain (consisting of NB, ARC1 and ARC2 subdomains) coupled to an LRR domain. TNLs carry an N-terminal TIR domain, while CNLs contain either a CC or an extended CC domain.

R protein classification

Currently, over 55 *R* genes have been cloned from different monocot and dicot plant species ((Martin et al., 2003) and references in Table 1). Although *R* genes confer resistance to very different pathogens, the encoded proteins share a limited number of conserved elements. Based on these domains R proteins can be classified into five classes (Figure 1). The vast majority contains a central Nucleotide-Binding (NB) subdomain as part of a larger entity called the NB-ARC domain, which is present in the human apoptotic protease-activating factor 1 (APAF-1), R proteins, and the *Caenorhabditus elegans* homolog CED-4 (van der Biezen and Jones, 1998). C-terminal to the NB-ARC domain lies a leucine-rich repeat (LRR) domain, which is sometimes followed by an extension of variable length. Hence, this group is collectively referred to as NB-LRR proteins. These NB-LRR proteins are divided into two classes on the basis of their N-terminal region. If this region shows homology to a protein domain found in the *Drosophila* Toll and human Interleukin-1 Receptor (IL-1R), it is called the TIR domain (Whitham et al., 1994) and the proteins are referred to as TIR-NB-LRR or TNL proteins (TNL class). Since some non-TIR proteins contain predicted coiled-coil structures (CC) in their N-terminal domain, non-TIR NB-LRR proteins are collectively referred to as CC-NB-LRR or CNL proteins (CNL class). Phylogenetic analyses of the NB-ARC domains of NB-LRR proteins revealed separate clustering of TNL and CNL proteins. This suggests co-evolution of the N-terminal and NB-ARC domains and is indicative for an ancient segregation of these two classes providing an extra basis for the subdivision of NB-LRR R proteins

(McHale et al., 2006). All NB-LRR proteins are believed to act intracellularly. A more limited number of R proteins acts extracellularly and they contain a predicted extracellular LRR (eLRR) domain at their N-terminus. This eLRR is connected via a transmembrane domain to a variable cytoplasmic C-terminal region. When the cytoplasmic domain contains a protein kinase domain the R protein is placed in the RLK class, that of Receptor-Like Kinases. If no such domain is present it is placed in the RLP class, that of Receptor-Like Proteins. The last class represents a rest group of R proteins that cannot be placed in any of the first four classes.

Besides the genes that have been isolated and confirmed to function as *R* gene, numerous *R* gene homologues have been identified in genome sequencing and annotation programs. In *Arabidopsis*, TNLs form the largest group of NB-LRR proteins (Meyers et al., 1999), whereas this class is absent in monocots (Meyers et al., 1999; Pan et al., 2000). This difference could reflect differences in host/pathogen co-evolution in mono- and dicots. The majority of solanaceous NB-LRR proteins belongs to the CNL class (Table 1), whereas only three TNLs have been identified: the tomato *Bs4*, the potato *Gro1-4* and the tobacco *N* gene conferring resistance to *Xanthomonas campestris*, *Globodora rostochioensis* and Tobacco Mosaic Virus (TMV), respectively (Table1). The RLP class contains the tomato Cf and Ve proteins that confer resistance to *Cladosporium fulvum* and *Verticillium albo-atrum*, respectively (Kawchuk et al., 2001; Rivas and Thomas, 2005). The two Ve proteins differ from the Cf proteins by the presence of a putative C-terminal endocytosis signal (Kawchuk et al., 2001). No R proteins that belong to the RLK class have yet been identified in the *Solanaceae*. Except for the rice *Xa21* gene, this group is made up of PRRs: the *Arabidopsis* EF-tu and flagellin FLS2 receptors (Gomez-Gomez and Boller, 2000; Chinchilla et al., 2006; Zipfel et al., 2006) and the tomato *Le*EIX (Ron and Avni, 2004). Tomato *Asc1* has been placed in the rest class since it does not encode a 'typical' R protein involved in gene-for-gene resistance: resistance to *Alternaria alternata* is brought about by reduced sensitivity to the AAL mycotoxin rather than by specific recognition of the pathogen (Brandwagt et al., 2000).

Avr proteins and R protein-mediated recognition

It seems ill-considered for a pathogen to disclose its presence to a plant by secreting *Avr* gene products that are recognized by an R protein. Naturally, *Avr* genes did not evolve to serve this purpose and indeed evidence accumulates that many Avrs are virulence factors (Jones and Dangl, 2006). Plant pathogenic bacteria deliver approximately 15-30 proteins into host cells using a specialized type III secretion system (TTSS) (Buttner and Bonas, 2006). Whether these effectors suppress or trigger host defence depends on the host being attacked (Vinatzer et al., 2006).

TABLE 1 Cloned solanaceous plant disease resistance genes

Gene[a]	Plant	Ref[b]	Avr gene	Pathogen	Ref[b]
TNL					
Bs4	*Solanum lycopersicum*	(Schornack et al., 2004)	AvrBs4, Hax4	*Xanthomonas campestris*	(Bonas et al., 1993; Kay et al., 2005)
Gro1-4	*Solanum tuberosum*	(Paal et al., 2004)		*Globodera rostochiensis*	
N	*Nicotiana tabacum*	(Whitham et al., 1994)	Helicase	TMV	(Erickson et al., 1999)
CNL					
Bs2	*Capsicum annuum*	(Tai et al., 1999)	AvrBs2	*Xanthomonas campestris*	(Swords et al., 1996)
Gpa2 *Rxh1*	*Solanum tuberosum*	(van der Vossen et al., 2000)		*Globodera pallida*	
Hero[c]	*Solanum lycopersicum*	(Ernst et al., 2002)		*Globodera rostochiensis, G. pallida*	
I-2	*Solanum lycopersicum*	(Ori et al., 1997; Simons et al., 1998)		*Fusarium oxysporum*	
Mi-1.2[c]	*Solanum lycopersicum*	(Milligan et al., 1998b; Vos et al., 1998)		*Meloidogyne incognita, M. arenaria, M. javanica, Bemisia tabacci*	
Prf[c]	*Solanum lycopersicum*	(Salmeron et al., 1996)	AvrPto, AvrPtoB	*Pseudomonas syringae*	(Ronald et al., 1992; Abramovitch et al., 2003)
R1[c]	*Solanum tuberosum*	(Ballvora et al., 2002)		*Phytophthora infestans*	
R3a	*Solanum tuberosum*	(Huang et al., 2005)	Avr3a	*Phytophthora infestans*	(Armstrong et al., 2005)
Rpi-blb1 *RB*	*Solanum bulbocastanum*	(Song et al., 2003; van der Vossen et al., 2003)		*Phytophthora infestans*	
Rpi-blb2[c]	*Solanum bulbocastanum*	(van der Vossen et al., 2005)		*Phytophthora infestans*	
Rx1	*Solanum tuberosum*	(Bendahmane et al., 1995)	CP	PVX	(Bendahmane et al., 1995)
Rx2	*Solanum tuberosum*	(Bendahmane et al., 2000)	CP	PVX	(Bendahmane et al., 2000)
Sw-5[c]	*Solanum*	(Brommonschenk		Tospovirus	

	lycopersicum	el et al., 2000)			
Tm-2	*Solanum lycopersicum*	(Lanfermeijer et al., 2005)	MP	ToMV	(Calder and Palukaitis, 1992)
Tm-2-2	*Solanum lycopersicum*	(Lanfermeijer et al., 2003)	MP	ToMV	(Calder and Palukaitis, 1992)
RLP					
Cf-2	*Solanum lycopersicum*	(Dixon et al., 1996)	Avr2	*Cladosporium fulvum*	(Luderer et al., 2002)
Cf-4	*Solanum lycopersicum*	(Thomas et al., 1997)	Avr4	*Cladosporium fulvum*	(Joosten et al., 1994)
Cf-4A *Hcr9-4E*	*Solanum lycopersicum*	(Takken et al., 1998)	Avr4E	*Cladosporium fulvum*	(Westerink et al., 2004)
Cf-5	*Solanum lycopersicum*	(Dixon et al., 1998)		*Cladosporium fulvum*	
Cf-9	*Solanum lycopersicum*	(Jones et al., 1994)	Avr9	*Cladosporium fulvum*	(van Kan et al., 1991)
Cf-9B *Hcr9-9B*	*Solanum lycopersicum*	(Parniske et al., 1997; Panter et al., 2002)		*Cladosporium fulvum*	
Ve1	*Solanum lycopersicum*	(Kawchuk et al., 2001)		*Verticillium albo-atrum*	
Ve2	*Solanum lycopersicum*	(Kawchuk et al., 2001)		*Verticillium albo-atrum*	
Other					
Asc-1	*Solanum lycopersicum*	(Brandwagt et al., 2000)	-	*Alternaria alternata*	

[a]Synonymous names in italics

[b]References that describe cloning of the gene

[c]The R proteins encoded by these genes contain an extended N-terminus

Effectors appear to manipulate many signalling processes, but only for a small number of effectors a host target has been identified (Grant et al., 2006). Clues on how they interfere with signal transduction processes of the host can sometimes be obtained from structural homology to other proteins. For instance, members of the XopJ/AvrRxv effector family appear to encode SUMO proteases, suggesting interference with SUMO signalling (Orth et al., 2000), while AvrPtoB is an active ubiquitin E3 ligase likely interfering with specific protein degradation of the host (Janjusevic et al., 2006). Avrs such as AvrRpt2 and AvrPphB act as proteases and cleave specific host proteins (Shao et al., 2002; Axtell et al., 2003; Shao et al., 2003; Kim et al., 2005b). For recent reviews on bacterial effectors we refer to (Mudgett, 2005; Abramovitch et al., 2006; Grant et al., 2006).

Less is known on fungal effectors. Four *Avr* genes have been cloned from the fungus *Cladosporium fulvum* (Table 1), which all encode small cysteine-rich extracellular

proteins found in the tomato apoplast. Avr2 acts as a protease inhibitor (Rooney et al., 2005), while Avr4 binds to chitin present in fungal cell walls, thereby protecting it from degradation by plant chitinases (van den Burg et al., 2006). The function of the remaining *C. fulvum* Avrs remains unresolved but they probably exert their function extracellulary (Joosten and De Wit, 1999; Thomma et al., 2005). Other plant pathogenic fungi, like rusts and powdery mildews, form more intimate contacts with their hosts by the formation of specialized feeding structures called haustoria. These specialized feeding structures penetrate the host plant cell wall, but remain separated from the host cytoplasm by the host cell envelope. Recently, several *Avr* genes have been identified from haustoria-forming fungi (Catanzariti et al., 2006; Dodds et al., 2006; Ridout et al., 2006). These genes encode proteins with a predicted signal peptide for secretion into the extrahaustorial matrix, but nonetheless act inside the host cell where they are perceived by matching NB-LRR proteins. How these Avrs are taken up by the host is currently not clear (Dodds et al., 2006; Ridout et al., 2006). For a recent review on fungal Avrs and secreted proteins we refer to (Rep, 2005).

The Avr3a protein from the oomycete *Phytophthora infestans* also acts inside the host cell as in the absence of the *R3* resistance gene it is able to suppress cell death triggered by the *P. infestans* elicitin INF1 (Bos et al., 2006). Avr3a and two other oomycete Avrs cloned from *Hyaloperonospora parasitica* share a conserved sequence motif, RxLR (Kamoun, 2006). This motif might be the signal for uptake into the host cell from the extrahaustorial space.

Based on the existence of monogenic resistance against animal pathogens such as nematodes and insects, the latter are also predicted to contain *Avr* genes (Vos et al., 1998; Williamson and Kumar, 2006). Unfortunately, animal *Avr* genes have not yet been identified (Kaloshian and Walling, 2005; Williamson and Kumar, 2006).

Because in all cases described above corresponding R and Avr proteins co-localize, one interpretation of the gene-for-gene relation assumes a direct interaction between the two proteins. Using yeast two-hybrid and in vitro pull-down approaches, a direct interaction was indeed confirmed in a few cases, i.e. between Pita / AvrPita (Jia et al., 2000), L / AvrL567 (Dodds et al., 2006), PopP2 / RRS-1 (Deslandes et al., 2003) and the TMV p50 helicase with the NB-ARC-LRR part of the tobacco N protein (Ueda et al., 2006). The latter interaction, however, was not found by others using in vivo pull-down assays (Peart et al., 2005; Mestre and Baulcombe, 2006), or rather an indirect interaction was detected (Caplan et al., 2008; also see below). A direct interaction was recently proposed for the Bs4 / AvrBs4 pair (Schornack et al., 2006) since AvrBs4 has a tetratricopeptide repeat (TPR)-like structure also found in the I-2 interacting protein phosphatase 5 (PP5) (de la Fuente van Bentem et al., 2005).

Since most bacterial Avrs probably act as effector proteins that target host cellular

components, R proteins might sense the presence of an Avr protein by monitoring the state of the host target. This indirect interaction model is called the guard hypothesis (Van der Biezen and Jones, 1999; Dangl and Jones, 2001). Although a guard that waits until its guardee is killed may seem a bit odd, this theory has gained support. The best studied example of modification of a host target by Avrs, resulting in R protein activation, is the phosphorylation or cleavage of *Arabidopsis* Rin4 protein by AvrB, AvrRpm1 and AvrRpt2, respectively (Mackey et al., 2002; Kim et al., 2005b). These events trigger activation of the NB-LRR proteins Rpm1 and Rps2. Also, the cleavage of the Pbs1 kinase bound to Rps5 by the avrPphB protease, thereby triggering Rps5 activation, supports the guard hypothesis (Shao et al., 2003). Three additional examples in support of the guard hypothesis have been described in tomato-pathogen model systems. Firstly, an interaction has been shown between the *Pseudomonas syringae* effectors AvrPto and AvrPtoB and the tomato kinase Pto, sensed by NB-LRR protein Prf. The Avr proteins interact directly with their target Pto (Tang et al., 1996; Kim et al., 2002), while Pto constitutively binds to the N-terminus of Prf (Mucyn et al., 2006). Although the presence of a tertiary complex could not be shown, interaction of all three components is essential for induction of defence signalling. Upon binding of AvrPto or AvrPtoB to Pto, a conformational change of this protein is proposed to trigger the defense signalling potential of the interacting Prf R protein (Mucyn et al., 2006).

A second example of indirect pathogen perception in tomato is the *Avr2/Cf-2* system. *Cf-2* resistance is strictly dependent on the tomato cysteine protease Rcr3 that is inhibited by the Avr2 protein from *C. fulvum*. Interestingly, the Rcr3 sequence from cultivated tomato (*Solanum lycopersicum* L.) differs slightly from the *S. pimpinellifolium* Rcr3, and *Sl*Rcr3 induces Cf-2 dependent necrosis in the absence of any Avr. This observation suggests that a small conformational difference in the *Sl*Rcr3 protein mimics the Avr2-inhibited *Sp*Rcr3 state so that it activates Cf-2 (Rooney et al., 2005).

The third example of indirect Avr binding is provided by the TNL protein N of tobacco. Using co-immunoprecipitations and bimolecular fluorescence complementation (BiFC) experiments, it was shown that N and p50, the part of the helicase protein that is required for its Avr function, associate in vivo. This association is mediated by an unknown protein binding to the TIR domain, called N interacting protein (NIP1). NIP1 is a good candidate to be the guardee of N (S. P. Dinesh-Kumar, personal communication). Besides the examples described above, indirect Avr recognition has been proposed for the tomato Mi-1.2 protein. Mi-1.2 is intriguing since it confers resistance to highly diverse animal pathogens: the root-knot nematode *Meloidogyne incognita,* the potato aphid *Macrosiphum euphorbiae* and the whitefly *Bemisia tabaci* (Milligan et al., 1998a; Vos et al., 1998; Nombela et al., 2003). Mi-1.2 mediated

resistance to nematodes is accompanied by an HR, while an HR is not observed in the interaction with whitefly and the potato aphid (Williamson, 1999). A mutant screen identified *Rme-1*, which is unlinked to *Mi-1.2*, but is required for Mi-mediated resistance against all three pathogens. As Rme-1 is not involved in other R gene pathways and acts upstream (or at the same step) of Mi-1.2 in the signalling cascade, it is a candidate for the Mi-1.2 guardee (Martinez de Ilarduya et al., 2004). However, cloning of the *Rme-1* gene is needed to confirm that Rme-1 functions as the Mi-1.2 guardee.

Based on the few examples for direct and indirect Avr perception it cannot be concluded at this stage whether there is a prevalence for one over the other. During evolution, R protein recognition specificities are likely to be generated at random, some targeting Avr products directly, and others recognizing host factor modifications. The group targeting Avrs directly can relatively easily be overcome by mutations in the Avr protein that abolish the interaction, but not its virulence function. Resistance based on indirect recognition is (at least theoretically) more difficult to overcome, since mutations avoiding recognition will also affect virulence.

Structural features of R protein domains

As described above, R proteins can be classified based on their protein domain architecture. Figure 1 schematically presents the four structural classes of R proteins. Unfortunately, crystal structures have not yet been obtained of any domain of plant R proteins. However, crystal structures of LRR and NB-ARC domains have been obtained from evolutionary related proteins. These crystal structures have been used for 3D structure modelling studies of plant LRR and NB-ARC domains (van der Hoorn et al., 2005; McHale et al., 2006; Takken et al., 2006). These studies have provided insight into some structural features of these domains and they are utilized to explain the effect of certain mutations on R protein activation and downstream signalling (McHale et al., 2006; Takken et al., 2006).

The Leucine-Rich Repeat domain

The LRR domain is the only domain present in all R proteins listed in Table 1. LRRs are present in many receptors of virtually any organism, where this domain is involved in ligand recognition (Enkhbayar et al., 2004). The LRR domain consists of two to 42 repeats each comprising a ß-sheet with the core consensus xxLxLxx (Enkhbayar et al., 2004). In plant LRRs, individual repeats are formed by 24-28 residues and contain a core of 14 residues with consensus sequence LxxLxxLxLxxC/Nxx. This core forms the ß-sheet and the attached loop-regions. Each core is separated from the next by a spacer of variable length. Crystal structures of over 20 LRR proteins have revealed differences in overall structure, but in all proteins

a series of parallel ß-strands form a right-handed super helical beta-sheet (Kobe and Kajava, 2001; Enkhbayar et al., 2004). The only plant LRR protein for which the crystal structure was solved is PGIP2, an eLRR protein that binds and inhibits polygalacturonases from fungi such as *Fusarium moniliforme* and *Aspergillus niger* (Leckie et al., 1999). The PGIP2 structure is characterized by the presence of a second ß-sheet (ß2) in each repeat, with consensus NxLxGx, connecting the first (ß1) with an α-helix in the spacer (Di Matteo et al., 2003).

In plant R proteins there are several differences between intra- and extracellular LRR domains. In the LRRs of TNLs and CNLs no clear subdomains are apparent, but a conserved motif is present in the third LRR (Meyers et al., 2003). Mutation of the D in this so-called VLDL motif in the potato Rx protein to an E produced a constitutively active protein (Bendahmane et al., 2002), whereas a mutation adjacent to this motif in the *Arabidopsis* CNL Rps5 had inhibitory epistatic effects on resistance (Warren et al., 1998). The role of this motif for NB-LRR protein function is not clear, but the sequence fits the consensus for a leucine-rich nuclear export signal (Bendahmane et al., 2002; la Cour et al., 2004).

Plant eLRR proteins are characterized by a longer repeat consensus sequence than intracellular LRRs; a 24-residue motif LxxLxxLxLxxNxLxGxIPxxLGx instead of the general 14-residue consensus (Federici et al., 2006). The consensus of the PGIP2 ß2 is conserved in the Cf proteins and since ligand binding presumably only involves ß1, ß2 might be involved in binding of other proteins (Rivas and Thomas, 2005; Federici et al., 2006) or in homo- or hetero dimerization with other eLRRs. The Cf and Ve eLRR domains can be subdivided into three subdomains, in Cf proteins these are referred to as: C1, 2 and 3 (Rivas and Thomas, 2005). C1 forms the major part of the eLRR domain and consists of 21-28 hypervariable repeats. C2 forms a spacer domain separating C1 from C3. C3 consists of three to four relatively conserved repeats (Rivas and Thomas, 2005). R protein eLRR domains, unlike the LRR domains in NB-LRR proteins, have many putative N-linked glycosylation (NGS) sites in the exposed regions. For Cf-9, the NGS sites in the C1 have been shown to be essential for Cf-9 function, whereas introduction of NGS sites in the C3 disrupts its function (van der Hoorn et al., 2005). Another unique feature of eLRRs is the presence of N- and C-terminal ‘capping’ domains. For the small tomato eLRR protein LRP, these capping domains were shown to form disulphide bonds that are necessary to protect the eLRR from proteolysis (Kolade et al., 2006).

The NB-ARC domain

The recently published crystal structures of the NB-ARC domains of APAF-1 and CED-4 revealed that the NB-ARC domain consists of clearly distinguishable subdomains. Besides the NB subdomain, the NB-ARC of APAF-1 contains three

additional subdomains (ARC1-ARC3) that form a four-helix bundle, a winged-helix fold and a helical bundle, respectively (Riedl et al., 2005). Subdomain ARC3 is absent in plant R proteins and CED-4, but ARC1 and ARC2 are conserved (Figure 2)(Yan et al., 2005; Albrecht and Takken, 2006). Proteins containing an NB-ARC domain are evolutionary related to the mammalian NACHT-LRR protein family (such as NAIP, CIITA, HET-E and TP1), many of which function in innate immunity (Inohara et al., 2002; Leipe et al., 2004; Albrecht and Takken, 2006). ARC1, 2 and 3 of APAF-1 correspond to the NAD1-3 subdomains of mammalian intracellular NACHT-LRR proteins (Albrecht and Takken, 2006).

The NB-ARC and NACHT-LRR proteins belong to the STAND super family of ATPases (Signal Transduction ATPases with Numerous Domains). The nucleotide-binding domain of these proteins is proposed to function as a molecular switch, where NTP-hydrolysis induces a conformational switch required to regulate signal transduction (Leipe et al., 2004). The NB subdomains of both NB-ARC and NACHT domains form an NTP binding fold consisting of a parallel five-stranded ß-sheet flanked by α-helixes (Takken et al., 2006), placing them in the large group of P-loop NTPases (Vetter and Wittinghofer, 1999). The ß-sheet is five-stranded and assumes a 2-3-4-1-5 topology (Figure 2). The strands ß1 and ß3 encompass the most conserved motifs of the NB subdomain: the P-loop itself (also called Walker A motif), and the Walker B motif. The P-loop is defined by the consensus sequence GxxxxGKS/T that bind ß- and γ- phosphates of the nucleotide through the Lys residue, and the Ser and Thr residues coordinate the Mg^{2+}-ion in the binding pocket. The Walker B motif is defined by the hhhhDD/E consensus site (where h represents a hydrophobic residue), in R proteins this motif is often hhhhDD. The first Glu residue (D) is also important for the coordination of the Mg^{2+}-ion while the acidic residue (D/E) is thought to act as a catalytic base during nucleotide hydrolysis (Leipe et al., 2004; Hanson and Whiteheart, 2005).

Besides the P-loop and Walker B motifs, several other motifs have been identified in the NB-ARC domain (Figure 2). The hhGRExE motif is part of a linker region connecting the NB subdomain with the N-terminus. In the ARC2 subdomain, a highly conserved motif is present called the MHD-motif. Other motifs annotated in the NB-ARC domain of R proteins include Resistance NBS motifs RNBS-A, -B, -C and –D, the GxP motif and motifs VII and VIII (Figure 2). For an overview on synonymous names for these motifs, we refer to (Takken et al., 2006). Not surprisingly, many residues in the conserved motifs are essential for NB-LRR protein function and are predicted to map at positions where they are able to interact with the nucleotide (Takken et al., 2006). For instance, the conserved His residue in the APAF-1 MHD motif interacts directly with the ß-phosphate of dATP (Riedl et al., 2005). Mutation of this motif in the R proteins I-2, Mi-1.2, L6 and Rx results in autoactivation (Moffett et

al., 2002; de la Fuente van Bentem et al., 2005; Howles et al., 2005; Chapter 3), possibly by interfering with nucleotide binding.

The NB-ARC domain of I-2, Mi-1.2 and N has been shown to specifically bind (d)ATP, similar to APAF-1 and CED4 (Tameling et al., 2002; Kim et al., 2005a; Yan et al., 2005; Ueda et al., 2006). The NB-ARC domain of these R proteins also catalyzes the hydrolysis of ATP to ADP, as shortly discussed below.

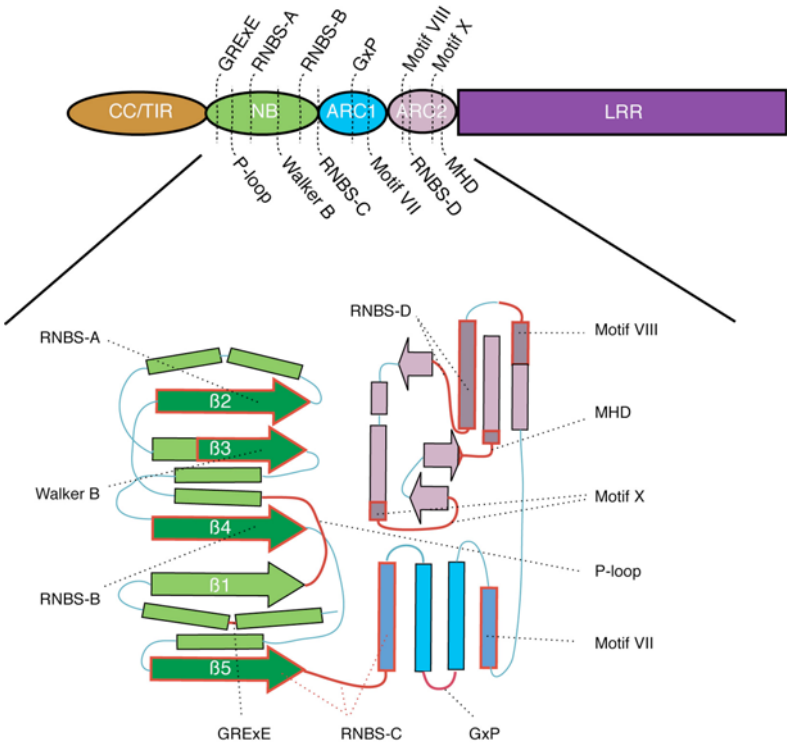

Figure 2

Proposed protein topology of the NB-ARC domain. (A) The position of conserved motifs in the NB (green), ARC1 (blue) and ARC2 (pink) subdomains is indicated in the schematic representation of a typical NB-LRR R protein. (B) Conserved motifs are marked (a darker colour and red surroundings) in a close-up of the protein topology of the NB-ARC domain. Arrows and bars represent ß-strands and α-helices, respectively.

ATP hydrolysis by NB-ARC domains

In APAF-1, binding of cytochrome c results in hydrolysis of ATP by the NB-ARC domain, followed by replacement of the formed ADP by ATP (Kim et al., 2005a). ATP hydrolysis and nucleotide exchange are both essential to produce the activated state. Like APAF-1, CED-4 requires ATP binding for function. However, hydrolysis or nucleotide exchange has not been observed for CED-4 (Yan et al., 2005).

Specific binding and hydrolysis of ATP was recently observed for the solanaceous R proteins I-2, Mi-1.2 and N (Tameling et al., 2002; Ueda et al., 2006). For I-2,

biochemical analysis of two autoactivating mutants revealed that these mutants are affected in ATP hydrolysis but not in nucleotide binding (Tameling et al., 2006). For N, the ATP- and not the ADP-bound state of the protein was shown to interact with the elicitor (Ueda et al., 2006). Together, these observations suggest that in the active, HR signalling state, ATP is bound to the NB-ARC. Mutations in the P-loop of several other R proteins were shown to abolish function (Dinesh-Kumar et al., 2000; Tao et al., 2000; Tornero et al., 2002). These data indicate that nucleotide binding is essential for R protein signalling. To define more exactly the effect of the nucleotide binding status of R proteins on R protein function, biochemical analyses of NB-ARC domains or even entire R proteins will be a valuable development. protein topology of the NB-ARC domain.

The N-terminal domain

As described above, the two NB-LRR classes are distinguished by the presence or absence of a TIR domain at the N-terminus. The TIR domain is conserved in metazoan Toll and IL-1R proteins (Xu et al., 2000), involved in innate immunity. Crystal structures have been published for human Toll-like receptors TLR1 and TLR2. Structures of plant TIR domains have not yet been resolved, but structures similar to animal family members are proposed, since amino acids shared between the TNL N and the metazoan Toll or IL-1R protein were shown to be essential for functioning of both (Dinesh-Kumar et al., 2000). The topology of the TIR domain consists of a parallel five-stranded β-sheet, five α-helices, and connecting loops. The loop between ß2 and α2 contains several highly conserved surface-exposed residues that are important for receptor signalling by recruiting interacting proteins (Xu et al., 2000).

CNL proteins often contain a predicted coiled-coil domain (α-helix-rich domain that contains seven-residue repeat sequences). In Table 1, we have discriminated two types of CC domains: a short CC domain and an extended CC domain. This extended domain has only been found in *Solanaceae* and might be specific for this family. Recently, a novel protein-protein interaction domain was identified in the extended CC domain of tomato Prf. This domain has been found in solanaceous R proteins with an extended CC domain only, and was called the Solanaceous Domain (SD) (Mucyn et al., 2006).

A recent sequence analysis has revealed a short conserved motif in the middle of the short CC. The nT motif was originally described due to its high conservation in monocot CC-NB-LRRs (Bai et al., 2002). This motif is less conserved in dicots but a core EDVID motif can be identified in many but not all CC-NB-LRR proteins and is one of the few motifs that can be identified as being broadly conserved across the CC domains of NB-LRRS of different families of plants (Rairdan et al., 2008). This

EDVID motif was proven to be required for Rx function, due at least in part to its requirement for an intra-molecular interaction involving the CC domain (Rairdan et al., 2008).

R protein domain functionality and interplay

As detailed above, R proteins are composed of several (sub)domains that appear to function consecutively during signal perception. In this section we address the following questions: (1) What is the specific function of each (sub)domain? (2) How do the domains interact? (3) How does this result in a protein that is able to recognize Avr proteins and trigger activation of defence responses?

Many studies have shown that the LRR domain is under diversifying selection, and specifically the surface-exposed residues in the β–sheet that are putatively involved in ligand recognition (Meyers et al., 1998; Noel et al., 1999; Mondragon-Palomino et al., 2002). Diversifying selection is compatible with a receptor surface that might be involved in Avr perception (Mondragon-Palomino et al., 2002). The prediction that the LRR confers Avr specific recognition has indeed been confirmed experimentally and this specificity can be changed with a few minor changes into a new one (Ellis et al., 1999; Jia et al., 2000; Van der Hoorn et al., 2001; Wulff et al., 2001; Dodds et al., 2006; Rairdan and Moffett, 2006). Interestingly, a significant degree of diversifying selection was also observed in the N-terminal region of some NB-LRR proteins, suggesting that this region is also important for the origination of new recognition specificities (Mondragon-Palomino et al., 2002) and this has been confirmed experimentally (Ellis et al., 1999; Luck et al., 2000). In addition to a role in recognition specificity, the N-terminal domain may be involved in the recruitment of downstream signalling components. A strong indication that the N-terminus is involved in downstream signalling is the differential requirement of downstream signalling components by CNLs and TNLs, reviewed in (Martin et al., 2003).

With the LRR and the N-terminal domain conferring pathogen recognition and downstream signalling, the central NB-ARC is thought to act as the molecular switch that controls the activation state of the protein (Takken et al., 2006). The “on” and “off” state of the switch being defined by the nucleotide that is bound to the NB-ARC domain (ATP versus ADP).

Important progress has been made over the last years in understanding the function of the intra-molecular interaction in the NB-LRR R proteins. R protein signalling by NB-LRRs appears to depend on dynamic interactions between the three major domains. Positive and negative regulatory regions are scattered over the entire protein as demonstrated by many auto-activating and loss-of-function mutations (Dinesh-Kumar et al., 2000; Tao et al., 2000; Axtell et al., 2001; Bendahmane et al., 2002; Tornero et al., 2002; Takken et al., 2006). These mutations suggest that

compatibility between the different domains is required to keep NB-LRR proteins in an auto-inhibited but activatable state. Support for such harmonisation between domains is provided by domain swap experiments between homologous R proteins. For instance, LRR exchange between homologues at the maize *Rp1* locus results in a necrotic phenotype (Sun et al., 2001). Likewise, domain swaps between Mi-1.2 and its paralogue Mi-1.1 resulted in autoactivating incompatibilities between the LRR of Mi-1.2 and either the first 161 amino acids of the amino terminal domain (NT-1), or the next 751 residues encompassing the NB-ARC domain of Mi-1.1 (Hwang et al., 2000). Autoactivating fusions were also obtained by swapping different, non-overlapping, LRR sequences in Rx for the equivalent region of Gpa2 (Rairdan and Moffett, 2006). These experiments suggest that the different domains interact with each other and that mis-pairing can result in spontaneous activation of the protein.

Studies on the potato protein Rx provided the first example of direct physical and functional intra-molecular interactions between the different protein domains found in NB-LRR proteins (Moffett et al., 2002). Co-expression of either the CC and NB-ARC-LRR fragments or the CC-NB-ARC and LRR fragments reconstituted Avr-dependent HR. This transcomplementation involved physical interaction between the domains, which was disrupted by co-expression of the PVX coat protein, the activator of Rx (Moffett et al., 2002; Rairdan and Moffett, 2006). Interestingly, the interaction between the CC domain and the NB-ARC-LRR fragment requires a functional EDVID motif in the CC domain (Rairdan et al., 2008). In vitro, the LRR domain of the tobacco TNL protein N was found to interact with the TIR-NB-ARC fragment and this interaction was lost when the elicitor was added (Ueda et al., 2006). The latter observation however, could not be confirmed in vivo, as no intramolecular interactions were detectable upon co-expression of N domains. Perhaps the intramolecular interactions in N are weaker than in Rx or are not effective for proteins expressed in trans (Mestre and Baulcombe, 2006). Immunoprecipitation studies with the R protein Bs2 also showed an intra-molecular interaction between the CC-NB-ARC and LRR parts, but instead of disrupting this interaction, the interaction was enhanced when the elicitor (AvrBs2) was co-expressed. No interaction could be observed between the CC fragment and NB-ARC-LRR of Bs2. Strikingly, the interaction between the CC-NB-ARC and LRR parts of Bs2 was no longer detectable upon silencing of SGT1 (Leister et al., 2005). These differences support the idea that SGT1 acts as a co-chaperone of R-protein complexes (Leister et al., 2005), as will be discussed later.

To investigate the function of the various subdomains of the NB-ARC involved in the intramolecular interactions with the N- and C-terminal domains, a series of domain swaps between Rx and Gpa2 were made. These studies showed that the Rx ARC1 subdomain is necessary for the interaction between the CC-NB-ARC and LRR

fragments (Rairdan and Moffett, 2006). Binding to LRR domains seems to be a general property of the ARC1 subdomain. For instance the CC-NB-ARC part of Rx was able to interact with the LRR domains of several other NB-LRRs as well (i.e. Bs2 and *Arabidopsis* HRT LRR domains). However, these interactions did not reconstitute a functional R protein capable of activating defence responses (neither autoactivation nor elicitor-dependent activation) (Rairdan and Moffett, 2006). Point mutations in the ARC1 subdomain had only a quantitative effect on the binding affinity for the LRR domain and reduced LRR binding affinity did not necessarily compromise functionality of the R protein. This observation supports an extensive and partially conserved interaction surface between the ARC1 and the LRR domain with individual contacts quantitatively contributing to the interaction. Subsequent deletion studies with the LRR of Rx revealed that the intact LRR domain is necessary for the interaction with the CC-NB-ARC part suggesting that the overall fold is needed for the interaction or that the interaction surface is scattered over the entire LRR domain (Rairdan and Moffett, 2006).

A function for the ARC2 subdomain became apparent when the Gpa2 ARC2 subdomain was swapped with the Rx ARC2 domain, as this resulted in a constitutively active protein. The LRR is believed to have a positive regulatory role in the activation process, as R proteins are generally inactive in the absence of their genuine LRR when expressed at their endogenous levels (Rathjen and Moffett, 2003; Rairdan and Moffett, 2006). Thus, the ARC2 domain of Gpa2 and LRR domain of Rx are sufficiently compatible to execute the positive regulatory role of the LRR and to induce HR, but the combination lacks the structural constraints to prevent autoactivation. Rairdan & Moffett therefore concluded that the ARC2 subdomain relays pathogen recognition mediated by the LRR domain into changes in R protein conformation, unleashing its downstream signalling potential (Rairdan and Moffett, 2006). A regulatory role for the ARC2 subdomain fits with the fact that mutations in the ARC2 subdomain often result in an autoactivating protein (Takken et al., 2006). These observations suggest fine-tuning and co-evolution between the N-terminal end of the LRR domain and the ARC2 subdomain in NB-LRR proteins. This idea might be tested by a survey of polymorphisms in NB-LRR proteins.

A model in which Avr perception alters the interaction between the LRR and ARC2 subdomains, repositioning critical motifs and thereby allowing the molecule to progress to an active conformation, is in agreement with domain swap experiments between Mi-1.2 and Mi-1.1 (Hwang and Williamson, 2003). These swaps demonstrated autoactivating incompatibilities between the LRR and a region encompassing the ARC2 (Hwang and Williamson, 2003). Additional intramolecular interactions for Mi-1.2 were suggested based on mutational analysis. A single amino acid replacement in the first half of the Mi-1.2 LRR by the Mi-1.1 residue (R961D)

leads to autoactivation, suggesting that this residue is needed for autoinhibition of HR signalling. This autoactivation phenotype was suppressed in trans by overexpression of a subdomain of the Mi-1.1 N-terminus (NT1), suggesting that HR signalling mediated by the LRR is normally suppressed by the NT1 (Hwang et al., 2000). The necessity of compatibility between the NT1 domain and residue 961 was also shown by swapping the Mi-1.1 NT1 into a Mi-1.2 background, which results in autoactivation. However, this NT1 domain is absent in CNL proteins with a shorter N-terminus (Table 1).

The ability of NB-LRR proteins to establish intramolecular interactions depends on the conformation of the NB subdomain, regulated by the nucleotide bound. For instance, mutations in the P-loop of Rx abolished the interaction between the CC fragment and the NB-ARC-LRR fragment, whereas the LRR and CC-NB-ARC interaction was not lost (Moffett et al., 2002). Also in Bs-2 the latter interaction does not require a functional P-loop (Leister et al., 2005), whereas in N it does in vitro (Ueda et al., 2006). Direct support for a conformational change in the NB-ARC domain upon binding different nucleotides came from the tomato CNL protein I-2. The ADP-bound state of the protein displayed increased affinity for the nucleotide compared to the ATP-bound state (Tameling et al., 2006). In addition, two autoactivation mutants of I-2 were shown to have a wild-type nucleotide binding affinity but a reduced ATPase activity. These data suggested that the ADP conformation reflects a resting state whereas the ATP conformation represents the activated state of the I-2 protein (Tameling et al., 2006). In contrast, in a model proposed for the N protein the ATP-bound state reflects the resting state (Ueda et al., 2006). Upon Avr perception by N, its ATPase activity is stimulated resulting in hydrolysis of the nucleotide and transition to the activated, ADP-bound state of the protein. Unfortunately, the I-2 and N data are not directly comparable as they were obtained using truncated proteins, containing either the CC-NB-ARC (I-2) or the NB-ARC-LRR (N). The crucial next step will be to perform nucleotide binding and hydrolysis experiments using full-length R proteins.

An important additional role of the NB-ARC domain was found for non-plant NB-ARC proteins. The NB-ARC domains of the mammalian NB-ARC protein APAF-1 and its *Drosophila* and *C. elegans* analogues DARK1 and CED4, have been shown to homo-oligomerize upon activation, to form wheel-like structures of respectively 7, 8, and 4 molecules. These ‘wheels of death’ provide a platform for binding and subsequent activation of downstream procaspases (Yan et al., 2005; Yu et al., 2005; Yu et al., 2006).

Recently, also for the tobacco TNL protein N oligomerization upon recognition of the Avr was observed (Mestre and Baulcombe, 2006). Oligomerization and resistance both require an intact P-loop, hence presumably the ability to bind nucleotides.

Interestingly, mutation of the RNBS-A motif does not affect elicitor-dependent oligomerization but still abolishes resistance (Mestre and Baulcombe, 2006), indicating that resistance is not an automatic consequence of oligomerization. The N TIR domain can also oligomerize on its own (Mestre and Baulcombe, 2006). However, oligomerization of the TIR domain was independent of the Avr protein. Mutation of three of the predicted solvent exposed residues in the TIR domain abolished HR signalling coinciding with a weaker homotypic interaction of the TIR domain. However, when these mutations where introduced in the full-length protein oligomerization still occurred. This suggests that the elicitor-triggered oligomerization of the full-length R protein mainly involves NB-ARC::NB-ARC interactions, similar to the CED-4, APAF-1 and DARK oligomers. Regretfully, the N NB-ARC domain alone was not stable upon transient expression to test this hypothesis (Mestre and Baulcombe, 2006). A major remaining question is now whether oligomerization is a general feature of NB-LRR R proteins or whether it is unique for N or possibly the TNL class.

Intermolecular interactions of R proteins

Besides the intramolecular interactions described above, R proteins interact with other proteins to form large, dynamic, multimeric protein complexes. Yeast two-hybrid screens and recently also co-immunoprecipitation experiments have identified R protein-interacting proteins.

For solanaceous NB-LRR proteins entire proteins as well as the different domains have been used as baits. For the LRR domain, thought to be the specificity determinant, this did not reveal putative “guardees” and/or Avr products. Rather, LRR interactors were found to be chaperones and chaperone-associated proteins. For example, the LRRs of N and I-2 physically interact with heat shock protein 90 (Hsp90) (Liu et al., 2004; de la Fuente van Bentem et al., 2005). Hsp90 is a chaperone mainly involved in folding receptor proteins into a signalling competent state (Pratt et al., 2004). Whereas the N-terminal part of the LRR domain of I-2 interacts with Hsp90, the C-terminal part was found to bind specifically to protein phosphatase 5 (PP5) (de la Fuente van Bentem et al., 2005). Binding is not exclusive for I-2 since in yeast two-hybrid assays PP5 was also found to interact with the solanaceous R proteins Mi-1.2 and Rx, and *Arabidopsis* Rps5 and Rpm1 (de la Fuente van Bentem et al., 2005) as well as N (S. P. Dinesh-Kumar, unpublished data). PP5 not only interacts with the LRR domain of NB-LRR proteins, but through its TPR domain also with the C-terminus of Hsp90. The biological function of the single copy gene PP5 in disease resistance remains elusive, however, since neither knock-down in tomato nor knock-out in *Arabidopsis* affects disease resistance (de la Fuente van Bentem et al., 2005). In contrast, silencing of the different Hsp90

homologs showed a requirement for Hsp90 in disease resistance and HR activation for a large number of NB-LRR and RLP R proteins (Hubert et al., 2003; Lu et al., 2003; Takahashi et al., 2003; Liu et al., 2004; de la Fuente van Bentem et al., 2005; Kaloshian and Walling, 2005; Gabriëls et al., 2006).

Another TPR-containing Hsp90-interacting co-chaperone is Sgt1. The role of Sgt1 and its interaction partner Rar1 in disease resistance has been strongly established (Austin et al., 2002; Azevedo et al., 2002; Peart et al., 2002). Several studies have demonstrated physical interaction between Hsp90, Sgt1, and Rar1 (Hubert et al., 2003; Takahashi et al., 2003; Liu et al., 2004). A role for Sgt1 as a co-chaperone in *Solanaceae* is illustrated by the N and Rx proteins, whose accumulation depends on Sgt1 (Azevedo et al., 2006; Mestre and Baulcombe, 2006) and the tomato Bs2 protein that requires Sgt1 for intramolecular interactions (Leister et al., 2005). Also outside the *Solanaceae* the combined activities of Rar1, Sgt1 and cytosolic Hsp90 are required to modulate R protein accumulation and signalling competence (Holt et al., 2005). Originally, Sgt1 was identified in yeast where it is involved in the regulation of the cell cycle and kinetochore assembly, and interacts with E3 ubiquitin ligases. Sgt1 is part of SCF E3 ubiquitin ligases via an interaction with SKP1 (Kitagawa et al., 1999). SCF E3 ligase complexes target proteins for degradation by the 26S proteasome (Willems et al., 2004). The SCF complex can associate with the COP9 signalosome (Lyapina et al., 2001; Schwechheimer et al., 2001) and interactions of COP9 and SCF subunits with either Sgt1 or Rar1 have been demonstrated in planta (Azevedo et al., 2002; Liu et al., 2002). Silencing of subunits of the SCF complex or COP9 signalosome impaired resistance mediated by N (Liu et al., 2002). Hence, besides being a chaperone, Sgt1 could be involved in R protein-mediated signalling by targeting negative regulators for degradation.

Despite extensive efforts no proteins have been identified that directly interact with the NB-ARC domain of NB-LRR proteins. This could mean that the NB-ARC is only involved in intramolecular interactions. For the N-terminal domains of NB-LRR proteins however, quite a number of interactors have been identified. This proposed “downstream signalling” domain was found to bind most of the guardees mentioned before, which supports the involvement of this domain in Avr perception. Examples of an *Arabidopsis* guardee that interacts with the N-terminal domain of an R protein is the Ser/Thr kinase Pbs1 that interacts with the CC domain of the *Arabidopsis* CNL Rps5 (Shao et al., 2003). A tertiary complex with the elicitor AvrPphB has been shown, in which cleavage of Pbs1 leads to activation of the R protein Rps5 (Ade et al., 2007; Shao et al., 2003). Another example is the interaction of Rin4 with the CC domain of the CNL proteins Rpm1 and Rps2. In addition to the interaction with Rin4, the N-terminal domains of Rpm1 and Rpp5 (CC-NB-ARC part) also interact with an ortholog of TIP49 (Holt et al., 2002). TIP49a is part of the transcriptional machinery

and interacts with the TATA binding protein (TBP) complex. Reduction of Arabidopsis TIP49a mRNA levels revealed that it does not affect Rpm1 function but it acts as a negative regulator of Rpp5 (Holt et al., 2002).
Another example of indirect Avr binding is provided by the TNL protein N of tobacco, that binds the Avr protein via NRIP1 (Caplan et al., 2008). In tomato, the guardee Pto interacts not only with the SD domain of CNL Prf and with AvrPto (Mucyn et al., 2006), but also with a set of plant proteins called Pto interacting proteins or Pti's. Pti-1 is a Ser/Thr kinase related to Pto (Zhou et al., 1995). Interestingly, Pti-4, -5 and -6 turned out to be ethylene responsive transcription factors that bind specifically to the GCC box in the promoter regions of a large number of genes encoding 'pathogenesis-related' (PR) proteins (Zhou et al., 1997; Gu et al., 2002).

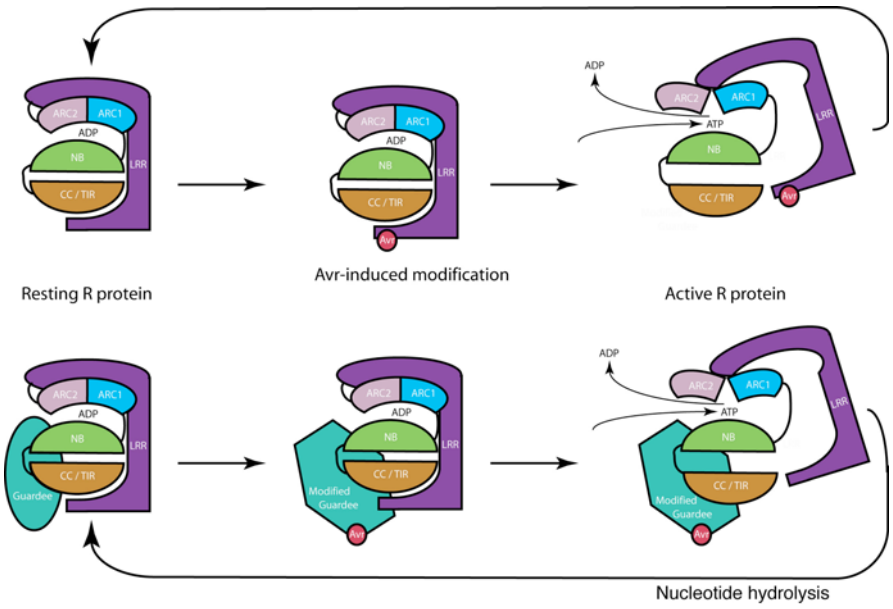

Figure 3
A current model for NB-LRR R protein function and activation. (A) Direct Avr-interaction model. In the absence of a pathogen, the NB-LRR protein is in the ADP-bound resting state. Upon binding of the Avr protein, the interaction between the LRR and the ARC1 and 2 is altered (transition state), resulting in nucleotide exchange and a different conformation of the protein. This altered ATP-bound conformation represents the active state of the NB-LRR protein. Hydrolysis of ATP returns the protein into its resting state. (B) Guard model. Rather than direct binding to the Avr protein modifies a guardee bound to the N-terminus. This modification is detected by the LRR altering its interaction with the ARC1 and 2.

Although some NB-LRR proteins have been shown to associate with membranes structures, the interactions described above provide a direct link between R proteins and regulation of gene expression. An indirect link between R proteins and the nucleus is provided by Rx. Two research groups independently identified RanGAP as an interactor of the Rx N-terminus (W. I. L. Tameling and D. C. Baulcombe and M.

Sacco and P. Moffett, personal communication). In mammalian cells, RanGAP associates with RAN, a Ras-related small GTPase that has an important function in nucleo-cytoplasmic trafficking and is part of a nuclear cargo-importing complex at the nuclear envelope (Rose et al., 2004; Meier, 2006). In mammalian cells this complex is involved in the translocation of receptor-Hsp90-immunophilin complexes. The TPR-containing immunophilins (such as PP5) are required to link the heteromeric complex to a motor protein (such as dynein) for directional movement along microtubules towards the nuclear pores (Pratt et al., 2004). Interestingly, two components of the nuclear pore complex, the importin alpha homologue MOS6 (AtImpα3) and a nucleoporin 96 homologue MOS3-1, were recently identified in a suppressor screen to be required for the SNC1 phenotype (Palma et al., 2005; Zhang and Li, 2005). SNC1 is an ectopically activated NB-LRR protein that triggers constitutive activation of defence signalling (Zhang et al., 2003). A mos3-1 single mutant is compromised in both basal resistance and R protein mediated resistance (Zhang and Li, 2005).

Together, the data above imply that some R proteins may require nuclear localization for their function and could be directly involved in transcriptional regulation. Until now, nuclear localization has been reported for two TNL proteins, Rrs1 and N, which confer resistance to *Ralstonia solanacearum* in *Arabidopsis thaliana* and TMV in tobacco, respectively ((Deslandes et al., 2002) and S. P. Dinesh-Kumar, personal communication). Rrs1 is unique in that it bears a WRKY transcription factor domain at its C-terminus (Deslandes et al., 2002), providing a direct link between R protein function and transcription regulation. Activation of this R protein occurs upon binding to the Avr protein PopP2, and both proteins localize to the nucleus (Deslandes et al., 2003). On the other hand the N protein is present both in the cytoplasm and the nucleus, similar to its matching Avr protein the p50 helicase. Interestingly, nuclear localization is required for N function since equipping N and p50 with nuclear export signals reveals that disease resistance is only lost when the N protein is excluded from the nucleus and not when p50 is redirected to the cytoplasm. This observation indicates that N has a function in the nucleus, similar to RRS-1 (S. P. Dinesh-Kumar, personal communication).

An analogous type of activation was found for the prototypic animal counterpart of R proteins, the MHC class II transactivator CIITA (Steimle et al., 1993). Upon viral infection, CIITA is activated and translocated to the nucleus where it activates transcription by binding to DNA binding proteins that bind to MHC-II promoter regions (Masternak et al., 2000; Ting and Davis, 2005). Interestingly, both translocation and transactivation of CIITA require a functional NB subdomain (Harton et al., 1999). The ARC2 subdomain of CIITA adopts a winged-helix fold similar to that predicted in NB-LRR proteins (Albrecht and Takken, 2006). Such a structure is often found to be

characteristic of DNA-binding transcription factors, suggesting that both R proteins and CIITA might be directly involved in DNA binding (Albrecht and Takken, 2006). If NB-LRR proteins indeed act directly as transcriptional activators, it might explain the small number of putative downstream signalling partners that have been identified and the relatively large number of components from the transcriptional machinery among them (see below). Left aside that many putative transcription factors that bind R proteins in yeast 2-hybrid screens would have been discarded as autoactivators.
To find interactors for the membrane-spanning R proteins, the RLP class of R proteins, the cytoplasmic tail of Cf-9 has been used as bait in yeast two-hybrid screens. A thioredoxin homologue, CITRX (Cf-9 Interacting ThioRedoxin) was identified in this way as a negative regulator of Cf-9/Avr9 mediated cell death and defense responses (Rivas et al., 2004). Silencing of *CITRX* in tomato and *N. benthamiana* resulted in an accelerated Cf-9/Avr9-triggered HR accompanied by the induction of defense-related genes (Rivas et al., 2004). This interaction seems to be Cf-9 specific as no interaction was found in in vitro pull-downs with the related Cf-2 protein and Cf-2 function was not affected upon *CITRX* silencing (Rivas et al., 2004). Recently, the protein kinase ACIK1 (Avr9/Cf-9 Induced Kinase) was shown to interact with CITRX (Nekrasov et al., 2006). Intriguingly, silencing experiments suggested that this protein is a positive regulator of Cf-9/Avr9 function and is required for full Cf-9 disease resistance (Rowland et al., 2005).

Partners in R protein signalling

As detailed above, the fishing expeditions for R protein interactors thus far yielded only small numbers of components possibly involved in R protein signalling. In contrast, forward genetic screens using virus-induced gene silencing (VIGS) have been highly successful and identified a relatively large number of candidate genes. A VIGS screen of 2400 cDNAs from a normalized *Nicotiana benthamiana* cDNA library revealed that Pto-dependent HR was compromised in 3% of the cases (del Pozo et al., 2004). In a similar VIGS screen using 4992 cDNAs, HR was compromised in 1.6% of the cases (Lu et al., 2003). Alternative screens were performed with custom-made libraries made from cDNA-AFLP fragments that were selected based on their differential expression pattern upon Avr perception. To identify genes involved in Cf-4/Avr4-dependent HR, 192 cDNA-AFLP fragments were selected that are differentially expressed upon expression of an *Avr4* transgene. These fragments were subsequently used for VIGS in *N. benthamiana* and twenty of them were found to correspond to genes required for Cf-4/Avr4 mediated HR (Gabriëls et al., 2006). A similar approach using Cf-9/Avr9 induced genes resulted in the identification of four genes out of the tested 43 that affect Cf-9 mediated HR (Rowland et al., 2005).

Although these VIGS screens identified relatively large numbers of genes whose silencing suppresses HR, only for a small number silencing also abolishes disease resistance. For instance, only six of 79 candidates identified in one of the Pto screens are required for *Pto*-mediated resistance to *P. syringae* pv *tabaci,* three of them derived from *Hsp90* genes (Lu et al., 2003). Likewise, of the 20 gene fragments that affect Cf-4-mediated HR, only six are essential for resistance to *Cladosporium fulvum* (Gabriëls et al., 2006).

The set of genes that is required for resistance can be roughly divided into five groups. The first consists of chaperones such as Hsp90 that have also been identified in other studies as R-protein interactors (Lu et al., 2003; Gabriëls et al., 2006). The second group has been found in each screen and consists of ribosomal proteins such as L19 (Lu et al., 2003; Gabriëls et al., 2006). The third group consist of proteins that are likely to be involved in classic signalling pathways like MAP kinase cascades (Ekengren et al., 2003) and other pathways employing protein kinases like ACIK1 (Rowland et al., 2005). The fourth group contains proteins involved in protein degradation via the 26S proteasome. Besides Sgt1, other examples are the two U-box proteins ACRE74/*Nt*CMPG1 and ACRE276 that are both ubiquitin E3 ligases (Gonzalez-Lamothe et al., 2006; Yang et al., 2006) and ACRE189, an F-box protein (Rowland et al., 2005). The fifth and last group consists of two NB-LRR proteins. The CNL NRG1 (N-requirement gene 1) appears to be specifically required for *N* function and not for other NB-LRR proteins (Peart et al., 2005). This indicates that CNL proteins may not only act as individual resistance proteins, but might also be involved in resistance mediated by TNL proteins. Similarly, the CNL NRC-1 (NB-LRR protein Required for Cf-4 function) was found to be required for Cf-4 and Cf-9 mediated resistance (Gabriëls et al., 2007). NRC-1 has also been shown to be required for HR mediated by the R proteins Prf, Rx and Mi-1.2 and for function of the RLK *Le*Eix (Gabriëls et al., 2007). The presence of more than one R protein-like factor in a single resistance pathway could indicate that resistance pathways are interwoven. Additional support for crosstalk of eLRR, TNL and CNL pathways comes from genetic studies. For instance, Cf-4 depends on EDS1, a lipase-like protein mainly required for resistance responses mediated by TNL proteins (Wiermer et al., 2005), hinting to the presence of a TNL in this pathway as well. The function of the TNL N was also found to be dependent on EDS1, while the CNL NRG1, which acts downstream of N, is not. Both are dependent on Sgt1, again showing the general importance of this protein for R signalling. Together, these data show that several resistance proteins require downstream NB-LRRs for cell death signalling (Peart et al., 2005).

Model for R protein function

Based on the data above a “generalised” model for the function of NB-LRR R proteins can be proposed (Figure 3). In the resting state R proteins are autoinhibited, and the NB-ARC domain interacts with both the LRR and the CC or TIR domains. This complex is molded and/or preserved in a signalling competent state by its interaction with the chaperone Hsp90 and one or more co-chaparones such as Sgt-1, Rar-1 and PP5. Perturbation of the LRR domain (either by mutations or by Avr recognition) allows transition to the active state. The Avrs can be recognized either directly, possibly by direct binding to the LRR, or indirectly by modification of a guardee that is bound to the N-terminus (CC/TIR). In the latter case, the modification of the guardee could be detected by the LRR. Such a model for indirect recognition is supported by the current data on the TNL protein N. The Avr protein (p50 helicase) is bound via an unkown protein to the TIR domain (S. P. Dinesh-Kumar, personal communication). In vitro, p50 can also interact directly with the LRR domain of N (Ueda et al., 2006). One intepretation of these data is that the LRR domain recognizes binding of p50 to the ‘guardee’ bound to the TIR domain. Conceivably, after (in)direct Avr recognition by the LRR its interaction with the ARC2 subdomain changes, resulting in a different conformation of the NB-ARC that allows nucleotide exchange (Tameling et al., 2006) or hydrolysis (Ueda et al., 2006). The exact intramolecular conformation at this stage is still unknown (e.g. dissociation of the N-terminus) and could very well differ between various R proteins (Moffett et al., 2002; Leister et al., 2005; Rairdan and Moffett, 2006; Ueda et al., 2006). The activated R protein either directly recruits downstream signalling components or could require oligomerization first, in analogy to the “wheel-of-death”. Downstream signalling components could very well be transcriptional regulators, as at least some R proteins need to be nuclearly localized for their function and one of the earliest defence signalling responses is changes in gene expression (Eulgem, 2005).

Hydrolysis of ATP by the NB-ARC could return activated R proteins to the autoinhibited state. Such a mechanism would explain why hydrolysis mutants are autoactivating, and why defence signalling is only initiated when the Avr concentration in the cell is sufficiently high. Future research will put this model to the test and reveal whether it applies to all or a subset of NB-LRR proteins.

Acknowledgements

The authors would like to acknowledge Wladimir Tameling, David Baulcombe, Savithramma Dinesh-Kumar, Greg Rairdan, Melanie Sacco, Peter Moffett and Roger Innes for sharing their data before publication. We are grateful to Martijn Rep for providing critical review and helpful comments on this manuscript. GvO is supported by the Research Council for Earth and Life Sciences (ALW) with financial aid from

the Netherlands Organization for Scientific Research (NWO). HB is supported by Netherlands Organization for Scientific Research (NWO VENI grant 863.04.018).

References

Abramovitch, R.B., Anderson, J.C., and Martin, G.B. (2006). Bacterial elicitation and evasion of plant innate immunity. Nat Rev Mol Cell Biol **7,** 601-611.

Abramovitch, R.B., Kim, Y.J., Chen, S., Dickman, M.B., and Martin, G.B. (2003). *Pseudomonas* type III effector AvrPtoB induces plant disease susceptibility by inhibition of host programmed cell death. EMBO J **22,** 60-69.

Ade, J., DeYoung, B.J., Golstein, C., and Innes, R.W. (2007). Indirect activation of a plant nucleotide binding site-leucine-rich repeat protein by a bacterial protease. Proceedings of the National Academy of Sciences of the United States of America **104,** 2531-2536.

Albrecht, M., and Takken, F.L.W. (2006). Update on the domain architectures of NLRs and R proteins. Biochem Biophys Res Commun **339,** 459-462.

Armstrong, M.R., Whisson, S.C., Pritchard, L., Bos, J.I.B., Venter, E., Avrova, A.O., Rehmany, A.P., Bohme, U., Brooks, K., Cherevach, I., Hamlin, N., White, B., Fraser, A., Lord, A., Quail, M.A., Churcher, C., Hall, N., Berriman, M., Huang, S., Kamoun, S., Beynon, J.L., and Birch, P.R.J. (2005). An ancestral oomycete locus contains late blight avirulence gene *Avr3a*, encoding a protein that is recognized in the host cytoplasm. Proc Natl Acad Sci USA **102,** 7766-7771.

Austin, M.J., Muskett, P., Kahn, K., Feys, B.J., Jones, J.D.G., and Parker, J.E. (2002). Regulatory role of *SGT1* in early *R* gene-mediated plant defenses. Science **295,** 2077-2080.

Axtell, M.J., Chisholm, S.T., Dahlbeck, D., and Staskawicz, B.J. (2003). Genetic and molecular evidence that the Pseudomonas syringae type III effector protein AvrRpt2 is a cysteine protease. Mol Microbiol **49,** 1537-1546.

Axtell, M.J., McNellis, T.W., Mudgett, M.B., Hsu, C.S., and Staskawicz, B.J. (2001). Mutational analysis of the Arabidopsis RPS2 disease resistance gene and the corresponding Pseudomonas syringae avrRpt2 avirulence gene. Mol Plant Microbe Interact **14,** 181-188.

Azevedo, C., Sadanandom, A., Kitagawa, K., Freialdenhoven, A., Shirasu, K., and Schulze-Lefert, P. (2002). The RAR1 interactor SGT1, an essential component of *R* gene-triggered disease resistance. Science **295,** 2073-2076.

Azevedo, C., Betsuyaku, S., Peart, J., Takahashi, A., Noel, L., Sadanandom, A., Casais, C., Parker, J., and Shirasu, K. (2006). Role of SGT1 in resistance protein accumulation in plant immunity. EMBO J **25,** 2007-2016.

Bai, J., Pennill, L.A., Ning, J., Lee, S.W., Ramalingam, J., Webb, C.A., Zhao, B., Sun, Q., Nelson, J.C., Leach, J.E., and Hulbert, S.H. (2002). Diversity in nucleotide binding site-leucine-rich repeat genes in cereals. Genome Res **12,** 1871-1884.

Ballvora, A., Ercolano, M.R., Weiss, J., Meksem, K., Bormann, C.A., Oberhagemann, P., Salamini, F., and Gebhardt, C. (2002). The *R1* gene for potato resistance to late blight (*Phytophthora infestans*) belongs to the leucine zipper/NBS/LRR class of plant resistance genes. Plant J **30,** 361-371.

Bendahmane, A., Kohn, B.A., Dedi, C., and Baulcombe, D.C. (1995). The coat protein of potato virus X is a strain-specific elicitor of *Rx*1-mediated virus resistance in potato. Plant J **8,** 933-941.

Bendahmane, A., Querci, M., Kanyuka, K., and Baulcombe, D.C. (2000). *Agrobacterium* transient expression system as a tool for the isolation of disease resistance genes: application to the *Rx2* locus in potato. Plant J **21,** 73-81.

Bendahmane, A., Farnham, G., Moffett, P., and Baulcombe, D.C. (2002). Constitutive gain-of-function mutants in a nucleotide binding site-leucine rich repeat protein encoded at the *Rx* locus of potato. Plant J **32,** 195-204.

Bonas, U., Conrads-Strauch, J., and Balbo, I. (1993). Resistance in tomato to *Xanthomonas campestris* pv *vesicatoria* is determined by alleles of the pepper-specific avirulence gene *avrBs3*. Mol Gen Genet **238,** 261-269.

Bos, J.I.B., Kanneganti, T.D., Young, C., Cakir, C., Huitema, E., Win, J., Armstrong, M.R., Birch, P.R.J., and Kamoun, S. (2006). The C-terminal half of Phytophthora infestans RXLR effector AVR3a is sufficient to trigger R3a-mediated hypersensitivity and suppress INF1-induced cell death in Nicotiana benthamiana. Plant J **48,** 165-176.

Brandwagt, B.F., Mesbah, L.A., Takken, F.L.W., Laurent, P.L., Kneppers, T.J.A., Hille, J., and Nijkamp, H.J.J. (2000). A longevity assurance gene homolog of tomato mediates resistance to *Alternaria alternata* f. sp. *lycopersici* toxins and fumonisin B1. Proc Natl Acad Sci USA **97,** 4961-4966.

Brommonschenkel, S.H., Frary, A., Frary, A., and Tanksley, S.D. (2000). The broad-spectrum tospovirus resistance gene *Sw-5* of tomato is a homolog of the root-knot nematode resistance gene *Mi*. Mol Plant Microbe Interact **13,** 1130-1138.

Buttner, D., and Bonas, U. (2006). Who comes first? How plant pathogenic bacteria orchestrate type III secretion. Curr Opin Microbiol **9,** 193-200.

Calder, V.L., and Palukaitis, P. (1992). Nucleotide sequence analysis of the movement genes of resistance breaking strains of tomato mosaic virus. J Gen Virol **73,** 165-168.

Caplan, J.L., Mamillapalli, P., Burch-Smith, T.M., Czymmek, K., and Dinesh-Kumar, S.P. (2008). Chloroplastic protein NRIP1 mediates innate immune receptor recognition of a viral effector. Cell **132,** 449-462.

Catanzariti, A.M., Dodds, P.N., Lawrence, G.J., Ayliffe, M.A., and Ellis, J.G. (2006). Haustorially expressed secreted proteins from flax rust are highly enriched for avirulence elicitors. Plant Cell **18,** 243-256.

Chinchilla, D., Bauer, Z., Regenass, M., Boller, T., and Felix, G. (2006). The Arabidopsis receptor kinase FLS2 binds flg22 and determines the specificity of flagellin perception. Plant Cell **18,** 465-476.

Chisholm, S.T., Coaker, G., Day, B., and Staskawicz, B.J. (2006). Host-microbe interactions: shaping the evolution of the plant immune response. Cell **124,** 803-814.

Dangl, J.L., and Jones, J.D.G. (2001). Plant pathogens and integrated defence responses to infection. Nature **411,** 826-833.

de la Fuente van Bentem, S., Vossen, J.H., de Vries, K.J., van Wees, S., Tameling, W.I.L., Dekker, H.L., de Koster, C.G., Haring, M.A., Takken, F.L.W., and Cornelissen, B.J.C. (2005). Heat shock protein 90 and its co-chaperone protein phosphatase 5 interact with distinct regions of the tomato I-2 disease resistance protein. Plant J **43,** 284-298.

del Pozo, O., Pedley, K.F., and Martin, G.B. (2004). MAPKKKalpha is a positive regulator of cell death associated with both plant immunity and disease. EMBO J **23,** 3072-3082.

Deslandes, L., Olivier, J., Theulieres, F., Hirsch, J., Feng, D.X., Bittner-Eddy, P., Beynon, J., and Marco, Y. (2002). Resistance to *Ralstonia solanacearum* in *Arabidopsis thaliana* is conferred by the recessive *RRS1-R* gene, a member of a novel family of resistance genes. Proc Natl Acad Sci USA **99,** 2404-2409.

Deslandes, L., Olivier, J., Peeters, N., Feng, D.X., Khounlotham, M., Boucher, C., Somssich, I., Genin, S., and Marco, Y. (2003). Physical interaction between RRS1-R, a protein conferring resistance to bacterial wilt, and PopP2, a type III effector targeted to the plant nucleus. Proc Natl Acad Sci USA **100,** 8024-8029.

Di Matteo, A., Federici, L., Mattei, B., Salvi, G., Johnson, K.A., Savino, C., De Lorenzo, G., Tsernoglou, D., and Cervone, F. (2003). The crystal structure of polygalacturonase-inhibiting protein (PGIP), a leucine-rich repeat protein involved in plant defense. Proc Natl Acad Sci USA **100,** 10124-10128.

Dinesh-Kumar, S.P., Tham, W.H., and Baker, B.J. (2000). Structure-function analysis of the tobacco mosaic virus resistance gene N. Proc Natl Acad Sci USA **97,** 14789-14794.

Dixon, M.S., Hatzixanthis, K., Jones, D.A., Harrison, K., and Jones, J.D.G. (1998). The tomato *Cf-5* disease resistance gene and six homologs show pronounced allelic variation in leucine-rich repeat copy number. Plant Cell **10,** 1915-1925.

Dixon, M.S., Jones, D.A., Keddie, J.S., Thomas, C.M., Harrison, K., and Jones, J.D.G. (1996). The tomato *Cf-2* disease resistance locus comprises two functional genes encoding leucine-rich repeat proteins. Cell **84,** 451-459.

Dodds, P.N., Lawrence, G.J., Catanzariti, A.M., Teh, T., Wang, C.I.A., Ayliffe, M.A., Kobe, B., and Ellis, J.G. (2006). Direct protein interaction underlies gene-for-gene specificity and coevolution of the flax resistance genes and flax rust avirulence genes. Proc Natl Acad Sci USA **103,** 8888-8893.

Ekengren, S.K., Liu, Y., Schiff, M., Dinesh-Kumar, S.P., and Martin, G.B. (2003). Two MAPK cascades, NPR1, and TGA transcription factors play a role in Pto-mediated disease resistance in tomato. Plant J **36,** 905-917.

Ellis, J.G., Lawrence, G.J., Luck, J.E., and Dodds, P.N. (1999). Identification of regions in alleles of the flax rust resistance gene *L* that determine differences in gene-for-gene specificity. Plant Cell **11,** 495-506.

Enkhbayar, P., Kamiya, M., Osaki, M., Matsumoto, T., and Matsushima, N. (2004). Structural principles of leucine-rich repeat (LRR) proteins. Proteins **54,** 394-403.

Erickson, F.L., Holzberg, S., Calderon-Urrea, A., Handley, V., Axtell, M., Corr, C., and Baker, B. (1999). The helicase domain of the TMV replicase proteins induces the *N*-mediated defence response in tobacco. Plant J **18,** 67-75.

Ernst, K., Kumar, A., Kriseleit, D., Kloos, D.U., Phillips, M.S., and Ganal, M.W. (2002). The broad-spectrum potato cyst nematode resistance gene (*Hero*) from tomato is the only member of a large gene family of NBS-LRR genes with an unusual amino acid repeat in the LRR region. Plant J **31,** 127-136.

Eulgem, T. (2005). Regulation of the Arabidopsis defense transcriptome. Trends Plant Sci **10,** 71-78.

Federici, L., Di Matteo, A., Fernandez-Recio, J., Tsernoglou, D., and Cervone, F. (2006). Polygalacturonase inhibiting proteins: players in plant innate immunity? Trends Plant Sci **11,** 65-70.

Flor, H.H. (1942). Inheritance of pathogenicity in *Melampsora lini.* Phytopathol **32,** 653-669.

Gabriëls, S.H.E.J., Takken, F.L.W., Vossen, J.H., de Jong, C.F., Liu, Q., Turk, S.C., Wachowski, L.K., Peters, J., Witsenboer, H.M., de Wit, P.J.G.M., and Joosten, M.H.A.J. (2006). cDNA-AFLP combined with functional analysis reveals novel genes involved in the hypersensitive response. Mol Plant Microbe Interact **19,** 567-576.

Gabriëls, S.H.E.J., Vossen, J.H., Ekengren, S.K., van Ooijen, G., Abd-El-Haliem, A.M., van den Berg, G.C., Rainey, D.Y., Martin, G.B., Takken, F.L.W., de Wit, P.J.G.M., and Joosten, M.H.A.J. (2007). An NB-LRR protein required for HR signalling mediated by both extra- and intracellular resistance proteins. Plant J **50,** 14-28.

Gomez-Gomez, L., and Boller, T. (2000). FLS2: an LRR receptor-like kinase involved in the perception of the bacterial elicitor flagellin in Arabidopsis. Mol Cell **5,** 1003-1011.

Gonzalez-Lamothe, R., Tsitsigiannis, D.I., Ludwig, A.A., Panicot, M., Shirasu, K., and Jones, J.D.G. (2006). The U-box protein CMPG1 is required for efficient activation of defense mechanisms triggered by multiple resistance genes in tobacco and tomato. Plant Cell **18,** 1067-1083.

Grant, S.R., Fisher, E.J., Chang, J.H., Mole, B.M., and Dangl, J.L. (2006). Subterfuge and Manipulation: Type III Effector Proteins of Phytopathogenic Bacteria. Annu Rev Microbiol **60,** 425-449.

Gu, Y.Q., Wildermuth, M.C., Chakravarthy, S., Loh, Y.T., Yang, C., He, X., Han, Y., and Martin, G.B. (2002). Tomato transcription factors pti4, pti5, and pti6 activate defense responses when expressed in Arabidopsis. Plant Cell **14,** 817-831.

Hanson, P.I., and Whiteheart, S.W. (2005). AAA+ proteins: have engine, will work. Nature Rev **6,** 519-529.

Harton, J.A., Cressman, D.E., Chin, K.C., Der, C.J., and Ting, J.P.-Y. (1999). GTP binding by class II transactivator: role in nuclear import. Science **285,** 1402-1405.

Holt, B.F., 3rd, Belkhadir, Y., and Dangl, J.L. (2005). Antagonistic control of disease resistance protein stability in the plant immune system. Science **309,** 929-932.

Holt, B.F., 3rd, Boyes, D.C., Ellerstrom, M., Siefers, N., Wiig, A., Kauffman, S., Grant, M.R., and Dangl, J.L. (2002). An evolutionarily conserved mediator of plant disease resistance gene function is required for normal Arabidopsis development. Dev Cell **2,** 807-817.

Howles, P., Lawrence, G., Finnegan, J., McFadden, H., Ayliffe, M., Dodds, P., and Ellis, J. (2005). Autoactive alleles of the flax *L6* rust resistance gene induce non-race-specific rust resistance associated with the hypersensitive response. Mol Plant Microbe Interact **18,** 570-582.

Huang, S., van der Vossen, E.A.G., Kuang, H., Vleeshouwers, V.G.A.A., Zhang, N., Borm, T.J.A., van Eck, H.J., Baker, B., Jacobsen, E., and Visser, R.G.F. (2005). Comparative genomics enabled the isolation of the *R3a* late blight resistance gene in potato. Plant J **42,** 251-261.

Hubert, D.A., Tornero, P., Belkhadir, Y., Krishna, P., Takahashi, A., Shirasu, K., and Dangl, J.L. (2003). Cytosolic HSP90 associates with and modulates the Arabidopsis RPM1 disease resistance protein. EMBO J **22,** 5679-5689.

Hwang, C.F., and Williamson, V.M. (2003). Leucine-rich repeat-mediated intramolecular interactions in nematode recognition and cell death signaling by the tomato resistance protein Mi. Plant J. **34,** 585-593.

Hwang, C.F., Bhakta, A.V., Truesdell, G.M., Pudlo, W.M., and Williamson, V.M. (2000). Evidence for a role of the N terminus and leucine-rich repeat region of the *Mi* gene product in regulation of localized cell death. Plant Cell **12,** 1319-1329.

Inohara, N., Ogura, Y., and Nunez, G. (2002). Nods: a family of cytosolic proteins that regulate the host response to pathogens. Curr Opin Microbiol **5,** 76-80.

Janjusevic, R., Abramovitch, R.B., Martin, G.B., and Stebbins, C.E. (2006). A bacterial inhibitor of host programmed cell death defenses is an E3 ubiquitin ligase. Science **311,** 222-226.

Jia, Y., McAdams, S.A., Bryan, G.T., Hershey, H.P., and Valent, B. (2000). Direct interaction of resistance gene and avirulence gene products confers rice blast resistance. EMBO J **19,** 4004-4014.

Jones, D.A., Thomas, C.M., Hammond-Kosack, K.E., Balint-Kurti, P.J., and Jones, J.D.G. (1994). Isolation of the tomato *Cf-9* gene for resistance to *Cladosporium fulvum* by transposon tagging. Science **266,** 789-793.

Jones, J.D.G., and Dangl, J.L. (2006). The plant immune system. Nature **444,** 323-329.

Joosten, M.H.A.J., and De Wit, P.J.G.M. (1999). The tomato-*Cladosporium fulvum* interaction: a versatile experimental system to study plant-pathogen interactions. Annu Rev Phytopathol **37,** 355-367.

Joosten, M.H.A.J., Cozijnsen, T.J., and De Wit, P.J.G.M. (1994). Host resistance to a fungal tomato pathogen lost by a single base-pair change in an avirulence gene. Nature **367,** 384-386.

Kaloshian, I., and Walling, L.L. (2005). Hemipterans as plant pathogens. Annu Rev Phytopathol **43,** 491-521.

Kamoun, S. (2006). A catalogue of the effector secretome of plant pathogenic oomycetes. Annu Rev Phytopathol **44,** 41-60

Kawchuk, L.M., Hachey, J., Lynch, D.R., Kulcsar, F., van Rooijen, G., Waterer, D.R., Robertson, A., Kokko, E., Byers, R., Howard, R.J., Fischer, R., and Prufer, D. (2001). Tomato Ve disease resistance genes encode cell surface-like receptors. Proc Natl Acad Sci USA **98,** 6511-6515.

Kay, S., Boch, J., and Bonas, U. (2005). Characterization of AvrBs3-like effectors from a *Brassicaceae* pathogen reveals virulence and avirulence activities and a protein with a novel repeat architecture. Mol Plant Microbe Interact **18,** 838-848.

Kim, H.E., Du, F., Fang, M., and Wang, X. (2005a). Formation of apoptosome is initiated by cytochrome c-induced dATP hydrolysis and subsequent nucleotide exchange on Apaf-1. Proc Natl Acad Sci USA **102,** 17545-17550.

Kim, H.S., Desveaux, D., Singer, A.U., Patel, P., Sondek, J., and Dangl, J.L. (2005b). The Pseudomonas syringae effector AvrRpt2 cleaves its C-terminally acylated target, RIN4, from Arabidopsis membranes to block RPM1 activation. Proc Natl Acad Sci USA **102,** 6496-6501.

Kim, Y.J., Lin, N.C., and Martin, G.B. (2002). Two distinct *Pseudomonas* effector proteins interact with the Pto kinase and activate plant immunity. Cell **109,** 589-598.

Kitagawa, K., Skowyra, D., Elledge, S.J., Harper, J.W., and Hieter, P. (1999). *SGT1* encodes an essential component of the yeast kinetochore assembly pathway and a novel subunit of the SCF ubiquitin ligase complex. Mol Cell **4,** 21-33.

Kobe, B., and Kajava, A.V. (2001). The leucine-rich repeat as a protein recognition motif. Curr Opin Struct Biol **11,** 725-732.

Kolade, O.O., Bamford, V.A., Ancillo Anton, G., Jones, J.D.G., Vera, P., and Hemmings, A.M. (2006). In vitro characterization of the cysteine-rich capping domains in a plant leucine rich repeat protein. Biochim Biophys Acta **1764,** 1043-1053.

la Cour, T., Kiemer, L., Molgaard, A., Gupta, R., Skriver, K., and Brunak, S. (2004). Analysis and prediction of leucine-rich nuclear export signals. Protein Eng Des Sel **17,** 527-536.

Lanfermeijer, F.C., Warmink, J., and Hille, J. (2005). The products of the broken *Tm-2* and the durable *Tm-2(2)* resistance genes from tomato differ in four amino acids. J Exp Bot **56,** 2925-2933.

Lanfermeijer, F.C., Dijkhuis, J., Sturre, M.J.G., de Haan, P., and Hille, J. (2003). Cloning and characterization of the durable tomato mosaic virus resistance gene Tm-2(2) from *Lycopersicon esculentum*. Plant Mol Biol **52,** 1037-1049.

Leckie, F., Mattei, B., Capodicasa, C., Hemmings, A., Nuss, L., Aracri, B., De Lorenzo, G., and Cervone, F. (1999). The specificity of polygalacturonase-inhibiting protein (PGIP): a single amino acid substitution in the solvent-exposed beta-strand/beta-turn region of the leucine-rich repeats (LRRs) confers a new recognition capability. EMBO J. **18,** 2352-2363.

Leipe, D.D., Koonin, E.V., and Aravind, L. (2004). STAND, a class of P-loop NTPases including animal and plant regulators of programmed cell death: multiple, complex domain architectures, unusual phyletic patterns, and evolution by horizontal gene transfer. J Mol Biol **343,** 1-28.

Leister, R.T., Dahlbeck, D., Day, B., Li, Y., Chesnokova, O., and Staskawicz, B.J. (2005). Molecular genetic evidence for the role of *SGT1* in the intramolecular complementation of Bs2 protein activity in *Nicotiana benthamiana*. Plant Cell **17,** 1268-1278.

Liu, Y., Schiff, M., Serino, G., Deng, X.W., and Dinesh-Kumar, S.P. (2002). Role of SCF ubiquitin-ligase and the COP9 signalosome in the *N* gene-mediated resistance response to *Tobacco mosaic virus*. Plant Cell **14,** 1483-1496.

Liu, Y., Burch-Smith, T., Schiff, M., Feng, S., and Dinesh-Kumar, S.P. (2004). Molecular chaperone Hsp90 associates with resistance protein N and its signaling proteins SGT1 and Rar1 to modulate an innate immune response in plants. J Biol Chem **279,** 2101-2108.

Lu, R., Malcuit, I., Moffett, P., Ruiz, M.T., Peart, J., Wu, A.J., Rathjen, J.P., Bendahmane, A., Day, L., and Baulcombe, D.C. (2003). High throughput virus-induced gene silencing implicates heat shock protein 90 in plant disease resistance. EMBO J. **22,** 5690-5699.

Luck, J.E., Lawrence, G.J., Dodds, P.N., Shepherd, K.W., and Ellis, J.G. (2000). Regions outside of the leucine-rich repeats of flax rust resistance proteins play a role in specificity determination. Plant Cell **12,** 1367-1377.

Luderer, R., Takken, F.L.W., Wit, P.J.G.M., and Joosten, M.H.A.J. (2002). *Cladosporium fulvum* overcomes *Cf-2*-mediated resistance by producing truncated AVR2 elicitor proteins. Mol Microbiol **45,** 875-884.

Lyapina, S., Cope, G., Shevchenko, A., Serino, G., Tsuge, T., Zhou, C., Wolf, D.A., Wei, N., Shevchenko, A., and Deshaies, R.J. (2001). Promotion of NEDD-CUL1 conjugate cleavage by COP9 signalosome. Science **292,** 1382-1385.

Mackey, D., Holt, B.F., Wiig, A., and Dangl, J.L. (2002). RIN4 interacts with *Pseudomonas syringae* type III effector molecules and is required for RPM1-mediated resistance in *Arabidopsis*. Cell **108,** 743-754.

Martin, G.B., Bogdanove, A.J., and Sessa, G. (2003). Understanding the functions of plant disease resistance proteins. Annu Rev Plant Biol **54,** 23-61.

Martinez de Ilarduya, O., Nombela, G., Hwang, C.F., Williamson, V.M., Muniz, M., and Kaloshian, I. (2004). *Rme1* is necessary for *Mi-1*-mediated resistance and acts early in the resistance pathway. Mol Plant Microbe Interact **17,** 55-61.

Masternak, K., Muhlethaler-Mottet, A., Villard, J., Zufferey, M., Steimle, V., and Reith, W. (2000). CIITA is a transcriptional coactivator that is recruited to MHC class II promoters by multiple synergistic interactions with an enhanceosome complex. Genes Dev **14,** 1156-1166.

McHale, L., Tan, X., Koehl, P., and Michelmore, R.W. (2006). Plant NBS-LRR proteins: adaptable guards. Genome Biol **7,** 212.

Meier, I. (2006). Composition of the plant nuclear envelope: theme and variations J Exp Bot **58,** 27-34

Mestre, P., and Baulcombe, D.C. (2006). Elicitor-mediated oligomerization of the tobacco N disease resistance protein. Plant Cell **18,** 491-501.

Meyers, B.C., Kozik, A., Griego, A., Kuang, H., and Michelmore, R.W. (2003). Genome-wide analysis of NBS-LRR-encoding genes in Arabidopsis. Plant Cell **15,** 809-834.

Meyers, B.C., Dickerman, A.W., Michelmore, R.W., Sivaramakrishnan, S., Sobral, B.W., and Young, N.D. (1999). Plant disease resistance genes encode members of an ancient and diverse protein family within the nucleotide-binding superfamily. Plant J **20,** 317-332.

Meyers, B.C., Chin, D.B., Shen, K.A., Sivaramakrishnan, S., Lavelle, D.O., Zhang, Z., and Michelmore, R.W. (1998). The major resistance gene cluster in lettuce is highly duplicated and spans several megabases. Plant Cell **10,** 1817-1832.

Milligan, S.B., Bodeau, J., Yaghoobi, J., Kaloshian, I., Zabel, P., and Williamson, V.M. (1998a). The root knot nematode resistance gene *Mi* from tomato is a member of the leucine zipper, nucleotide binding, leucine-rich repeat family of plant genes. Plant Cell **10,** 1307-1319.

Milligan, S.B., Bodeau, J., Yaghoobi, J., Kaloshian, I., Zabel, P., and Williamson, V.M. (1998b). The root knot nematode resistance gene *Mi* from tomato is a member of the leucine zipper, nucleotide binding, leucine-rich repeat family of plant genes. Plant Cell **10,** 1307-1319.

Moffett, P., Farnham, G., Peart, J., and Baulcombe, D.C. (2002). Interaction between domains of a plant NBS-LRR protein in disease resistance-related cell death. EMBO J **21,** 4511-4519.

Mondragon-Palomino, M., Meyers, B.C., Michelmore, R.W., and Gaut, B.S. (2002). Patterns of positive selection in the complete NBS-LRR gene family of *Arabidopsis thaliana*. Genome Res **12,** 1305-1315.

Mucyn, T.S., Clemente, A., Andriotis, V.M.E., Balmuth, A.L., Oldroyd, G.E.D., Staskawicz, B.J., and Rathjen, J.P. (2006). The tomato NBARC-LRR protein Prf Interacts with Pto kinase in vivo to regulate specific plant immunity. Plant Cell **18**, 2792-2806

Mudgett, M.B. (2005). New insights to the function of phytopathogenic bacterial type III effectors in plants. Annu Rev Plant Biol **56,** 509-531.

Nekrasov, V., Ludwig, A.A., and Jones, J.D.G. (2006). CITRX thioredoxin is a putative adaptor protein connecting Cf-9 and the ACIK1 protein kinase during the Cf-9/Avr9- induced defence response. FEBS Lett **580,** 4236-4241.

Noel, L., Moores, T.L., van der Biezen, E.A., Parniske, M., Daniels, M.J., Parker, J.E., and Jones, J.D.G. (1999). Pronounced intraspecific haplotype divergence at the *RPP5* complex disease resistance locus of Arabidopsis. Plant Cell **11,** 2099-2112.

Nombela, G., Williamson, V.M., and Muniz, M. (2003). The root-knot nematode resistance gene *Mi-1.2* of tomato is responsible for resistance against the whitefly *Bemisia tabaci*. Mol Plant Microbe Interact **16,** 645-649.

Nürnberger, T., Brunner, F., Kemmerling, B., and Piater, L. (2004). Innate immunity in plants and animals: striking similarities and obvious differences. Immunol Rev **198,** 249-266.

Ori, N., Eshed, Y., Paran, I., Presting, G., Aviv, D., Tanksley, S., Zamir, D., and Fluhr, R. (1997). The *I2C* family from the wilt disease resistance locus *I2* belongs to the nucleotide binding, leucine-rich repeat superfamily of plant resistance genes. Plant Cell **9,** 521-532.

Orth, K., Xu, Z., Mudgett, M.B., Bao, Z.Q., Palmer, L.E., Bliska, J.B., Mangel, W.F., Staskawicz, B., and Dixon, J.E. (2000). Disruption of signaling by Yersinia effector YopJ, a ubiquitin-like protein protease. Science **290,** 1594-1597.

Paal, J., Henselewski, H., Muth, J., Meksem, K., Menendez, C.M., Salamini, F., Ballvora, A., and Gebhardt, C. (2004). Molecular cloning of the potato *Gro1-4* gene conferring resistance to pathotype Ro1 of the root cyst nematode *Globodera rostochiensis*, based on a candidate gene approach. Plant J **38,** 285-297.

Palma, K., Zhang, Y., and Li, X. (2005). An importin alpha homolog, MOS6, plays an important role in plant innate immunity. Curr Biol **15,** 1129-1135.

Pan, Q., Liu, Y.S., Budai Hadrian, O., Sela, M., Carmel Goren, L., Zamir, D., and Fluhr, R. (2000). Comparative genetics of nucleotide binding site-leucine rich repeat resistance gene homologues in the genomes of two dicotyledons: tomato and *Arabidopsis*. Genetics **155,** 309-322.

Panter, S.N., Hammond-Kosack, K.E., Harrison, K., Jones, J.D.G., and Jones, D.A. (2002). Developmental control of promoter activity is not responsible for mature onset of *Cf-9B*-mediated resistance to leaf mold in tomato. Mol Plant Microbe Interact **15,** 1099-1107.

Parniske, M., Hammond-Kosack, K.E., Golstein, C., Thomas, C.M., Jones, D.A., Harrison, K., Wulff, B.B.H., and Jones, J.D.G. (1997). Novel disease resistance specificities result from sequence exchange between tandemly repeated genes at the *Cf-4/9* locus of tomato. Cell **91,** 821-832.

Peart, J.R., Mestre, P., Lu, R., Malcuit, I., and Baulcombe, D.C. (2005). NRG1, a CC-NB-LRR Protein, together with N, a TIR-NB-LRR Protein, Mediates Resistance against Tobacco Mosaic Virus. Curr Biol **15,** 968-973.

Peart, J.R., Lu, R., Sadanandom, A., Malcuit, I., Moffett, P., Brice, D.C., Schauser, L., Jaggard, D.A.W., Xiao, S., Coleman, M.J., Dow, M., Jones, J.D.G., Shirasu, K., and Baulcombe, D.C. (2002). Ubiquitin ligase-associated protein SGT1 is required for host and nonhost disease resistance in plants. Proc Natl Acad Sci USA **99,** 10865-10869.

Pratt, W.B., Galigniana, M.D., Harrell, J.M., and DeFranco, D.B. (2004). Role of hsp90 and the hsp90-binding immunophilins in signalling protein movement. Cell Signal **16,** 857-872.

Rairdan, G.J., and Moffett, P. (2006). Distinct domains in the ARC region of the potato resistance protein Rx mediate LRR binding and inhibition of activation. Plant Cell **18,** 2082-2093.

Rairdan, G.J., Collier, S.M., Sacco, M.A., Baldwin, T.T., Boettrich, T., and Moffett, P. (2008). The coiled-coil and nucleotide binding domains of the Potato Rx disease resistance protein function in pathogen recognition and signaling. Plant Cell **20,** 739-751.

Rathjen, J.P., and Moffett, P. (2003). Early signal transduction events in specific plant disease resistance. Curr Opin Plant Biol **6,** 300-306.

Rep, M. (2005). Small proteins of plant-pathogenic fungi secreted during host colonization. FEMS Microbiol Lett **253,** 19-27.

Ridout, C.J., Skamnioti, P., Porritt, O., Sacristan, S., Jones, J.D.G., and Brown, J.K.M. (2006). Multiple avirulence paralogues in cereal powdery mildew fungi may contribute to parasite fitness and defeat of plant resistance. Plant Cell **18,** 2402-2414.

Riedl, S.J., Li, W., Chao, Y., Schwarzenbacher, R., and Shi, Y. (2005). Structure of the apoptotic protease-activating factor 1 bound to ADP. Nature **434,** 926-933.

Rivas, S., and Thomas, C.M. (2005). Molecular interactions between tomato and the leaf mold pathogen *Cladosporium fulvum*. Ann Rev Phytopathol **43,** 395-436.

Rivas, S., Rougon-Cardoso, A., Smoker, M., Schauser, L., Yoshioka, H., and Jones, J.D.G. (2004). CITRX thioredoxin interacts with the tomato Cf-9 resistance protein and negatively regulates defence. EMBO J **23,** 2156-2165.

Ron, M., and Avni, A. (2004). The receptor for the fungal elicitor ethylene-inducing xylanase is a member of a resistance-like gene family in tomato. Plant Cell **16,** 1604-1615.

Ronald, P.C., Salmeron, J.M., Carland, F.M., and Staskawicz, B.J. (1992). The cloned avirulence gene *avrPto* induces disease resistance in tomato cultivars containing the *Pto* resistance gene. J Bacteriol **174,** 1604-1611.

Rooney, H.C., Van't Klooster, J.W., van der Hoorn, R.A., Joosten, M.H., Jones, J.D., and de Wit, P.J. (2005). Cladosporium Avr2 inhibits tomato Rcr3 protease required for Cf-2-dependent disease resistance. Science **308,** 1783-1786.

Rose, A., Patel, S., and Meier, I. (2004). The plant nuclear envelope. Planta **218,** 327-336.

Rowland, O., Ludwig, A.A., Merrick, C.J., Baillieul, F., Tracy, F.E., Durrant, W.E., Fritz-Laylin, L., Nekrasov, V., Sjolander, K., Yoshioka, H., and Jones, J.D.G. (2005). Functional analysis of *Avr9/Cf-9 rapidly elicited* genes identifies a protein kinase, ACIK1, that is essential for full Cf-9-dependent disease resistance in tomato. Plant Cell **17,** 295-310.

Salmeron, J.M., Oldroyd, G.E.D., Rommens, C.M.T., Scofield, S.R., Kim, H.S., Lavelle, D.T., Dahlbeck, D., and Staskawicz, B.J. (1996). Tomato *Prf* is a member of the leucine-rich repeat class of plant disease resistance genes and lies embedded within the *Pto* kinase gene cluster. Cell **86,** 123-133.

Schornack, S., Meyer, A., Romer, P., Jordan, T., and Lahaye, T. (2006). Gene-for-gene-mediated recognition of nuclear-targeted AvrBs3-like bacterial effector proteins. J Plant Physiol **163,** 256-272.

Schornack, S., Ballvora, A., Gurlebeck, D., Peart, J.R., Baulcombe, D.C., Ganal, M., Baker, B., Bonas, U., and Lahaye, T. (2004). The tomato resistance protein Bs4 is a predicted non-nuclear TIR-NB-LRR protein that mediates defense responses to severely truncated derivatives of AvrBs4 and overexpressed AvrBs3. Plant J **37,** 46-60.

Schwechheimer, C., Serino, G., Callis, J., Crosby, W.L., Lyapina, S., Deshaies, R.J., Gray, W.M., Estelle, M., and Deng, X.W. (2001). Interactions of the COP9 signalosome with the E3 ubiquitin ligase SCFTIR1 in mediating auxin response. Science **292,** 1379-1382.

Shao, F., Merritt, P.M., Bao, Z., Innes, R.W., and Dixon, J.E. (2002). A Yersinia effector and a Pseudomonas avirulence protein define a family of cysteine proteases functioning in bacterial pathogenesis. Cell **109,** 575-588.

Shao, F., Golstein, C., Ade, J., Stoutemyer, M., Dixon, J.E., and Innes, R.W. (2003). Cleavage of Arabidopsis PBS1 by a bacterial type III effector. Science **301,** 1230-1233.

Simons, G., Groenendijk, J., Wijbrandi, J., Reijans, M., Groenen, J., Diergaarde, P., Van der Lee, T., Bleeker, M., Onstenk, J., De Both, M., Haring, M., Mes, J., Cornelissen, B., Zabeau, M., and Vos, P. (1998). Dissection of the fusarium *I2* gene cluster in tomato reveals six homologs and one active gene copy. Plant Cell **10,** 1055-1068.

Song, J., Bradeen, J.M., Naess, S.K., Raasch, J.A., Wielgus, S.M., Haberlach, G.T., Liu, J., Kuang, H., Austin-Phillips, S., Buell, C.R., Helgeson, J.P., and Jiang, J. (2003). Gene *RB* cloned

from *Solanum bulbocastanum* confers broad spectrum resistance to potato late blight. Proc Natl Acad Sci USA **100,** 9128-9133.

Steimle, V., Otten, L.A., Zufferey, M., and Mach, B. (1993). Complementation cloning of an MHC class II transactivator mutated in hereditary MHC class II deficiency (or bare lymphocyte syndrome). Cell **75,** 135-146.

Strange, R.N., and Scott, P.R. (2005). Plant disease: a threat to global food security. Annu Rev Phytopathol **43,** 83-116.

Sun, Q., Collins, N.C., Ayliffe, M., Smith, S.M., Drake, J., Pryor, T., and Hulbert, S.H. (2001). Recombination between paralogues at the *rp1* rust resistance locus in maize. Genetics **158,** 423-438.

Swords, K.M.M., Dahlbeck, D., Kearney, B., Roy, M., and Staskawicz, B.J. (1996). Spontaneous and induced mutations in a single open reading frame alter both virulence and avirulence in *Xanthomonas campestris* pv. *vesicatoria avrBs2*. J Bacteriol **178,** 4661-4669.

Tai, T.H., Dahlbeck, D., Clark, E.T., Gajiwala, P., Pasion, R., Whalen, M.C., Stall, R.E., and Staskawicz, B.J. (1999). Expression of the *Bs2* pepper gene confers resistance to bacterial spot disease in tomato. Proc Natl Acad Sci USA **96,** 14153-14158.

Takahashi, A., Casais, C., Ichimura, K., and Shirasu, K. (2003). HSP90 interacts with RAR1 and SGT1 and is essential for RPS2-mediated disease resistance in *Arabidopsis*. Proc Natl Acad Sci USA **100,** 11777-11782.

Takken, F.L.W., Albrecht, M., and Tameling, W.I.L. (2006). Resistance proteins: molecular switches of plant defence. Curr Opin Plant Biol **9,** 383-390.

Takken, F.L.W., Schipper, D., Nijkamp, H.J.J., and Hille, J. (1998). Identification and Ds-tagged isolation of a new gene at the *Cf-4* locus of tomato involved in disease resistance to *Cladosporium fulvum* race 5. Plant J **14,** 401-411.

Tameling, W.I.L., Elzinga, S.D., Darmin, P.S., Vossen, J.H., Takken, F.L.W., Haring, M.A., and Cornelissen, B.J.C. (2002). The tomato *R* gene products I-2 and Mi-1 are functional ATP binding proteins with ATPase activity. Plant Cell **14,** 2929-2939.

Tameling, W.I.L., Vossen, J.H., Albrecht, M., Lengauer, T., Berden, J.A., Haring, M.A., Cornelissen, B.J.C., and Takken, F.L.W. (2006). Mutations in the NB-ARC domain of I-2 that impair ATP hydrolysis cause autoactivation. Plant Physiol **140,** 1233-1245.

Tang, X.Y., Frederick, R.D., Zhou, J.M., Halterman, D.A., Jia, Y.L., and Martin, G.B. (1996). Initiation of plant disease resistance by physical interaction of *Avrpto* and *Pto* kinase. Science **274,** 2060-2063.

Tao, Y., Yuan, F., Leister, R.T., Ausubel, F.M., and Katagiri, F. (2000). Mutational analysis of the Arabidopsis nucleotide binding site-leucine- rich repeat resistance gene RPS2. Plant Cell **12,** 2541-2554.

Thomas, C.M., Jones, D.A., Parniske, M., Harrison, K., Balint-Kurti, P.J., Hatzixanthis, K., and Jones, J.D.G. (1997). Characterization of the tomato *Cf-4* gene for resistance to *Cladosporium fulvum* identifies sequences that determine recognitional specificity in Cf-4 and Cf-9. Plant Cell **9,** 2209-2224.

Thomma, B.P.H.J., Van Esse, H.P., Crous, P.W., and De Wit, P.J.G.M. (2005). Cladosporium fulvum (syn. Passalora fulva), a highly specialized plant pathogen as a model for functional studies on plant pathogenic Mycosphaerellaceae. Mol Plant Pathol **6,** 379-393.

Ting, J.P., and Davis, B.K. (2005). CATERPILLER: A Novel Gene Family Important in Immunity, Cell Death, and Diseases. Annu Rev Immunol **23,** 387-414.

Tornero, P., Chao, R.A., Luthin, W.N., Goff, S.A., and Dangl, J.L. (2002). Large-scale structure-function analysis of the Arabidopsis RPM1 disease resistance protein. Plant Cell **14,** 435-450.

Ueda, H., Yamaguchi, Y., and Sano, H. (2006). Direct interaction between the tobacco mosaic virus helicase domain and the ATP-bound resistance protein, N factor during the hypersensitive response in tobacco plants. Plant Mol Biol **61,** 31-45.

van den Burg, H.A., Harrison, S.J., Joosten, M.H.A.J., Vervoort, J., and de Wit, P.J.G.M. (2006). Cladosporium fulvum Avr4 protects fungal cell walls against hydrolysis by plant chitinases accumulating during infection Mol Plant Microbe Interact **19,** 1420–1430.

van der Biezen, E.A., and Jones, J.D.G. (1998). The NB-ARC domain: a novel signalling motif shared by plant resistance gene products and regulators of cell death in animals. Curr Biol **8,** R226-227.

Van der Biezen, E.A., and Jones, J.D.G. (1999). Plant disease-resistance proteins and the gene-for-gene concept. Trends Biochem Sci **23,** 454-456.

Van der Hoorn, R.A.L., Roth, R., and De Wit, P.J.G.M. (2001). Identification of distinct specificity determinants in resistance protein Cf-4 allows construction of a Cf-9 mutant that confers recognition of avirulence protein AVR4. Plant Cell **13,** 273-285.

van der Hoorn, R.A.L., Wulff, B.B.H., Rivas, S., Durrant, M.C., van der Ploeg, A., De Wit, P.J.G.M., and Jones, J.D.G. (2005). Structure-function analysis of Cf-9, a receptor-like protein with extracytoplasmic leucine-rich repeats. Plant Cell **17,** 1000-1015.

van der Vossen, E., Sikkema, A., Hekkert, B.L., Gros, J., Stevens, P., Muskens, M., Wouters, D., Pereira, A., Stiekema, W., and Allefs, S. (2003). An ancient R gene from the wild potato species Solanum bulbocastanum confers broad-spectrum resistance to Phytophthora infestans in cultivated potato and tomato. Plant J **36,** 867-882.

van der Vossen, E.A.G., Gros, J., Sikkema, A., Muskens, M., Wouters, D., Wolters, P., Pereira, A., and Allefs, S. (2005). The *Rpi-blb2* gene from *Solanum bulbocastanum* is an *Mi-1* gene homolog conferring broad-spectrum late blight resistance in potato. Plant J **44,** 208-222.

van der Vossen, E.A.G., Rouppe van der Voort, J.N.A.M., Kanyuka, K., Bendahmane, A., Sandbrink, H., Baulcombe, D.C., Bakker, J., Stiekema, W.J., and Klein-Lankhorst, R.M. (2000). Homologues of a single resistance-gene cluster in potato confer resistance to distinct pathogens: a virus and a nematode. Plant J **23,** 567-576.

van Kan, J.A.L., van den Ackerveken, G.F.J.M., and de Wit, P.J.G.M. (1991). Cloning and characterization of cDNA of avirulence gene *avr9* of the fungal pathogen *Cladosporium fulvum*, causal agent of tomato leaf mold. Mol Plant Microbe Interact **4,** 52-59.

Vetter, I.R., and Wittinghofer, A. (1999). Nucleoside triphosphate-binding proteins: different scaffolds to achieve phosphoryl transfer. Q Rev Biophys **32,** 1-56.

Vinatzer, B.A., Teitzel, G.M., Lee, M.W., Jelenska, J., Hotton, S., Fairfax, K., Jenrette, J., and Greenberg, J.T. (2006). The type III effector repertoire of Pseudomonas syringae pv. syringae B728a and its role in survival and disease on host and non-host plants. Mol Microbiol **62,** 26-44.

Voinnet, O. (2005). Induction and suppression of RNA silencing: insights from viral infections. Nat Rev Genet **6,** 206-220.

Vos, P., Simons, G., Jesse, T., Wijbrandi, J., Heinen, L., Hogers, R., Frijters, A., Groenendijk, J., Diergaarde, P., Reijans, M., Fierens Onstenk, J., De Both, M., Peleman, J., Liharska, T., Hontelez, J., and Zabeau, M. (1998). The tomato *Mi-1* gene confers resistance to both root-knot nematodes and potato aphids. Nature Biotech **16,** 1365-1369.

Warren, R.F., Henk, A., Mowery, P., Holub, E., and Innes, R.W. (1998). A mutation within the leucine-rich repeat domain of the *Arabidopsis* disease resistance gene *RPS5* partially suppresses multiple bacterial and downy mildew resistance genes. Plant Cell **10,** 1439-1452.

Westerink, N., Brandwagt, B.F., De Wit, P.J.G.M., and Joosten, M.H.A.J. (2004). *Cladosporium fulvum* circumvents the second functional resistance gene homologue at the *Cf-4* locus (*Hcr9-4E*) by secretion of a stable avr4E isoform. Mol Microbiol **54,** 533-545.

Whitham, S., Dinesh-Kumar, S.P., Choi, D., Hehl, R., Corr, C., and Baker, B. (1994). The product of the tobacco mosaic virus resistance gene *N*: similarity to toll and the interleukin-1 receptor. Cell **78,** 1101-1115.

Wiermer, M., Feys, B.J., and Parker, J.E. (2005). Plant immunity: the EDS1 regulatory node. Curr Opin Plant Biol **8,** 383-389.

Willems, A.R., Schwab, M., and Tyers, M. (2004). A hitchhiker's guide to the cullin ubiquitin ligases: SCF and its kin. Biochim Biophys Acta **1695,** 133-170.

Williamson, V.M. (1999). Plant nematode resistance genes. Curr Opin Plant Biol **2,** 327-331.

Williamson, V.M., and Kumar, A. (2006). Nematode resistance in plants: the battle underground. Trends Genet **22,** 396-403.

Wulff, B.B.H., Thomas, C.M., Smoker, M., Grant, M., and Jones, J.D.G. (2001). Domain swapping and gene shuffling identify sequences required for induction of an Avr-dependent hypersensitive response by the tomato Cf-4 and Cf-9 proteins. Plant Cell **13,** 255-272.

Xu, Y., Tao, X., Shen, B., Horng, T., Medzhitov, R., Manley, J.L., and Tong, L. (2000). Structural basis for signal transduction by the Toll/interleukin-1 receptor domains. Nature **408,** 111-115.

Yan, N., Chai, J., Lee, E.S., Gu, L., Liu, Q., He, J., Wu, J.W., Kokel, D., Li, H., Hao, Q., Xue, D., and Shi, Y. (2005). Structure of the CED-4-CED-9 complex provides insights into programmed cell death in *Caenorhabditis elegans*. Nature **437,** 831-837.

Yang, C.W., Gonzalez-Lamothe, R., Ewan, R.A., Rowland, O., Yoshioka, H., Shenton, M., Ye, H., O'Donnell, E., Jones, J.D.G., and Sadanandom, A. (2006). The E3 ubiquitin ligase activity of *Arabidopsis* PLANT U-BOX17 and its functional tobacco homolog ACRE276 are required for cell death and defense. Plant Cell **18,** 1084-1098.

Yu, X., Wang, L., Acehan, D., Wang, X., and Akey, C.W. (2006). Three-dimensional structure of a double apoptosome formed by the *Drosophila* Apaf-1 related killer. J Mol Biol **355,** 577-589.

Yu, X., Acehan, D., Menetret, J.F., Booth, C.R., Ludtke, S.J., Riedl, S.J., Shi, Y., Wang, X., and Akey, C.W. (2005). A structure of the human apoptosome at 12.8 Å resolution provides insights into this cell death platform. Structure **13,** 1725-1735.

Zhang, Y., and Li, X. (2005). A putative nucleoporin 96 Is required for both basal defense and constitutive resistance responses mediated by *suppressor of npr1-1, constitutive 1*. Plant Cell **17,** 1306-1316.

Zhang, Y., Goritschnig, S., Dong, X., and Li, X. (2003). A gain-of-function mutation in a plant disease resistance gene leads to constitutive activation of downstream signal transduction pathways in suppressor of npr1-1, constitutive 1. Plant Cell **15,** 2636-2646.

Zhou, J., Tang, X., and Martin, G.B. (1997). The Pto kinase conferring resistance to tomato bacterial speck disease interacts with proteins that bind a *cis*-element of pathogenesis-related genes. EMBO J **16,** 3207-3218.

Zhou, J.M., Loh, Y.T., Bressan, R.A., and Martin, G.B. (1995). The tomato gene *Pti1* encodes a serine/threonine kinase that is phosphorylated by Pto and is involved in the hypersensitive response. Cell **83,** 925-935.

Zipfel, C., and Felix, G. (2005). Plants and animals: a different taste for microbes? Curr Opin Plant Biol **8,** 353-360.

Zipfel, C., Kunze, G., Chinchilla, D., Caniard, A., Jones, J.D.G., Boller, T., and Felix, G. (2006). Perception of the bacterial PAMP EF-Tu by the receptor EFR restricts *Agrobacterium*-mediated transformation. Cell **125,** 749-760.

Chapter 3

Mutational analysis of the MHD motif in resistance proteins reveals its functional role as sensor to transduce nucleotide-dependent conformational changes

Gerben van Ooijen*, Gabriele Mayr[1*], Mobien M. A. Kasiem, Mario Albrecht[1], Ben J. C. Cornelissen and Frank L. W. Takken

[1] Max Planck Institute for Informatics, Saarbrücken, Germany
*These authors contributed equally to this paper
Published in: Journal of Experimental Botany, 2008, Volume 59, 1383-1397

Resistance (R) proteins in plants are involved in pathogen recognition and subsequent activation of innate immune responses. Most resistance proteins contain a central nucleotide-binding domain, NB-ARC, which is also found in metazoan proteins Apaf-1 and CED-4. In R proteins, this NB-ARC domain consists of three subdomains: NB, ARC1 and ARC2. The NB-ARC domain is a functional ATPase domain, and its nucleotide-binding state is proposed to regulate activity of the R protein. A highly conserved methionine-histidine-aspartate (MHD) motif is present at the carboxy-terminus of ARC2. We report an extensive mutational analysis of the MHD motif in the R proteins I-2 and Mi-1. Several novel autoactivating mutations of the MHD invariant histidine and conserved aspartate are identified. The combination of MHD mutants with autoactivating hydrolysis mutants in the NB subdomain shows that the autoactivation phenotypes are not additive. This finding indicates an important regulatory role for the MHD motif in the control of R protein activity. To explain these observations, a three-dimensional model of the NB-ARC domain of I-2 is built based on the Apaf-1 template structure. The model was used to identify residues important for I-2 function. Substitution of the selected residues, and functional analysis of the mutants, resulted in the expected phenotypes. The hence validated model enables structural and functional interpretation of our mutagenesis results and demonstrates that the MHD motif replaces the sensor II motif found in AAA+ (ATPases Associated with diverse cellular Activities) proteins.

Introduction

To deal with pathogens, plants have evolved an advanced immune system to counteract pathogen-attack. This immune system enables plants to discriminate between self and non-self, and to induce specific defense responses upon pathogen perception. Recognition of non-self can be mediated by so-called Resistance or R proteins (Martin et al., 2003). Upon recognition of specific pathogen-derived molecules, called Avirulence (AVR) proteins, R proteins trigger the induction of plant defenses to restrict pathogen proliferation (Jones and Dangl, 2006). A hallmark of R protein mediated resistance is the hypersensitive response (HR), often visible as a localized cell death response around the infection site.

Over the last decade, many R genes have been cloned and the majority is predicted to encode intracellular multi-domain proteins (Martin et al., 2003; van Ooijen et al., 2007). These R proteins contain a C-terminal Leucine Rich Repeat (LRR) domain fused to a central Nucleotide Binding (NB) domain (NB-LRR proteins). The core nucleotide-binding fold in NB-LRR proteins is part of a larger entity called the NB-ARC domain because of its presence in Apaf-1 (Apoptotic protease-activating factor-1), R proteins and CED-4 (*Caenorhabditis elegans* Death-4 protein) (van der Biezen and Jones, 1998). Structurally related domains, named NACHT (NAIP, CIITA, HET-E and TP1) or NOD (for Nucleotide-Oligomerization Domain), can be found in other animal proteins. Many of these proteins act as receptors sensing intracellular perturbations (Leipe et al., 2004; Ting et al., 2006; Rairdan and Moffett, 2007). Like in R proteins, the NACHT or NOD domains in these proteins are fused to a repeat structure such as an LRR or WD40 repeat (Leipe et al., 2004). The combined activities of the nucleotide-binding domain and the repeat structure probably evolved independently in the plant and animal kingdoms, and might reflect the biochemical suitability of this combination to link ligand recognition with subsequent activation of downstream pathways (Leipe et al., 2004; Ausubel, 2005).

Proteins containing a NB-ARC/NACHT/NOD domain belong to the Signal Transduction ATPases with Numerous Domains (STAND) superfamily (Leipe et al., 2004). It was predicted that the STAND ATPase domain transmits conformational changes, induced by nucleotide exchange or hydrolysis, to other domains of the protein, thereby allowing it to generate a signal (Leipe et al., 2004).

No plant NB-ARC domain crystal structure has been published, but for the human STAND ATPase Apaf-1 such a structure has been solved and was found to contain a bound ADP (Riedl et al., 2005). This 3D structure revealed that the NB-ARC domain is actually composed of four distinct subdomains: the Nucleotide-Binding (NB) fold and ARC1, -2 and -3 subdomains. ARC1 forms a four-helix bundle, ARC2 adopts a winged-helix fold, and ARC3 constitutes another helical bundle. Specific ADP-binding is achieved through eight direct and four H_2O-mediated interactions with various

conserved residues present in the NB, ARC1 and ARC2 subdomains (Riedl et al., 2005). In *C. elegans* CED-4 (Yan et al., 2005) and plant NB-LRR R proteins, ARC1 and ARC2 are conserved, whereas ARC3 is absent (Albrecht and Takken, 2006). Numerous conserved motifs (hhGRExE, Walker A or P-loop, Walker B, GxP, RNBS-A to D, and MHD) have been identified throughout the NB-ARC domain in R proteins (Meyers et al., 1999; Pan et al., 2000) and seem to correspond to residues in Apaf-1 that are involved in nucleotide binding. The functional importance of these motifs is exemplified by the many mutations of motif residues that were demonstrated to result in either loss-of-function or autoactivation of the NB-LRR protein (Grant et al., 1995; Salmeron et al., 1996; Dinesh-Kumar et al., 2000; Tao et al., 2000; Axtell et al., 2001; Bendahmane et al., 2002; Tameling et al., 2002; Tornero et al., 2002; de la Fuente van Bentem et al., 2005; Howles et al., 2005; Tameling et al., 2006; Gabriëls et al., 2007). Autoactivation means that HR is initiated in the absence of pathogen or AVR protein.

The identification of loss-of-function mutations in the nucleotide binding pocket indicated that nucleotide binding is important for NB-LRR R protein function (Tameling et al., 2002). Previous studies in our lab have indeed confirmed that the NB-ARC domain in the R proteins I-2 and Mi-1 binds nucleotides in vitro. This nucleotide binding is required for I-2 function since a P-loop mutant impaired in binding is inactive (Tameling et al., 2002). R proteins have also been demonstrated to hydrolyse ATP in vitro. Two I-2 autoactivating mutants with specific point mutations in the NB subdomain were found to have wild-type nucleotide binding affinities, but to exhibit reduced ATPase activity (Tameling et al., 2006). These observations support a model for R protein function in which the activated state is ATP-bound and the ADP-bound state represents the resting state (Takken et al., 2006; Tameling et al., 2006). Likewise, the ADP-bound state represents the inactive state in Apaf-1 (Riedl et al., 2005). Upon activation, Apaf-1 binds ATP and undergoes conformational changes enabling the formation of an oligomer (Riedl et al., 2005; Riedl and Salvesen, 2007). Regarding NB-LRR R proteins, homo-oligomerization has so far been confirmed only for the tobacco protein N (Mestre and Baulcombe, 2006).

Whereas the NB subdomain forms a catalytic nucleotide-binding and nucleotide-hydrolyzing pocket, our understanding of the role of the adjacent ARC1 and ARC2 subdomains in regulation of R protein activity is limited. No autoactivating mutations have been described in the ARC1 subdomain and only eight loss-of-function mutations are known (Grant et al., 1995; Bendahmane et al., 2002; Tornero et al., 2002). The ARC1 subdomain of the potato NB-LRR protein Rx has been shown to interact with the Rx LRR domain, but also with the heterologous Bs2 and HRT LRR domains when expressed *in trans* (Rairdan and Moffett, 2006). These data suggest that this domain has a structural role and acts as molecular scaffold for LRR binding.

Many autoactivating mutations have been identified in the ARC2 subdomain, the majority of them maps to a highly conserved carboxy-terminal motif named after its consensus sequence methionine-histidine-aspartate, the MHD motif. An aspartate to valine substitution in the MHD motif was first identified by random mutagenesis in Rx and resulted in autoactivation upon transient expression in *N. benthamiana* leaves (Bendahmane et al., 2002). Later on, mutation of D was shown to result in autoactivation in other R proteins like I-2 and L6, (de la Fuente van Bentem et al., 2005; Howles et al., 2005) and in the NB-ARC protein NRC1 (Gabriëls et al., 2007). NRC1 (for NB-LRR protein Required for HR-associated Cell death 1) does not encode an R protein, but is required for induction of HR by several R proteins upon their activation (Gabriëls et al., 2007).

Autoactivating NB-LRR mutants were not only generated by point mutations, but were also obtained by domain swaps between closely related paralogues of Mi-1, Rx, Rp1 and L6 (Hwang et al., 2000; Sun et al., 2001; Howles et al., 2005; Rairdan and Moffett, 2006). Extensive domain-swap studies using Rx and the related Gpa2 protein suggested that the ARC2 subdomain, via its interaction with the LRR, transduces pathogen recognition by the LRR domain into R protein activation (Rairdan and Moffett, 2006). ARC2 thus seems crucial to condition both autoinhibition in the absence of a pathogen, as well as activation of the R protein in the presence of a pathogen.

The strict conservation of the MHD motif in the ARC2 domain across most clades of the STAND superfamily (Leipe et al., 2004) indicates that this motif is important for these molecular functions. Therefore, to gain more insight into a possible key regulatory role of ARC2 and to investigate the role of the MHD motif in more detail, we generated additional mutations in the MHD motif of the R proteins I-2 and Mi-1 and transiently expressed these proteins in *N. benthamiana*. To link the role of the MHD motif to the nucleotide-binding properties of the NB subdomain, double mutants were made that combine the known autoactivation mutations in the NB-subdomain of I-2 to those in the MHD motif.

To further elucidate the molecular role of the MHD motif in R proteins, an in-silico analysis was performed. We chose the crystal structure of Apaf-1 (Riedl et al., 2005) to model the 3D structure of the NB-ARC domain of I-2. Although sequence identity between Apaf-1 and R proteins is low (20%), we could demonstrate that Apaf-1 still represents a suitable template because functionally important residues are well conserved. To validate the model, five residues suggested by the model to be important for function were selected for mutation and were indeed found to be of functional importance for R protein activation. Our 3D model of the NB-ARC domain of I-2 provides a useful additional view of the functional role of the MHD motif and explains the effect of other autoactivating and loss-of-function mutants.

Results

Autoactivating aspartate to valine mutations in the MHD motif of Mi-1 and Rpi-blb1

Mutation of D to V in the MHD motif of the NB-LRR proteins conferring viral (Rx) or fungal resistance (I-2 and L6), and in NRC1, which is required for many R proteins to initiate HR signaling, has been shown to result in autoactivation of these proteins (Bendahmane et al., 2002; de la Fuente van Bentem et al., 2005; Howles et al., 2005; Gabriëls et al., 2007). To examine whether the D to V mutation also results in autoactivation in a nematode, aphid and whitefly resistance protein (Mi-1) and an oomycete resistance protein (Rpi-blb1), we introduced the corresponding mutation in these two proteins. Autoactivation of the mutant proteins was assessed by transient *Agrobacterium tumefaciens*-mediated transformation in five-weeks-old *Nicotiana*

Figure 1
Mutation of the MHD motif aspartate to valine leads to autoactivation. *Nicotiana benthamiana* leaves were agroinfiltrated with constructs to express R proteins mutated in the MHD motif (aspartate to valine). Pictures of representative leaves were taken two (**A**) or four days after agroinfiltration (**B**). **(A)** Counter-clockwise, starting from top-left: Rx^{D460V}, $I\text{-}2^{D495V}$, $Rpi\text{-}blb1^{D475V}$, $Mi\text{-}1^{D841V}$. **(B)** Counter-clockwise, starting from top-left: $Mi\text{-}1^{D841V}$, Rx^{D460V}, $I\text{-}2^{D495V}$, $Rpi\text{-}blb1^{D475V}$.

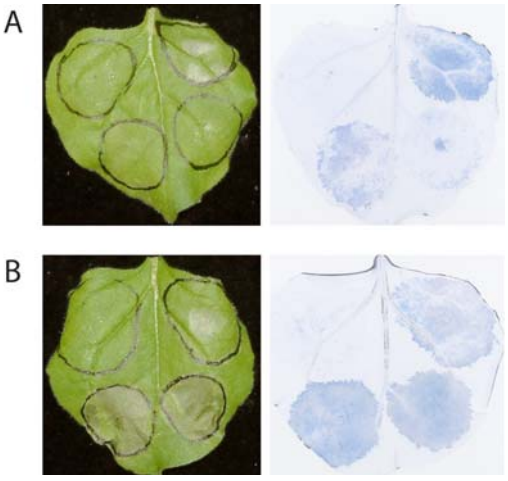

Figure 2
Combination of autoactivation mutations in the NB and ARC2 subdomains. *Nicotiana benthamiana* leaves were agroinfiltrated with constructs to express (mutant) I-2 alleles. Representative leaves were photographed at four days after agroinfiltration. **(A)** Counter-clockwise, starting from top-left: wild-type I-2, $I\text{-}2^{S233F}$, $I\text{-}2^{D283E}$, $I\text{-}2^{S233F/D283E}$. Cell death is visualised by trypan blue staining of the same leaf (right panel). **(B)** Counter-clockwise, starting from top-left: wild-type I-2, $I\text{-}2^{D495V}$, $I\text{-}2^{S233F/D495V}$, $I\text{-}2^{D283E/D495V}$.

benthamiana leaves. Expression of the proteins was driven by the 35S promoter. Pictures were taken at two and four days after agroinfiltration. Figure 1 shows that indeed Mi-1^{D841V} and Rpi-blb1^{D475V} induce a hypersensitive response visible as clear necrosis of the infiltrated sector. The autoactive alleles I-2^{D495V} and Rx^{D460V} are shown as positive controls for HR development. Rx^{D460V} and Rpi-blb1^{D475V} show a rapid HR that is fully developed at two days (Fig. 1A), whereas Mi-1^{D841V} and I-2^{D495V} trigger a slower response that does not lead to a full necrotic sector until three and four days after agroinfiltration, respectively (Fig. 1B). Expression of the wild type protein does not induce HR at the indicated time points (Fig. 2, 4B and data not shown).

The observed autoactivation phenotype of the aspartate-to-valine mutants confirms an important and conserved function for D in the MHD motif of various R proteins conferring resistance to a virus (Rx), a fungus (I-2), an oomycete (Rpi-blb1), and animals (Mi-1). Apparently, mutation of this residue consistently releases R protein autoinhibition, resulting in an autoactivation phenotype or, alternatively, induces another change mimicking the activated state.

Autoactivating mutations in the MHD motif and the NB subdomain do not act synergistically

We have shown previously that the autoactivation phenotype of the I-2^{D495V} mutant depends an a functional nucleotide-binding subdomain since a mutant combining the D495V with the K207R mutation in the P-loop (Walker A) is inactive (Tameling et al., 2006). The K207R mutation in the P-loop of the NB subdomain is a loss-of-function mutation that results in strongly reduced nucleotide-binding capacity (Tameling et al., 2006). Two weak autoactivating mutations in I-2, D283E (in Walker B) and S233F (in RNBS-A), caused reduced ATP hydrolysis rates (Tameling et al., 2006). These mutations are predicted to shift the presumed equilibrium towards the ATP-bound (active) state. Combination of two weak autoactivating mutations in the NB subdomain into a double mutant is therefore predicted to result in an even stronger shift, and hence a more pronounced autoactivation phenotype.

To analyse whether this is the case, the mutations were combined and timing and severity of the HR response after agroinfiltration was scored as a measure for the relative autoactivity of the I-2 mutants. As depicted in figure 2A, combination of both weak autoactivating NB mutations results in a synergetic phenotype. Onset of HR induced by the I-2$^{S233F/D283E}$ double mutant is visible at four days after agroinfiltration on all leaves tested, whereas I-2^{S233F} or I-2^{D283E} single mutants did not show HR at this time point (Fig. 2A). A trypan blue staining of the infiltrated leaf confirms that a weak HR (cell death is visible as blue staining) is induced by the two single mutants, whereas the HR triggered by the double mutant is much more pronounced. The wild-

type I-2 protein does not induce cell death as shown by the absence of any blue colouration. Although the I-2$^{S233F/D283E}$ double mutant is able to induce a clear HR phenotype after four days, the HR is still not as strong as that observed for I-2^{D495V} (Fig. 1), which is in line with an autoinhibitory role of the ARC2 subdomain.

With the NB subdomain being the nucleotide binding and hydrolyzing site, domain swaps of Rx suggest that the ARC2 subdomain, containing the MHD motif, is the regulatory element controlling nucleotide exchange and hence ARC2 activity (Rairdan and Moffett, 2006). Mutating the ARC2 MHD motif might release this autoinhibitory effect on the NB. Combining the MHD mutation with hydrolysis mutations in the NB subdomain would, in this scenario, have a minimal, if any, additive effect on the autoactivation phenotype.

To test this hypothesis, both autoactivating mutations were combined in I-2; the autoactivating mutation D495V in the ARC2 subdomain was paired with either the D283E or S233F in the NB subdomain. As shown in Figure 2B, I-2^{D495V} but not wild-type I-2 induces clear necrosis four days after agroinfiltration. Infiltration of double mutants I-2$^{S233F/D495V}$ and I-2$^{D283E/D495V}$ does not lead to a stronger induction of HR, as confirmed by trypan blue staining of the same leaf (Fig. 2B). Thus, at least visibly, combining the two weak autoactivating mutants with the strong autoactivating D495V mutation in ARC2 does indeed not result in a faster or stronger HR. These data suggest that the MHD motif is a major negative regulatory element controlling the NB subdomain.

Alignment of MHD motifs

Since the D-V mutation of the MHD motif has been found to result in autoactivation of all NB-LRR proteins tested so far, we made an extensive multiple sequence alignment (MSA) of the extended MHD motif of the 50 cloned NB-LRR proteins with confirmed resistance activity, thereby updating a previously published MSA of this region (Howles et al., 2005). For completeness, also the plant NB-LRR proteins NRC1 and NRG1 are included since both are involved in R protein signaling pathways (Peart et al., 2005; Gabriëls et al., 2006). Apaf-1 was included to illustrate the conservation of this motif in a sequence related human protein. The MSA was sorted to match a phylogenetic tree that was generated based on the aligned motifs. Although phylogeny based on such a short sequence is error-prone, clear clusters stand out (Figure 3). This clustering complies with the relationships of R proteins based on the identity of their N-terminal domains. This N-terminal domain contains either predicted coiled-coil (CC) motifs (the CNLs) or shares homology with the *Drosophila* Toll and human Interleukin-1 receptors (TIR, the TNLs) (reviewed in (Martin et al., 2003; van Ooijen et al., 2007)). As can be appreciated from Figure 3, the TNL group (aubergine characters) clusters together and the consensus sequence

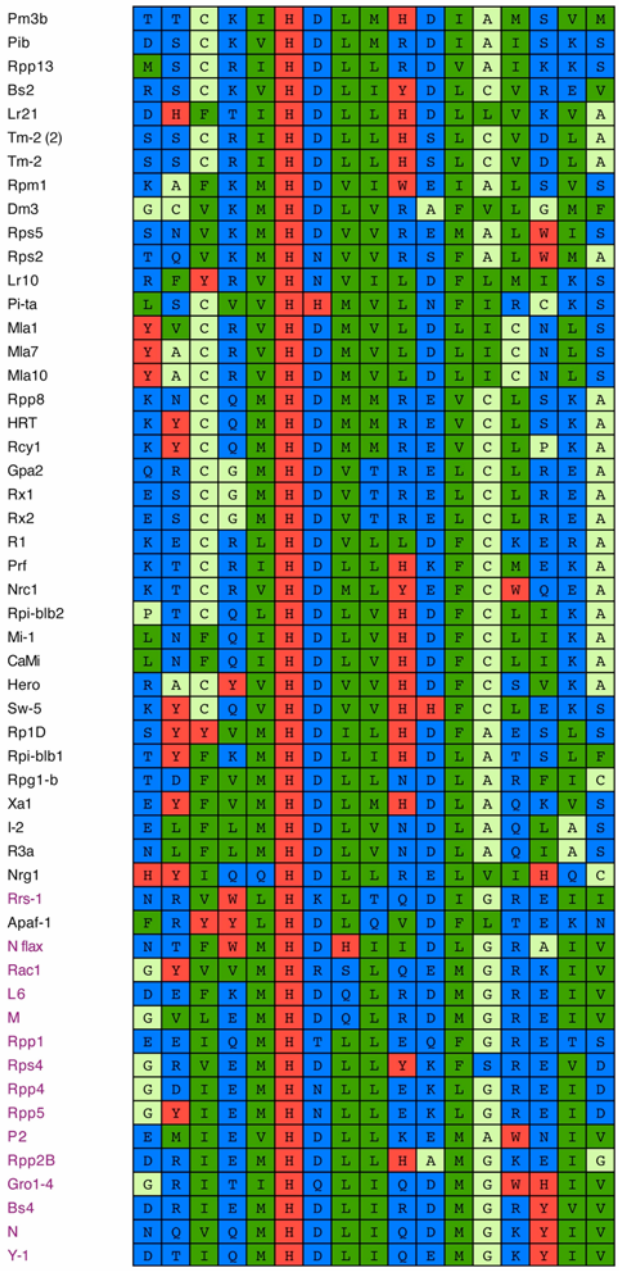

Figure 3

Multiple sequence alignment of the extended MHD motif in 50 R proteins with confirmed resistance activity, the downstream resistance signaling NB-ARC-LRR proteins NRC1 and NRG1, and human Apaf-1. CC-NB-LRR proteins are marked in blue, and TIR-NB-ARC-LRR proteins in red. Amino acid residues are colored based on their chemical type; beige: small hydrophobic (A, C, G, P), blue: hydrophilic (D, E, K, N, Q, R, S, T), red: aromatic (H, W, Y), green: large hydrophobic (F, I, L, M, V). TNLs are marked in aubergine.

of its MHD motif is C-terminally elongated compared to those of CNLs. The conservation of this motif in human Apaf-1 is clear as well.

As can be deduced from the MSA in Figure 3, the most conserved residue in the MHD motif is the histidine that is invariable in all NB-LRR R proteins. The histidine is always N-terminally flanked by a hydrophobic residue (a methionine in 53% of the cases), whereas the C-terminal neighbouring residue is an aspartate in most cases (83%). This means that, although conservation of the aspartate is considerable, it is not invariant. The histidine is the only invariable residue in the MHD motif, which suggests an essential role for this residue.

Table 1 Substitutions of I-2 H494

Amino acid		No. of clones	Phenotype
A	Alanine	5	+++
C	Cysteine	1	++
D	Aspartic acid	8	++
E	Glutamic acid	2	++
G	Glycine	10	++
K	Lysine	3	++
N	Asparagine	1	++
R	Arginine	13	++
S	Serine	7	++
T	Threonine	7	++
V	Valine	6	++
M	Methionine	2	+
Y	Tyrosine	4	+
F	Phenylalanine	4	+/-
P	Proline	3	+/-
L	Leucine	12	-
Q	Glutamine	5	-
W	Tryptophan	1	-
I	Isoleucine	0	nd
H	Histidine	85	-
*	stop	5	-

Mutation of the histidine in the MHD motif

Because the histidine is the most conserved residue in the MHD motif of plant NB-LRR R proteins, we decided to analyze the effect of mutating this residue on I-2 function. We first generated a small library of I-2 clones that encode proteins that are variable for residue H494. This library was made by site-directed mutagenesis using the megaprimer method (Ke and Madison, 1997). In the mutagenic primer, the H494-encoding codon (CAT) was replaced for NNS (in which N can be any nucleotide and

S can be either G or C). Introduction of S reduces the number of possible codons to 32, thereby increasing the relative percentage of the single-codon amino acids tryptophan and methionine. To have a good representation of all possible codons, an approximately six-fold excess of the 32 possible codons (184 clones) was sequenced. The obtained variants, and the number of clones coding for each amino acid at position 494, are shown in Table 1. Of the 19 possible amino acid replacements plus three stop codons, isoleucine was the only one that was not present in the sequenced set of clones. An overrepresentation of the wild-type histidine residue was obtained, probably due to inefficient removal of the wild-type insert.

The phenotype of the H494 variants was analyzed by transient expression in *N. benthamiana* leaves using agroinfiltration and assessment of timing and extent of cell death of the infiltrated region. Except for the stop codon mutants and the wild-type, we did not observe HR either when a glutamate, leucine or tryptophan replaced the histidine at position 494. The 15 other replacements resulted in autoactivation. However, variation in the amplitude of timing and intensity of HR was observed (Table 1). The results in Table 1 represent the average observed effects of at least two independent clones where possible. HR was ranked from very strong (+++) to no visual effect (-). To illustrate the range of HR, Figure 4A shows I-2 mutants H494A (+++), H494R (++), H494V (+), H494F (+/-), H494L (-) and H494Q (-). The same activity range is also evident upon trypan blue staining of this leaf (Fig. 4A, right panel). Substitution of H494 for alanine reproducibly resulted in the fastest induction of HR. Limited cell death was also visualised upon expression of I-2^{H494L} and I-2^{H494Q}, suggesting that the latter two could still weakly autoactivate. However, since the intensity of the blue staining is comparable to that for wildtype I-2, it likely represents background staining.

To investigate whether corresponding mutations in a related NB-LRR protein, Mi-1, confer similar phenotypes as obtained for I-2, we generated Mi-1 MHD motif mutants H840A, H840R, H840V, H840Q and as a negative control H840stop. Similar to I-2, Mi-1^{H840A} leads to the strongest autoactivation (Fig. 4B), whereas Mi-1^{H840R} and Mi-1^{H840V} show intermediate phenotypes. Wild-type Mi-1 and Mi-1^{H840Q} do not induce HR, but induce a similar light blue staining as the Mi-1^{H840stop} control.

Autoactivation by Mi-1 MHD mutants is not due to higher expression levels in the plant

To test whether autoactivation induced by mutations in the MHD are due to differences in protein expression levels rather than a direct effect of the mutation, the expression levels of the various mutants were analyzed. To detect the R proteins after *in planta* expression, antibodies against I-2 and Mi-1 were raised in rabbit.

Either a synthetic I-2 peptide or the Mi-1 NB-ARC domain with part of its N-terminal flanking sequence (Mi-1 amino acids 161-899) were used as antigen. The latter recombinant Mi-1 protein was heterologously produced in *E. coli* as described in the Methods section. Using affinity purified I-2 antibodies, we were unable to detect the R protein in protein extracts isolated from agroinfiltrated *N. benthamiana* leaves, although the antibody successfully recognized *E. coli*-produced I-2 protein (data not shown). These results indicate that I-2 expression levels *in planta* are probably below the detection level of the I-2 antibody (data not shown and (Tameling et al., 2006)). Efforts to detect N- or C-terminally epitope-tagged I-2 failed and since all tags tested rendered the autoactivation mutant I-2^{D495V} inactive, these efforts where not continued.

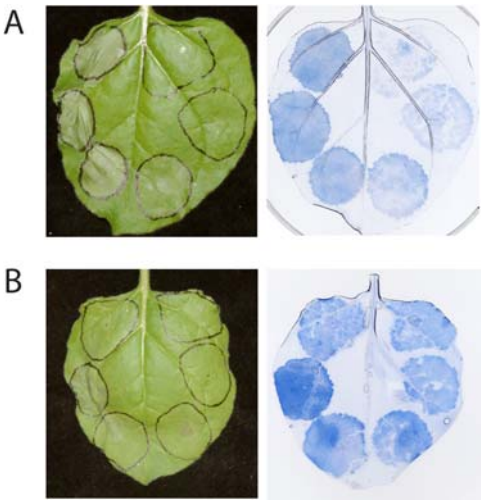

Figure 4
Mutation of the MHD motif histidine leads to a range of autoactivating phenotypes. *Nicotiana benthamiana* leaves were agroinfiltrated with constructs to express I-2 or Mi-1 mutants variant for the MHD motif histidine. (**A)** I-2 mutants variant for H494. Counter-clockwise, starting from top-left: I-2^{H494A}, I-2^{H494R}, I-2^{H494V}, I-2^{H494F}, I-2^{H494L}, I-2^{H494Q}. Picture was taken four days after agroinfiltration. Cell death is visualised by trypan blue staining of the same leaf (right panel). (**B)** Mi-1 mutants variant for H840. Counter-clockwise, starting from top-left: wild-type Mi-1, Mi-1^{H840A}, Mi-1^{H840R}, Mi-1^{H840V}, Mi-1^{H840Q}, Mi-1^{H840stop}. Picture was taken four days after agroinfiltration. Cell death is visualised by trypan blue staining of the same leaf (right panel).

In contrast to I-2, *in planta* produced Mi-1 could readily be detected using the Mi-1 antibody. The Mi-1 antibody detects both full-length Mi-1 and a truncated version lacking the LRR in total protein extracts from *N. benthamiana* leaves, following transient expression using agroinfiltration (Supplemental Fig. S1). No Mi-1-specific bands were detected on western blots from protein extracts of leaves agroinfiltrated with Mi-1 LRR (amino acids 900-1257), showing specificity of the antibody for the N-terminal part of Mi-1. Besides the Mi-1 protein, a ~80 kDa band was consistently found in all *N. benthamiana* extracts, including these from non-infiltrated leaves. The nature of this *N. benthamiana* specific protein is not known, but like Mi-1 it was not recognised on blots incubated with pre-immune serum (Supplemental Fig. S1). To analyze the expression levels of Mi-1 mutants, constructs encoding Mi-1^{D841V} and H840 mutants showing strong (H840A), intermediate (H840V) or no (H840Q)

autoactivating phenotype were agroinfiltrated. Infiltrated leaves were harvested after 24 hours, well before onset of HR, and subsequently used for total protein extraction. For comparison, the expression level of wild-type Mi-1 was included. A western blot of total soluble protein from agroinfiltrated leaves was stained with Ponceau S to confirm equal loading. This blot was subsequently probed with the Mi-1 antibody and Figure 5 shows the Mi-1 variants migrating at the predicted weight of ~145 kDa. The expression levels of autoactivating mutants do not differ significantly from the wild-type control. These results substantiate that induction of HR by Mi-1 mutants is not caused by differences in protein level and can solely be attributed to the specific mutations.

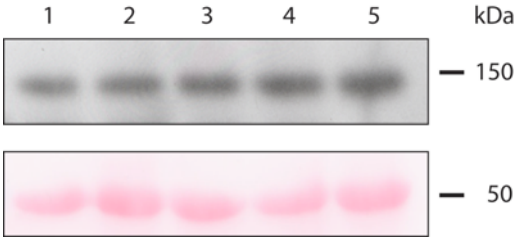

Figure 5 – Expression levels of wild-type and mutant Mi-1. *Nicotiana benthamiana* leaves were agroinfiltrated with constructs to express (mutant) Mi-1. One day after agroinfiltration, protein extracts were subjected to SDS-PAGE followed by Ponceau S staining of Rubisco **(B)** and immunoblotting with anti-Mi **(A)**. 1: Mi-1 wild-type, 2: Mi-1^{D841V}, 3: Mi-1^{H840A}, 4: Mi-1^{H840V}, 5: Mi-1^{H840Q}.

Structure-based multiple sequence alignment of R proteins

To provide an explanation for the phenotypes of the MHD mutants, a 3D model of the I-2 NB-ARC domain was built. To construct the structure model, we first examined sequence conservation and domain organization of R proteins by generating a structure-based multiple sequence alignment (Fig. 6). Two homologous proteins with known structure, human Apaf-1 and *C. elegans* CED-4, were included (Riedl et al., 2005; Yan et al., 2005). The initial alignment was refined manually, taking into account secondary structure predictions of R proteins, and known structure assignments of Apaf-1 and CED-4. Sequence identity between I-2 and Apaf-1 NB-ARC domains is low (24%) and concentrated within or adjacent to conserved motifs present in the three subdomains of the NB-ARC domain of R proteins (Fig. 6).

As can be seen in Figure 6, most known R protein motifs are also conserved in Apaf-1 and CED-4. The most important exception is the MHD motif itself, which is conserved in Apaf-1 but not in CED-4. The RNBS-C motif is not conserved either in CED-4 and has very low conservation in Apaf-1. Only two residues of this motif are in common with R proteins. The RNBS-D is conserved neither in CED-4 nor in Apaf-1. In the Apaf-1 crystal structure, the corresponding region is not involved in formation of the ADP binding pocket and is located on a helix within ARC2. Another remarkable

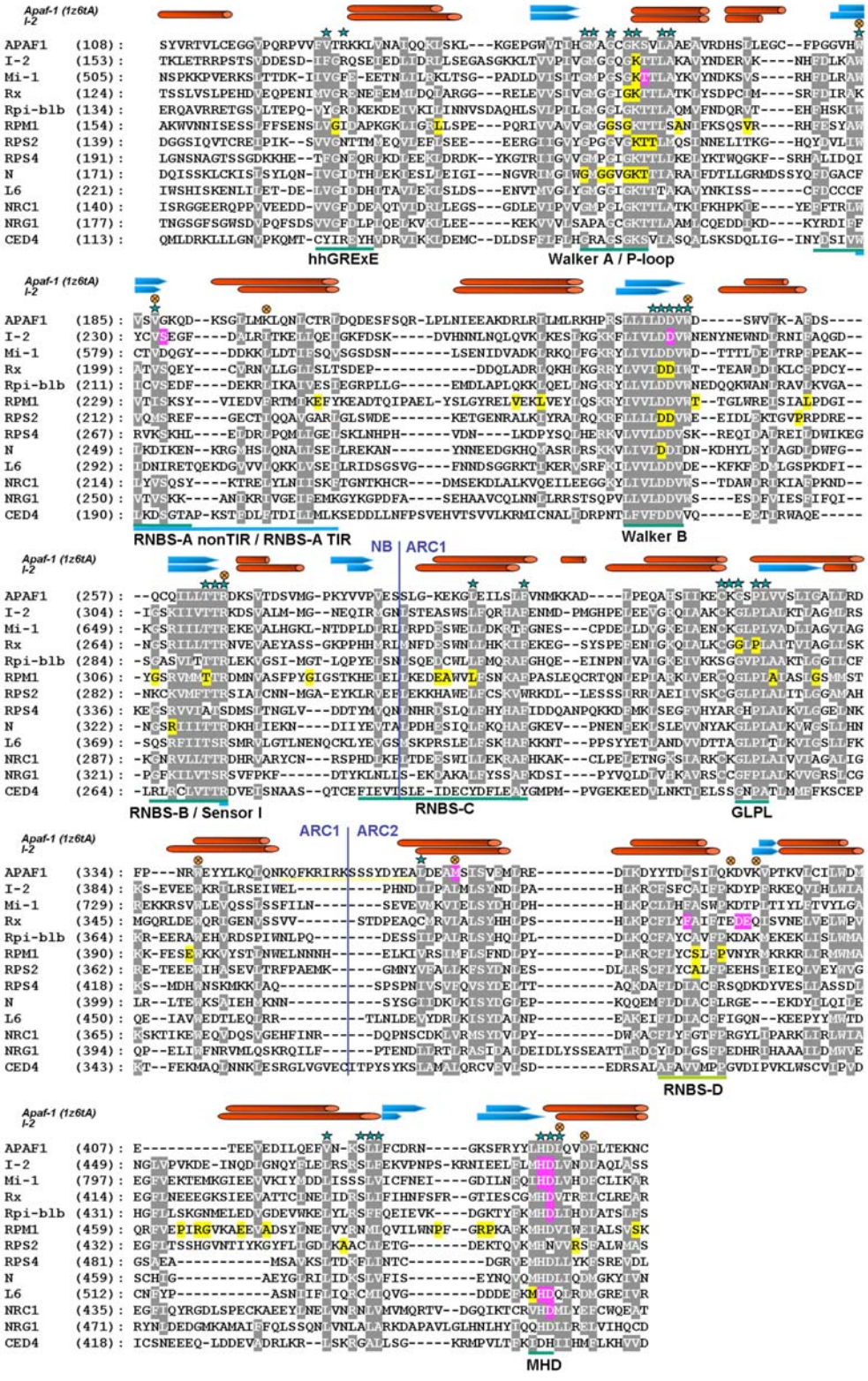
Apaf-1 (1z6tA)
I-2
APAF1 (108) :
I-2 (153) :
Mi-1 (505) :
Rx (124) :
Rpi-blb (134) :
RPM1 (154) :
RPS2 (139) :
RPS4 (191) :
N (171) :
L6 (221) :
NRC1 (140) :
NRG1 (177) :
CED4 (113) :
hhGRExE
Walker A / P-loop
APAF1 (185) :
I-2 (230) :
Mi-1 (579) :
Rx (199) :
Rpi-blb (211) :
RPM1 (229) :
RPS2 (212) :
RPS4 (267) :
N (249) :
L6 (292) :
NRC1 (214) :
NRG1 (250) :
CED4 (190) :
RNBS-A nonTIR / RNBS-A TIR
Walker B
NB | ARC1
APAF1 (257) :
I-2 (304) :
Mi-1 (649) :
Rx (264) :
Rpi-blb (284) :
RPM1 (306) :
RPS2 (282) :
RPS4 (336) :
N (322) :
L6 (369) :
NRC1 (287) :
NRG1 (321) :
CED4 (264) :
RNBS-B / Sensor I
RNBS-C
GLPL
ARC1 | ARC2
APAF1 (334) :
I-2 (384) :
Mi-1 (729) :
Rx (345) :
Rpi-blb (364) :
RPM1 (390) :
RPS2 (362) :
RPS4 (418) :
N (399) :
L6 (450) :
NRC1 (365) :
NRG1 (394) :
CED4 (343) :
RNBS-D
APAF1 (407) :
I-2 (449) :
Mi-1 (797) :
Rx (414) :
Rpi-blb (431) :
RPM1 (459) :
RPS2 (432) :
RPS4 (481) :
N (459) :
L6 (512) :
NRC1 (435) :
NRG1 (471) :
CED4 (418) :
MHD

Figure 6

Structure-based multiple sequence alignment of the NB, ARC1 and ARC2 subdomains of NB-LRR R proteins, Apaf-1 and CED-4. The secondary structure assignment of the Apaf-1 protein (PDB code 1z6t, chain A) and the secondary structure prediction of I-2 are depicted at the top of the alignment (beta-strands in blue, alpha-helices in red). Domain borders are indicated as vertical blue lines. Motifs are annotated as horizontal green and blue lines below the aligned sequences. Amino acid positions experimentally shown to lead to an HR response are highlighted in pink, loss-of-function mutations in yellow. Amino acids located in the ADP binding site of Apaf-1 and well-conserved in R proteins are marked by green stars. Residue positions of potential interest for experiments are marked by orange crossed circles.

difference between Apaf1/CED-4 and R proteins is a loop connecting the ARC1 and ARC2 subdomains, which is considerably shorter in R proteins. Despite these differences, we observe a remarkable conservation of the residues forming the nucleotide binding pocket. This is illustrated in Figure 6, where all residues are marked that are conserved in R proteins and located in the Apaf-1 ADP binding pocket. Most of these amino acids are located in previously defined motifs, except for Apaf-1 serine 422 in the ARC2 subdomain. This serine participates in a water-mediated hydrogen bond to the ADP ribose. A direct hydrogen bond with the β-phosphate of ADP was observed for histidine 438 in the Apaf-1 MHD motif (Riedl et al., 2005). These two important amino acids as well as most of the other conserved ADP binding pocket residues are missing in CED-4. The ARC2 subdomain in R proteins is generally more similar to Apaf-1 than to CED-4. In conclusion, the conserved cluster of residues in the ADP binding pocket make the Apaf-1 ADP bound structure the preferable modelling template for the NB-ARC domain of R proteins.

Protein structure model of I-2 and localization of mutations

Based on the multiple sequence alignment (Fig. 6), we propose a similar secondary structure and a conserved 3D arrangement of protein subdomains and nucleotide binding mode in the NB-ARC domain of R proteins as found for ADP-bound Apaf-1. Therefore, this Apaf-1 crystal structure (PDB code 1z6t, chain A) was chosen as modelling template for I-2 (Fig. 7 and S2). As in case of the Apaf-1 NB-ARC domain, in the NB-ARC structural model of I-2 the ADP molecule is deeply buried in a pocket formed at the interface of the NB, ARC1 and ARC2 subdomains.

Mapping of known loss-of-function mutations identified in the NB-ARC domains of R proteins onto the I-2 structural model reveals that they are located at many different positions scattered throughout the molecule (Fig. 6, motifs indicated in Fig. 7, and (Takken et al., 2006)). When located in the ADP binding pocket, the loss-of-function mutations point to the adenosine binding site of the pocket, possibly affecting ADP

binding. This observation agrees well with the finding that nucleotide binding is essential for R protein function (Tameling et al., 2006).

In contrast to loss-of-function mutations, autoactivating mutations are exclusively located on the opposite side of the interface between the NB and ARC2 subdomains. Here, they map in, or close to, the ADP binding pocket where they are located near the phosphates, which suggests a role in phosphate binding and/or hydrolysis (Fig. 7). This is in good agreement with the observation that hydrolysis mutants are autoactivating (Tameling et al., 2006).

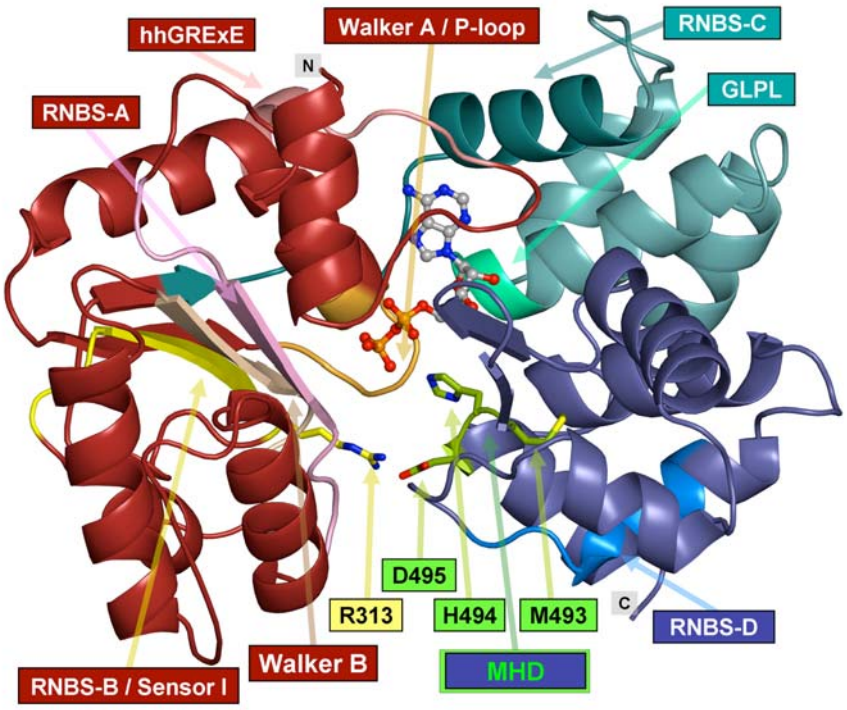

Figure 7

Computationally derived 3D structure model of the NB-ARC domain of the resistance protein I-2. The model was created using the ADP bound structure of human Apaf-1 (PDB code 1z6t, chain A) as structural template for I-2. The locations of R protein motifs are marked with arrows. Amino acids of the MHD motif as well as the sensor I arginine are shown in stick representation. ADP atoms are depicted as balls-and-sticks. Subdomain coloring is: NB: red, ARC1: green, ARC2: blue. Atom coloring is: oxygen: red, nitrogen: blue, phosphorus: orange.

Specific point mutations validate the I-2 NB-ARC structure model

The observed clustering of autoactivating mutations suggests that the model depicted in Figure 7 is a reliable representation of the NB-ARC domain of R proteins. Using this model, residues can be identified that, based on their structural position in the 3D structure, are important for R protein activity. Based on the model, we

selected five mutations at predicted important structural positions (Fig. S2). One mutation (R313A) was made in the sensor I motif and is a predicted loss-of-function mutant. Three mutations were made at the interface of the NB and ARC2 (i.e. W229A, V232A and W285A). One mutation, S474A, was made outside this interface and is not predicted to be of importance and thus should not effect R protein function. As can be seen in Figure 8A, expression of the I-2^{R313A} sensor I mutant induces less cell death (visualised by trypan blue) than expression of wild-type I-2 from the same binary vector. This observation suggests that the mutant is incapable of inducing cell death and might represent a loss of function mutant. Of the other 3 mutants with predicted functional relevance, I-2^{V232A} was found to represent an autoactivation mutant triggering clear HR (Fig. 8B), whereas W229A and W285A represent likely loss-of-function mutants (Fig. 8C and D). As expected, the I-2^{S474A} mutant is indeed neither gain- nor loss-of-function as it shows similar cell death levels like the wild-type I-2 protein (Fig. 8E).
These results support the validity of the NB-ARC model presented in Figure 7, and corroborates its use to derive a molecular function for the MHD motif as discussed below.

Discussion

The central NB-ARC domain in R proteins has been proposed to function as a molecular switch that defines the activation state of the protein depending on the nucleotide bound (Rairdan and Moffett, 2006; Takken et al., 2006; Tameling et al., 2006). In this functional model, the NB subdomain is the primary nucleotide binding and hydrolysis pocket, the ARC1 subdomain is required for the intramolecular interaction with the LRR, and the ARC2 subdomain transduces pathogen perception by the LRR into R protein activation (Rairdan and Moffett, 2006; Tameling et al., 2006). To examine how the ARC2 regulates R protein activity, we focused on the MHD motif in this subdomain. The results presented here indicate that the histidine in the MHD motif is a key component of the 'switch' of R protein activity.

Functional roles of the MHD residues

Both the histidine and the aspartate in the MHD motif are among the most conserved residues in R proteins, pointing to an important functional and structural role (Fig. 3 and 7). As part of a framework of conserved amino acids in the deeply buried ADP binding pocket, the histidine is in an apparently critical position (Fig. 7). This location suggests that it fulfils the same role as proposed for the corresponding histidine in Apaf-1, which is to directly bind and position the β-phosphate of the ADP (Riedl et al., 2005; Albrecht and Takken, 2006). Such a direct interaction of the winged-helix domain with the nucleotide is a unique feature of Apaf-1 and is not found in related

AAA+ ATPases (Riedl et al., 2005). The latter use a conserved arginine residue in the so-called sensor II motif in the helical bundle (corresponding to the ARC1 subdomain) to coordinate the bound nucleotide and control intersubunit interactions (Ogura et al., 2004). The region around the conserved arginine is referred to as sensor II by analogy with an arginine in adenylate kinases that mediates conformational changes upon ATP binding (Müller and Schulz, 1992; Guenther et al., 1997). Unlike in the AAA+ proteins, no sensor II motif is present in STAND proteins like Apaf-1 and R proteins. In Apaf-1, the binding of H438 to the beta-phosphate of the ADP stabilizes the compact closed conformation of the NB-ARC domain (Riedl et al., 2005). Through ADP binding, the histidine and serine participate in the interaction between the NB and the ARC2 subdomains. Mutation of the MHD histidine and aspartate may weaken ADP–protein and inter-subdomain interactions resulting in the destabilization of the closed ADP-bound conformation. Consequently, nucleotide exchange could be favoured, resulting in a constitutively active conformation of the R protein. In this way, the MHD motif takes over both AAA+ protein sensor II functions; coordination of the bound nucleotide and control of intersubunit interactions. Such a major positive regulatory role for the MHD is in line with the observation that combining an MHD mutant with a NB hydrolysis mutant does not result in a faster HR response (Fig. 2).

A sensor II function for the MHD motif could also explain the autoactivating phenotype obtained upon mutation of the aspartate. This aspartate is located C-terminally of the histidine at the positively charged end of an alpha-helix, a position preferably occupied by negatively charged amino acids stabilising the helix dipole. Mutating the aspartate or any other residue present at this position (Fig. 3) might reposition the helix, thereby dislocating the preceding histidine and weakening its interaction with the ADP.

In an ADP-bound conformation, the MHD aspartate may contact the so-called sensor I arginine through a salt bridge (as predicted by the WHAT-IF server). This conserved arginine (Apaf-1 R265, corresponding to R313 in I-2 (Fig. 7)) in the sensor I motif senses the presence of a γ-phosphate on the bound nucleotide in related AAA+ proteins and relays this information to other domains of the protein (Ogura and Wilkinson, 2001). Because only the ADP bound structure has been solved for Apaf-1, it is not known how it senses a γ-phosphate, but the corresponding arginine directly interacts with the γ-phosphate in the crystal structure of ATP-bound CED-4 (Yan et al., 2005). The sensor I maps to the NB subdomain and is hallmarked by the hhhhToR signature, which is referred to as the RNBS-B motif in plant R proteins ((Meyers et al., 1998) and Fig. 6). The importance of this motif was suggested by loss-of function mutations of the two neighboring threonine amino acids in Rpm1 and Prf ((Salmeron et al., 1996; Tornero et al., 2002) and Fig. 6), which could result in a

side chain dislocation of the adjacent sensor I arginine. Direct proof for functional importance of the sensor I arginine was shown by substitution for an alanine. As shown in Figure 8A, this mutation results in a loss-of-function phenotype. In light of this, mutation of the MHD aspartate might not only directly affect ADP binding through a delocalization of the preceding histidine, but could also lead by itself to a more open conformation of the NB-ARC as it can no longer interact with sensor I. An open conformation would result in weaker binding of ADP, allowing exchange for ATP and resulting in R protein activation.

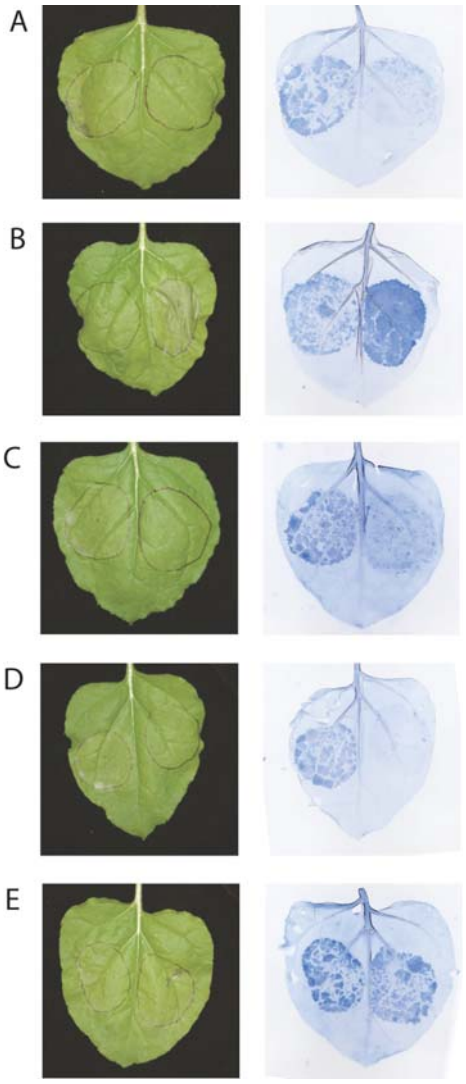

Figure 8
Mutation of predicted important residues alters R protein function. *Nicotiana benthamiana* leaves were agroinfiltrated with constructs to express wild-type or mutant I-2 protein. After pictures were taken (left panels), the same leafs were stained for cell death using trypan blue (right panels). Wild-type I-2 is expressed in the left leaf half, mutants in the right. **(A)** I-2^{R313A} **(B)** I-2^{V232A}, **(C)** I-2^{W229A}, **(D)** I-2^{W285A}, **(E)** I-2^{S474A}.

To conclude, the MHD histidine may be in direct contact with the ADP, and its mutation could directly destabilize the inactive ADP-bound protein complex, allowing nucleotide exchange and activation of the protein. Mutation of the aspartate could both dislocate the histidine making it less effective in repressing the R protein and/or negatively influence the interaction between the NB and ARC2 subdomains, thereby destabilizing the closed, inactive protein conformation.

Implications of the I-2 structural model on residues outside the MHD motif

The availability of a structural model of the NB-ARC domain of R proteins allows the formation of hypotheses on the molecular mechanism underlying autoactivation

phenotypes induced by mutation of residues outside the MHD motif. Most auto-activating mutations in R proteins map to the interface of the NB and the ARC2 subdomains, such as I-2^{S233F}, I-2^{D283E}, Rx^{D399V} and Rx^{E400K} (Bendahmane et al., 2002; Tameling et al., 2006). Our structural model of I-2 shows that I-2 residues S233 and D283 are on the same side of the NB subdomain and are facing Rx residues D399 and E400, which are located on the opposite side, on the ARC2 subdomain.

I-2 mutations S233F and D283E in the NB subdomain (Supplemental Fig. S2) have been shown to reduce the ATP hydrolysis rate (Tameling et al., 2006). Rx residues D399 and E400 in Rx (Bendahmane et al., 2002) are relatively distant from the ATP. These residues are therefore unlikely to be directly involved in ATP hydrolysis. These ARC2 residues, however, contact the residues in the neighbouring NB subdomain and may thus be involved in stabilizing the inactive domain complex. Mutation of these residues may destabilize the inactive conformation, allowing the protein to adopt its activated state. This hypothesis is in agreement with the assumption that STAND ATPases like R proteins undergo conformational changes upon activation (Moffett et al., 2002; Leipe et al., 2004; Rairdan and Moffett, 2006; Takken et al., 2006; Bent and Mackey, 2007; van Ooijen et al., 2007).

The observed clustering of known mutations in our structural model allowed identification of additional mutations that should affect protein function (Fig. 6). These residues are amino acids that are well-conserved and also in the spatial vicinity of experimentally verified sites. Their 3D locations are depicted in the structural model of I-2 (Supplemental Fig. S2). Two conserved residues were selected in the RNBS-A (W299A and V232) because of their predicted positions at the interface between NB and ARC2. Transient expression of the V232A resulted in autoactivating and an intense blue staining upon trypan blue staining (Fig. 8B). This observations supports the hypothesis that this loop is important for interactions between these two subdomain. The W229A mutant was shown to induce less cell death than wild-type I-2, suggesting that it is either hypoactive or inactive (Fig. 8C). In the NB-ARC structure (Supplemental Fig. S2), this tryptophan is deeply buried and has numerous non-covalent interactions with other amino acids, e.g. the Walker B D282. Mutation likely abrogates the stability of the protein fold leavind a non-functional protein.

W285 in the Walker B motif was selected because of its position near the aspartates that are required for ATPase activity. Mutation of this residue resulted in an inactive or hypoactive protein, confirming that this residue is important for function (Figure 8D).

An intriguing difference between R proteins and Apaf-1 as well as CED-4 is the loop connecting ARC1 and ARC2. In CED-4, this loop harbours a tyrosine that, together with the sensor I arginine and the P-loop lysine, is crucial for coordinating the gamma-phosphate of ATP (Yan et al., 2005). Likely, this loop is flexible, enabling

ARC2 dislocation upon activation. The loop is of variable length, but considerably shorter in R proteins (Fig. 6 and Supplemental Fig. S2) and also lacks sequence conservation. In the Apaf-1 structure, the loop covers part of the interface between the NB and ARC2 subdomains and is involved in interdomain re-organization upon activation. This implies that even though the proposed ADP-bound conformation of the NB-ARC domain in R proteins is similar to that of APAF-1, the ATP-bound state might differ.

In conclusion, our data support the current models for R protein function in which the NB-ARC acts as a molecular switch (Takken et al., 2006; Tameling et al., 2006; Bent and Mackey, 2007; van Ooijen et al., 2007). Although a crystal structure is required to confirm the provided 3D model, it can already serve as a framework for the formulation of hypotheses on how mutations exert their effect. This structural model provides insight into the function of the conserved elements within the NB-ARC domain and sheds light on the molecular mechanisms through which R proteins orchestrate plant defence.

ACKNOWLEDGEMENTS

We like to thank Harold Lemereis and Ludek Tikovski for plant handling. Thijs Hendrix is acknowledged for raising the Mi-1 antibody. Martijn Rep is acknowledged for critical review of the manuscript. pKG6210 containing the Mi-1 genomic region was provided by Keygene N.V., The Netherlands. A construct containing the Rpi-blb1 gene was kindly provided by Dr. E. van der Vossen, Wageningen University, Wageningen, The Netherlands.

G.v.O. is supported by the Research Council for Earth and Life Sciences (ALW) with financial aid from the Netherlands Organization for Scientific

Research (NWO). G.M. and M.A. have been financially supported by the German National Genome Research Network (NGFN). The research has been conducted in the context of the BioSapiens Network of Excellence funded by the European Commission under grant number LSHG-CT-2003-503265.

Materials and methods

Construction of vectors

Wild-type I-2 (wp42) and derived mutants D495V (wp45), S233F (wp54) and D283E (wp60) in pGreen (Hellens et al., 2000) have been described (Tameling et al., 2002; de la Fuente van Bentem et al., 2005; Tameling et al., 2006). All oligonucleotides (marked FP) used in this study were purchased from MWG, Germany, and can be found in Table 2. I-2^{D495V} was combined with I-2^{S233F} or I-2^{D283E} by swapping a 0.8 kb *Sal*I/*Bam*HI fragment from wp54 and wp60 into wp45. To make the double I-2$^{S233F/D283E}$ mutant a 3-points ligation was performed; wp45 was digested with *Sal*I/*Acc*65I and fragments of wp60 (*Acc*65I/*Bst*XI) and wp54 (*Sal*I/*Bst*XI) were inserted to obtain I-2$^{S233F/D283E}$.

To generate the H494 mutant library the I-2 coding sequence was PCR amplified from wp42 using primers FP794 and FP796 and gateway *att*B flanks were introduced in a second amplification using FP872 and

FP873. The resulting PCR product was recombined into pDONR207 (Invitrogen) via a Gateway BP clonase (Invitrogen) reaction to obtain pMK13. To establish random mutagenesis of residue 494, a degenerate primer FP1158 containing NNS as a codon for residue 494 was used in combination with FP490. The obtained 336 bp PCR product was subsequently used as a mutagenic megaprimer (Ke and Madison, 1997) in combination with FP216, to amplify a 0.8 kb fragment from wp42. This fragment was digested with *Bam*HI/*Nde*I and ligated into pMK13 using the same sites and subsequently recombined to binary vector CTAPi (Rohila et al., 2004) using a Gateway LR reaction (Invitrogen, Carlsbad, USA). Because the I-2 sequence contains its endogenous stop codon there is no translational fusion to the TAP tag. pMK13 was used as a template for circular mutagenesis (Hemsley et al., 1989) to generate I-2 mutants W229A, V232A, W285A, R313A, and S474A using primer pairs FP1834/FP1835, FP1836/FP1837, FP1838/FP1839, FP1840/FP1841, FP1844/FP1845, respectively. The resulting mutant isoforms were subsequently recombined to CTAPi (Rohila et al., 2004) by a Gateway LR reaction (Invitrogen). Creation of pSE23, a binary construct containing Mi-1 under control of its endogenous promoter, and the Mi-1^{T557S} mutation is described before (Gabriëls et al., 2007). The coding sequence of Mi-1, including its stop codon and intron, was amplified from pSE23 by PCR using primers FP764 and FP766, and Gateway *att*B flanks were added by adapter PCR using primers FP872 and FP873. The PCR product was transferred to binary vector CTAPi (Rohila et al., 2004) by the Gateway one-tube protocol for cloning *att*B-PCR products directly into destination vectors (Invitrogen) to create pG74. Mi-1 D841V was generated using pG74 as a template for mutagenic overlap extension PCR (Higuchi et al., 1988) using primer sets FP860/FP873 and FP861/FP872. Likewise, the constructs containing Mi-1 H840R,

Tab2 Oligonucleotide sequence

FP	Sequence
211	ctggtcgaccaaccataatgctacttaaataagg
216	gacatgcatttgaaaacatgg
490	taatccatgtccgagaaata
754	caagatgcatgttctcatcc
755	catacaggttcaagtatc
756	ccacctgtctaactcatccactaccc
764	aaaaagcaggctctatggaaaaacgaaaagatatt
766	agaaagctgggttctacttaaataaggggatattctt
771	aaaaagcaggctctatggctgaagctttcatt
793	agaaagctgggttttaaatatatatattcacattag
794	aaaaagcaggctctatggagattggcttagcag
796	agaaagctgggttttaaatatatttccaatcgata
860	ccaaattcatgttcttgtgcatga
861	gtcatgcacaagaacatgaatttgg
872	ggggacaagtttgtacaaaaaagcaggct
873	ggggaccactttgtacaagaaagctgggt
1095	cgggatcccatgggttgatactgaatgg
1099	gtatgccgggttcaggtgcagcaactttggcatacaaagtatac
1100	gatatactgaatttccaaattgctgatcttgtgcatgacttttg
1102	gtatactttgtatgccaaagttgctgcacctgaacccggcatac
1103	caaaagtcatgcacaagatcagcaatttggaaattcagtatatc
1158	gaggaattattccttatgnnsgaccttgtcaatgatttag
1541	ctgaatttccaaattcttgatcttgtgcatgac
1542	gtcatgcacaagatcaagaatttggaaattcag
1543	ctgaatttccaaattcgtgatcttgtgcatgac
1544	gtcatgcacaagatcacgaatttggaaattcag
1545	ctgaatttccaaattgttgatcttgtgcatgac
1546	gtcatgcacaagatcaacaatttggaaattcag
1547	ctgaatttccaaatttaggatcttgtgcatgac
1548	gtcatgcacaagatcctaaatttggaaattcag
1598	ctgaatttccaaattcaggatcttgtgcatgac
1599	gtcatgcacaagatcctgaatttggaaattcag
1834	cattttgatttgaaagcggcgtattgcgtttctgaagg
1835	ccttcagaaacgcaatacgccgctttcaaatcaaaatg
1836	gaaagcgtggtattgcgcttctgaaggatttgatgc
1837	gcatcaaatccttcagaagcgcaataccacgctttc
1838	gttttggatgatgtggcgaatgaaaattacaacg
1839	cgttgtaattttcattcgccacatcatccaaaac
1840	gatcattgtgacgacagcccaaagacagtgttgcc
1841	ggcaacactgtctttggctgtcgtcacaatgatc
1844	gagttgagatcaagagcattatttgaaaaggtccc
1845	gggacctttcaaataatgctcttgatctcaactc

Mismatches are underlined in mutagenic primers

H840V, H840stop and H840Q were generated using overlap extension with sets of either wild-type primer FP872 or FP873 in combination with mutagenic primers FP1543/FP1544, FP1545/FP1546, FP1547/FP1548 and FP1581/FP1582, respectively. The resulting 3.8 kb products were digested with *Bsp*119I/*Eco*72I and cloned into pG74 cut with the same enzymes.pG104 was obtained by ligating a 3.3 kb *Bam*HI/*Sal*I digested Mi-1 PCR product that was amplified with FP1095 and FP211 into pGEX-4T-1 (GE Healthcare) digested *Bam*HI/*Xho*I. For construction of Mi-1$^{KT556/557AA}$ and Mi-1^{H840A}, pG104 was used as a template for circular mutagenesis (Hemsley et al., 1989). The mutations were introduced using primer sets FP1099/FP1102 and FP1100/FP1103 to create pG108 and pG109, respectively. An Eco72I/Bsp119I fragment was exchanged between pG108 or pG109 and pG74 to obtain Mi-1$^{KT556/557AA}$ and Mi-1^{H840A}.
For heterologous Mi-1 protein production in *E. coli* for rabbit immunization, plasmid pKG6210 (Keygene N.V.) containing genomic Mi-1 promoter and coding sequence was used to transfer a Mi-1 *Nco*I/*Bsm*I fragment into pAS2-1 (Clontech Laboratories) digested *Nco*I/*Sma*I to obtain pSE06. An *Msc*I/*Sal*I fragment from pSE06 was ligated in pGEX-KG (Guan and Dixon, 1991) digested *Sma*I/*Sal*I to obtain pG01.
Rpi-blb1 constructs are amplified using FP771 and FP793 from pBINPLUS-RGA2-blb (van der Vossen et al., 2003). Gateway adapters were added to the coding sequence using FP872 and FP873, and the product was cloned into pDONR207 via a Gateway BP reaction to create pO2. Mutation D475V was introduced using the megaprimer method (Ke and Madison, 1997). The megaprimer was generated using primers FP754 and FP755 and, after purification the fragment, was extended using FP756. The product was digested *Eco*RI/*Bgl*II, and this 1.6 kb insert is ligated in a 3-point ligation with pO2 fragments generated by *Eco*RI/*Pst*I and *Pst*I/*Bgl*II to obtain pDONR207 containing Rpi-blb1^{D475V} with an intact stop codon. The insert was transferred to binary vector CTAPi in a Gateway LR reaction (Invitrogen). Correct sequences of all clones was confirmed by sequencing.

Agrobacterium-mediated transient transformation and protein extraction.
Agrobacterium tumefaciens strain GV3101(pMP90) (Koncz and Schell, 1986) was transformed with binary constructs (Takken et al., 2000) and grown to OD_{600}=0.8 in YEB medium supplemented with 20 µM acetosyringone and 10 mM MES pH 5.6. Cells were pelleted and resuspended in infiltration medium (1x MS, 10 mM MES pH 5.6, 2% w/v sucrose) and infiltrated at OD_{600}=0.2 (for I-2, Rx and Rpi-blb1 constructs) or 1 (for Mi-1 constructs) into four-weeks-old *Nicotiana benthamiana* leaves.
For protein extraction, nine independent leaves were harvested and pooled 24 hours after agroinfiltration and frozen in liquid nitrogen. After grinding the tissue, it was allowed to thaw in 2 ml protein extraction buffer per gram of tissue (25 mM Tris pH 7.5, 1 mM EDTA, 150 mM NaCl, 10% Glycerol, 5 mM DTT, 1 x Roche Complete protease inhibitor cocktail and 2% PVPP). Extracts were cleared by centrifugation at 12,000 krcf at 4º C for 10 minutes and the supernatant was passed over 4 layers of Miracloth to obtain a total protein lysate. Samples were mixed with Laemmli sample buffer, and equal amounts of total protein were run at 8% SDS-PAGE gels and blotted on PVDF membranes using semi-dry blotting. Equal loading was assayed by Ponceau S staining of Rubisco. 5% Skimmed milk powder was used as blocking agent.

Trypan blue staining
Leaves were boiled for 5 minutes in a 1:1 mixture of ethanol and 0.33 mg/ml trypan blue in lactophenol, and destained overnight in 2.5 g/ml chloral hydrate in dH_2O.

Multiple sequence alignment of the MHD motif
R protein sequences found in the NCBI database were aligned using the MacVector ClustalW analysis tool (Oxford Molecular Group). The aligned sequences are sorted according to a phylogenetic tree constructed by neighbour-joining and midpoint-rooting in MacVector.

Antibody production

Anti-I-2 was produced in rabbit by Eurogentec, Seraing, Belgium, against synthetic peptide FEKVPNPSKRNIEE, which maps just N-terminal of the MHD motif and is affinity purified.
pG01 was transformed to *E. coli* BL21 (DE3) and expression of fusion protein GST-Mi-1, amino acids 161-899, was induced by addition of IPTG. The fusion protein was isolated using glutathione sepharose (GE Healthcare). The Mi-1 part was released from the glutathione beads using biotinylated human thrombin (Sigma). Thrombin was subsequently removed using streptavidin beads (Stratagene). Immunization was performed by injecting twice 250 µg purified Mi-1 (aa 161-899) protein into two New Zealand White rabbits with a 12-week interval. 14 weeks after the first injection, serum was collected and analyzed for specific cross-reactivity to purified Mi-1 in comparison to the pre-immune sera. Serum showing the highest signal was used to detect Mi-1 in planta. For Western blot detection, both the Mi-1 antibody and the secondary antibody goat anti-rabbit (Rockland Inc.) are used in a dilution of 1:4000 in PBSt.

Structure-based multiple sequence alignment of the NB-ARC domain

We created a multiple sequence alignment of the following R proteins and related sequences from the UniProtKB database using the program MUSCLE (Edgar, 2004): human Apaf-1 (O14727), tomato I-2 (Q9XET3) and Mi-1 (O81137), potato Rx (Q9XGF5), wild potato Rpi-blb (Q7XBQ9), mouse-ear cress RPM1 (Q39214), RPS2 (Q42484) and RPS4 (Q9XGM3), TMV resistance protein N (Q40392), linseed L6 (Q40253), tomato NRC1 (A1X877), *N. benthamiana* NRG1 (Q4TVR0), and nematode CED-4 (P30429). The secondary structure assignment of the PDB structure of Apaf-1 (identifier 1z6t, chain A) was obtained from the DSSP database (http://www.cmbi.kun.nl/gv/dssp/) and added to the alignment. To predict the secondary structure of R-proteins, we contacted the protein structure prediction server PSIPRED (http://bioinf.cs.ucl.ac.uk/psipred/). We improved the alignment manually by minor adjustments based on structure prediction results and pairwise superposition of the PDB structures of Apaf-1 (identifier 1z6t, chain A) and CED-4 (identifier 2a5y, chain B). Since the relative spatial orientation of the otherwise well-conserved NB, ARC1 and ARC2 subdomains of Apaf-1 and CED-4 differs, we applied the FATCAT program for structure superposition (Ye and Godzik, 2003), which considers conformational flexibility. Subdomain borders were taken from (Albrecht and Takken, 2006). Shading of more than 60% physicochemically conserved residues was produced by GeneDoc (http://www.psc.edu/biomed/genedoc/).

3D structure model of I-2

Based on the structure-based multiple sequence alignment of the NB-ARC domain, a pairwise sequence-structure alignment of tomato R protein I-2 and human Apaf-1 was constructed and formed the input into the 3D-modeling server WHAT IF (Vriend, 1990). This server returned a full-atom structure model of the NB-ARC domain of I-2. The structure of Apaf-1 (PDB code 1z6t, chain A) comprises the residues 108-450 (UniProt sequence O14727) and is mapped on the I-2 residues 153-506 (UniProt sequence Q9XET3). Interatomic contacts (van der Waals interactions, salt bridges, hydrogen bonds) were calculated by the WHAT IF server (Vriend, 1990).
The protein structure image of the model was illustrated using PyMOL (http://www.pymol.org).

Supplementary data

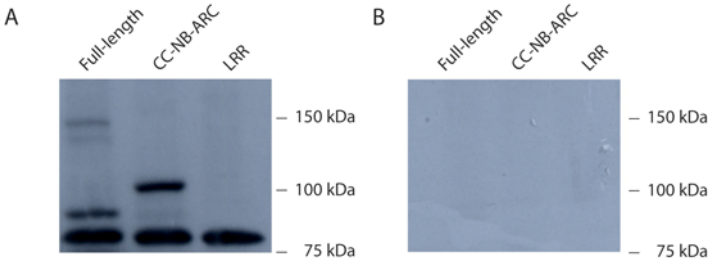

Figure S1

The Mi-1 antibody specifically recognizes transiently expressed Mi-1 protein. Western blots of 10 % SDS-PAGE gels loaded with total protein extracts of *Nicotiana benthamiana* leaves harvested 24 hours after agroinfiltration with constructs to express either full-length Mi-1, Mi-1 CC-NB-ARC, or Mi-1 LRR as indicated. One blot is probed with the Mi-1 antibody (**A**), the other with pre-immune serum (**B**). In both cases, peroxidase-linked goat anti-rabbit is used as a secondary antibody. Both full-length Mi-1 and Mi-1 CC-NB-ARC migrate according to their predicted molecular masses of ~145 and ~103 kDa.

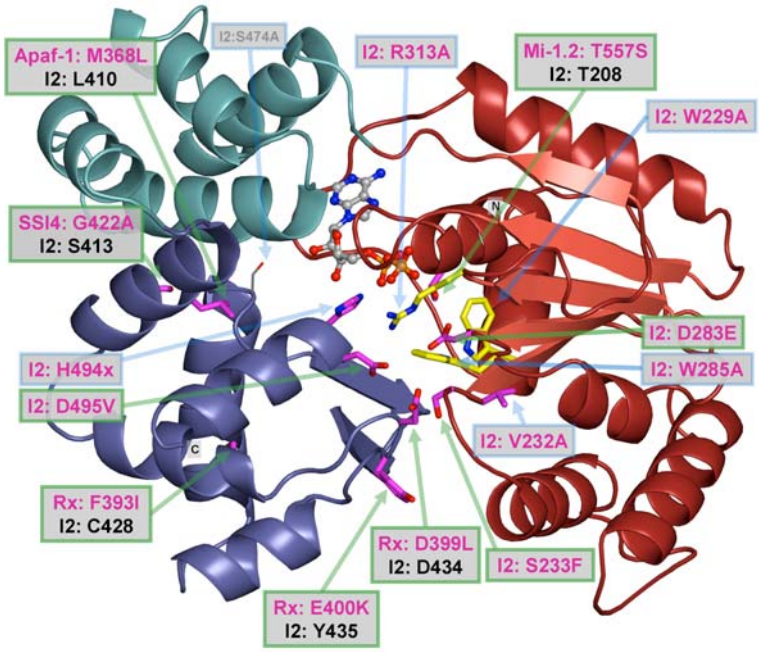

Figure S2

Structure model of the NB-ARC domain of I-2 indicates predicted important positions. Computationally derived 3D structure model of the NB-ARC domain of the resistance protein I-2. The model was created using the ADP bound structure of human Apaf-1 (PDB code 1z6t, chain A) as structural template for I-2. The protein name and the position of each mutation are indicated in magenta, the corresponding residues of I-2 are added in black. The locations of R protein mutations leading to HR are depicted as magenta sticks, leading to loss-of-function as yellow sticks. Mutations described in this study are framed in blue, otherwise in green. ADP atoms are depicted as balls-and-sticks. Subdomain coloring is: NB: red, ARC1: green, ARC2: blue. Atom coloring is: oxygen: red, nitrogen: blue, phosphorus: orange.

References

Albrecht, M., and Takken, F.L.W. (2006). Update on the domain architectures of NLRs and R proteins. Biochem Biophys Res Commun **339,** 459-462.

Ausubel, F.M. (2005). Are innate immune signaling pathways in plants and animals conserved? Nat Immunol **6,** 973-979.

Axtell, M.J., McNellis, T.W., Mudgett, M.B., Hsu, C.S., and Staskawicz, B.J. (2001). Mutational analysis of the *Arabidopsis RPS2* disease resistance gene and the corresponding *Pseudomonas syringae avrRpt2* avirulence gene. Mol Plant Microbe Interact **14,** 181-188.

Bendahmane, A., Farnham, G., Moffett, P., and Baulcombe, D.C. (2002). Constitutive gain-of-function mutants in a nucleotide binding site-leucine rich repeat protein encoded at the *Rx* locus of potato. Plant J **32,** 195-204.

Bent, A., and Mackey, D. (2007). Elicitors, Effectors, and R Genes: The New Paradigm and a Lifetime Supply of Questions. Annu Rev Phytopathol **45,** 399-436.

de la Fuente van Bentem, S., Vossen, J.H., de Vries, K.J., van Wees, S., Tameling, W.I.L., Dekker, H.L., de Koster, C.G., Haring, M.A., Takken, F.L.W., and Cornelissen, B.J.C. (2005). Heat shock protein 90 and its co-chaperone protein phosphatase 5 interact with distinct regions of the tomato I-2 disease resistance protein. Plant J **43,** 284-298.

Dinesh-Kumar, S.P., Tham, W.H., and Baker, B.J. (2000). Structure-function analysis of the tobacco mosaic virus resistance gene *N*. Proc Natl Acad Sci USA **97,** 14789-14794.

Edgar, R.C. (2004). MUSCLE: multiple sequence alignment with high accuracy and high throughput. Nucleic acids res **32,** 1792-1797.

Gabriëls, S.H.E.J., Takken, F.L.W., Vossen, J.H., de Jong, C.F., Liu, Q., Turk, S.C., Wachowski, L.K., Peters, J., Witsenboer, H.M., de Wit, P.J.G.M., and Joosten, M.H.A.J. (2006). cDNA-AFLP combined with functional analysis reveals novel genes involved in the hypersensitive response. Mol Plant Microbe Interact **19,** 567-576.

Gabriëls, S.H.E.J., Vossen, J.H., Ekengren, S.K., van Ooijen, G., Abd-El-Haliem, A.M., van den Berg, G.C.M., Rainey, D.Y., Martin, G.B., Takken, F.L.W., de Wit, P.J.G.M., and Joosten, M.H.A.J. (2007). An NB-LRR protein required for HR signalling mediated by both extra- and intracellular resistance proteins. Plant J **50,** 14-28.

Grant, M.R., Godiard, L., Straube, E., Ashfield, T., Lewald, J., Sattler, A., Innes, R.W., and Dangl, J.L. (1995). Structure of the Arabidopsis *RPM1* gene enabling dual specificity disease resistance. Science **269,** 843-846.

Guan, K.L., and Dixon, J.E. (1991). Eukaryotic proteins expressed in Escherichia coli: an improved thrombin cleavage and purification procedure of fusion proteins with glutathione S-transferase. Anal biochem **192,** 262-267.

Guenther, B., Onrust, R., Sali, A., O'Donnell, M., and Kuriyan, J. (1997). Crystal structure of the delta' subunit of the clamp-loader complex of E. coli DNA polymerase III. Cell **91,** 335-345.

Hellens, R., Mullineaux, P., and Klee, H. (2000). Technical Focus:a guide to *Agrobacterium* binary Ti vectors. Trends Plant Sci **5,** 446-451.

Hemsley, A., Arnheim, N., Toney, M.D., Cortopassi, G., and Galas, D.J. (1989). A simple method for site-directed mutagenesis using the polymerase chain reaction. Nucleic acids res **17,** 6545-6551.

Higuchi, R., Krummel, B., and Saiki, R.K. (1988). A general method of *in vitro* preparation and specific mutagenesis of DNA fragments: study of protein and DNA interactions. Nucleic acids res **16,** 7351-7367.

Howles, P., Lawrence, G., Finnegan, J., McFadden, H., Ayliffe, M., Dodds, P., and Ellis, J. (2005). Autoactive alleles of the flax *L6* rust resistance gene induce non-race-specific rust resistance associated with the hypersensitive response. Mol Plant Microbe Interact **18,** 570-582.

Hwang, C.F., Bhakta, A.V., Truesdell, G.M., Pudlo, W.M., and Williamson, V.M. (2000). Evidence for a role of the N terminus and leucine-rich repeat region of the *Mi* gene product in regulation of localized cell death. Plant Cell **12,** 1319-1329.

Jones, J.D.G., and Dangl, J.L. (2006). The plant immune system. Nature **444,** 323-329.

Ke, S.H., and Madison, E.L. (1997). Rapid and efficient site-directed mutagenesis by single-tube 'megaprimer' PCR method. Nucleic acids res **25,** 3371-3372.

Koncz, C., and Schell, J. (1986). The promoter of Tl-DNA gene *5* controls the tissue-specific expression of chimaeric genes carried by a novel type of *Agrobacterium* binary vector. Mol Gen Genet **204,** 383-396.

Leipe, D.D., Koonin, E.V., and Aravind, L. (2004). STAND, a class of P-loop NTPases including animal and plant regulators of programmed cell death: multiple, complex domain architectures, unusual phyletic patterns, and evolution by horizontal gene transfer. J Mol Biol **343,** 1-28.

Martin, G.B., Bogdanove, A.J., and Sessa, G. (2003). Understanding the functions of plant disease resistance proteins. Annu Rev Plant Biol **54,** 23-61.

Mestre, P., and Baulcombe, D.C. (2006). Elicitor-mediated oligomerization of the tobacco N disease resistance protein. Plant Cell **18,** 491-501.

Meyers, B.C., Dickerman, A.W., Michelmore, R.W., Sivaramakrishnan, S., Sobral, B.W., and Young, N.D. (1999). Plant disease resistance genes encode members of an ancient and diverse protein family within the nucleotide-binding superfamily. Plant J **20,** 317-332.

Meyers, B.C., Chin, D.B., Shen, K.A., Sivaramakrishnan, S., Lavelle, D.O., Zhang, Z., and Michelmore, R.W. (1998). The major resistance gene cluster in lettuce is highly duplicated and spans several megabases. Plant Cell **10,** 1817-1832.

Moffett, P., Farnham, G., Peart, J., and Baulcombe, D.C. (2002). Interaction between domains of a plant NBS-LRR protein in disease resistance-related cell death. EMBO J **21,** 4511-4519.

Müller, C.W., and Schulz, G.E. (1992). Structure of the complex between adenylate kinase from Escherichia coli and the inhibitor Ap5A refined at 1.9 Å resolution. A model for a catalytic transition state. J Mol Biol **244,** 159-177.

Ogura, T., and Wilkinson, A.J. (2001). AAA+ superfamily ATPases: common structure--diverse function. Genes Cells **6,** 575-597.

Ogura, T., Whiteheart, S.W., and Wilkinson, A.J. (2004). Conserved arginine residues implicated in ATP hydrolysis, nucleotide-sensing, and inter-subunit interactions in AAA and AAA+ ATPases. J Struct Biol **146,** 106-112.

Pan, Q., Liu, Y.S., Budai Hadrian, O., Sela, M., Carmel Goren, L., Zamir, D., and Fluhr, R. (2000). Comparative genetics of nucleotide binding site-leucine rich repeat resistance gene homologues in the genomes of two dicotyledons: tomato and *Arabidopsis*. Genetics **155,** 309-322.

Peart, J.R., Mestre, P., Lu, R., Malcuit, I., and Baulcombe, D.C. (2005). NRG1, a CC-NB-LRR protein, together with N, a TIR-NB-LRR protein, mediates resistance against Tobacco Mosaic Virus. Curr Biol **15,** 968-973.

Rairdan, G., and Moffett, P. (2007). Brothers in arms? Common and contrasting themes in pathogen perception by plant NB-LRR and animal NACHT-LRR proteins. Microbes Infect **9,** 677-686.

Rairdan, G.J., and Moffett, P. (2006). Distinct domains in the ARC region of the potato resistance protein Rx mediate LRR binding and inhibition of activation. Plant Cell **18,** 2082-2093.

Riedl, S.J., and Salvesen, G.S. (2007). The apoptosome: signalling platform of cell death. Nature rev **8,** 405-413.

Riedl, S.J., Li, W., Chao, Y., Schwarzenbacher, R., and Shi, Y. (2005). Structure of the apoptotic protease-activating factor 1 bound to ADP. Nature **434,** 926-933.

Rohila, J.S., Chen, M., Cerny, R., and Fromm, M.E. (2004). Improved tandem affinity purification tag and methods for isolation of protein heterocomplexes from plants. Plant J **38,** 172-181.

Salmeron, J.M., Oldroyd, G.E.D., Rommens, C.M.T., Scofield, S.R., Kim, H.S., Lavelle, D.T., Dahlbeck, D., and Staskawicz, B.J. (1996). Tomato *Prf* is a member of the leucine-rich repeat class of plant disease resistance genes and lies embedded within the *Pto* kinase gene cluster. Cell **86,** 123-133.

Sun, Q., Collins, N.C., Ayliffe, M., Smith, S.M., Drake, J., Pryor, T., and Hulbert, S.H. (2001). Recombination between paralogues at the *rp1* rust resistance locus in maize. Genetics **158,** 423-438.

Takken, F.L.W., Albrecht, M., and Tameling, W.I.L. (2006). Resistance proteins: molecular switches of plant defence. Curr Opin Plant Biol **9,** 383-390.

Takken, F.L.W., Luderer, R., Gabriëls, S.H.E.J., Westerink, N., Lu, R., de Wit, P.J.G.M., and Joosten, M.H.A.J. (2000). A functional cloning strategy, based on a binary PVX-expression vector, to isolate HR-inducing cDNAs of plant pathogens. Plant J **24,** 275-283.

Tameling, W.I.L., Elzinga, S.D., Darmin, P.S., Vossen, J.H., Takken, F.L.W., Haring, M.A., and Cornelissen, B.J.C. (2002). The tomato *R* gene products I-2 and Mi-1 are functional ATP binding proteins with ATPase activity. Plant Cell **14,** 2929-2939.

Tameling, W.I.L., Vossen, J.H., Albrecht, M., Lengauer, T., Berden, J.A., Haring, M.A., Cornelissen, B.J.C., and Takken, F.L.W. (2006). Mutations in the NB-ARC domain of I-2 that impair ATP hydrolysis cause autoactivation. Plant Physiol **140,** 1233-1245.

Tao, Y., Yuan, F., Leister, R.T., Ausubel, F.M., and Katagiri, F. (2000). Mutational analysis of the Arabidopsis nucleotide binding site-leucine- rich repeat resistance gene *RPS2*. Plant Cell **12,** 2541-2554.

Ting, J.P., Kastner, D.L., and Hoffman, H.M. (2006). CATERPILLERs, pyrin and hereditary immunological disorders. Nat Rev Immunol **6,** 183-195.

Tornero, P., Chao, R.A., Luthin, W.N., Goff, S.A., and Dangl, J.L. (2002). Large-scale structure-function analysis of the *Arabidopsis* RPM1 disease resistance protein. Plant Cell **14,** 435-450.

van der Biezen, E.A., and Jones, J.D.G. (1998). The NB-ARC domain: a novel signalling motif shared by plant resistance gene products and regulators of cell death in animals. Curr Biol **8,** R226-228.

van der Vossen, E., Sikkema, A., Hekkert, B.L., Gros, J., Stevens, P., Muskens, M., Wouters, D., Pereira, A., Stiekema, W., and Allefs, S. (2003). An ancient R gene from the wild potato species Solanum bulbocastanum confers broad-spectrum resistance to Phytophthora infestans in cultivated potato and tomato. Plant J **36,** 867-882.

van Ooijen, G., van den Burg, H.A., Cornelissen, B.J.C., and Takken, F.L.W. (2007). Structure and function of resistance proteins in solanaceous plants Annu Rev Phytopathol **45,** 43-72.

Vriend, G. (1990). WHAT IF: a molecular modeling and drug design program. J Mol Graphics **8,** 52-56, 29.

Yan, N., Chai, J., Lee, E.S., Gu, L., Liu, Q., He, J., Wu, J.W., Kokel, D., Li, H., Hao, Q., Xue, D., and Shi, Y. (2005). Structure of the CED-4-CED-9 complex provides insights into programmed cell death in *Caenorhabditis elegans*. Nature **437,** 831-837.

Ye, Y., and Godzik, A. (2003). Flexible structure alignment by chaining aligned fragment pairs allowing twists. Bioinformatics **19 Suppl 2,** II246-II255.

Chapter 4

Transcomplementation, but not physical association of the CC-NB-ARC and LRR domains of tomato R protein Mi-1.2 is altered by mutations in the ARC2 subdomain

Gerben van Ooijen, Gabriele Mayr[1], Mario Albrecht[1], Ben J. C. Cornelissen and Frank L. W. Takken

[1] Max Planck Institute for Informatics, Saarbrücken, Germany
Published in: Molecular Plant, 2008, Volume 1, 401-410

Race-specific disease resistance in plants is mediated by Resistance (R) proteins that recognise pathogen attack and initiate defence responses. Most R proteins contain a central NB-ARC domain and a C-terminal leucine-rich repeat (LRR) domain. We analysed the intramolecular interaction of the LRR domain of tomato R protein Mi-1.2 with its N-terminus. We expressed the CC-NB-ARC and LRR parts *in trans* and analysed functional transcomplementation and physical interactions. We show that these domains functionally transcomplement when expressed *in trans*. Known autoactivating LRR domain swaps were found to induce a hypersensitive response (HR) upon co-expression *in trans*. Likewise, autoactivating mutants in the NB subdomain transcomplemented to induce HR. Point mutations in the ARC2 subdomain that induce strong autoactivation in the full-length Mi-1.2 protein, however, fail to induce HR in the transcomplementation assay. These data indicate distinct functions for the three NB-ARC subdomains in induction of HR signalling. Furthermore, dissociation of the LRR is not required to release its negative regulation, as in all combinations of CC-NB-ARC and LRR domains tested a physical interaction was observed.

Introduction

Race-specific resistance in plants is mediated by specific surveillance proteins called resistance (R) proteins (Tameling and Takken, 2007). Upon pathogen perception, R proteins trigger a strong defence response often culminating in a hypersensitive response (HR), a form of programmed cell death mechanism aimed at restricting pathogen proliferation. Most R proteins are large intracellular proteins that contain a central Nucleotide Binding (NB-) domain fused to a C-terminal leucine-rich repeat (LRR) domain.

The LRR domain consists of a variable number of leucine-rich repeat units and harbours negative as well as positive regulatory functions. The positive regulatory role for R protein function is apparent as the LRR domain is indispensable and deletion normally does not result in constitutive activity (Bendahmane et al., 2002; Hwang and Williamson, 2003; Rathjen and Moffett, 2003). The negative regulatory function becomes clear when an LRR is improperly matched to the rest of an R protein. For instance, swapping the Mi-1.2 LRR region into paralogue Mi-1.1 results in autoactivity, i.e. activation of defence responses in the absence of the pathogen. The reciprocal swap results in loss of nematode resistance in transgenic roots (Hwang et al., 2000). Likewise, autoactivation upon LRR exchange has been observed for maize Rp1 homologues (Sun et al., 2001) and by swapping parts of the potato Rx LRR domain for the corresponding (highly homologous) Gpa2 sequences (Rairdan and Moffett, 2006). These experiments suggest that the LRR domain interacts with the rest of the protein and that improper pairing can result in de-repression of the protein. Direct physical and functional interaction of the R protein LRR domain with the rest of the protein has indeed been shown, first for potato Rx (Moffett et al., 2002) and later for tobacco N (Ueda et al., 2006), pepper Bs2 (Leister et al., 2005) and *Arabidopsis* RPS5 (Ade et al., 2007). Altogether, these observations indicate that subtle intramolecular interactions between the LRR domain and the N-terminus are required for proper R protein function.

The most well-conserved protein domain in NB-LRR proteins is the NB-ARC domain. This nucleotide-binding domain is found in proteins such as human Apaf-1, plant R proteins and *C. elegans* Ced-4 (ARC), hence its name NB-ARC. When the crystal structures of NB-ARC domains were established for Apaf-1 and CED-4 (Riedl et al., 2005; Yan et al., 2005), it became apparent that the NB-ARC consists of structurally defined subdomains. No plant NB-ARC domain has been crystallised so far, but based on homology modelling it has been proposed that the R protein NB-ARC consists of three subdomains; a nucleotide-binding fold (NB), a four-helix bundle (ARC1) and a winged-helix fold (ARC2) (Albrecht and Takken, 2006). These subdomains are spatially well-defined and are proposed to have functionally distinct roles, as elaborated below. The NB-ARC domain of R proteins I-2, Mi-1 and N have

been shown to be a functional module for nucleotide binding and hydrolysis (Tameling et al., 2002; Ueda et al., 2006). For I-2 it has been proposed that the ATP-bound state represents the active state and hydrolysis of the nucleotide is proposed to return the R protein into its resting state (Takken et al., 2006; Tameling et al., 2006). The nucleotide is likely bound at the interface between the NB, the ARC1 and ARC2, whose interactions are dependent on the nucleotide type (Takken et al., 2006).

Some aspects of the ARC1 subdomain function have been revealed by a series of domain swaps between R proteins Rx and Gpa2 (Rairdan and Moffett, 2006). These studies showed that the Rx ARC1 subdomain is necessary for the interaction of the N-terminus with the LRR domain. LRR binding seems to be a general feature of the ARC1 subdomain, since the Rx N-terminus was able to interact with the LRR domains of several other NB-LRR proteins. An extensive interaction surface with several individual contacts quantitatively contributing to the interaction was shown between the ARC1 and the LRR domain (Rairdan and Moffett, 2006). Together with the fact that no autoactive mutants have been described in this region suggests that the ARC1 subdomain is merely a scaffold regulating the intramolecular interactions with the LRR domain.

The ARC2 subdomain is proposed to relay pathogen recognition, mediated by the LRR domain into changes in R protein conformation, unleashing its downstream signaling potential. Swapping the Gpa2 ARC2 subdomain with the Rx ARC2 domain results in a constitutively active chimera (Rairdan and Moffett, 2006). Apparently, the ARC2 subdomain of Gpa2 and the LRR domain of Rx are sufficiently compatible to induce HR, but are not harmonized to prevent autoactivation. A role for the ARC2 subdomain in signal transduction fits with the fact that many autoactivating mutations in R proteins map to the ARC2 (Bendahmane et al., 2002; Shirano et al., 2002; de la Fuente van Bentem et al., 2005; Howles et al., 2005; Gabriëls et al., 2007). Support for such a regulatory function for the ARC2 is provided by mutational analysis of the conserved MHD motif in the ARC2 and modeling of the I-2 NB-ARC domain on the related human protein Apaf-1 (Chapter 3).

NB-LRR proteins can be roughly divided into two main subclasses depending on their N-terminal domain flanking the NB-ARC (Tameling and Takken, 2007; van Ooijen et al., 2007). This domain is either a region with homology to the *Drosophila* Toll and human Interleukin-1 Receptor proteins (the TIR domain), or a region of 120-200 amino acids without such homology, sometimes containing coiled-coil (CC) motifs. In solanaceous plants, several CC-NB-ARC-LRR proteins have a significantly larger N-terminal domain, and the presence of this extended N-terminus might indicate a difference in function between these and the ‘regular’ CC-NB-ARC-LRR proteins (Mucyn et al., 2006; Rairdan and Moffett, 2007). The R protein Mi-1.2

(Milligan et al., 1998; Vos et al., 1998) belongs to the group of CC-NB-ARC-LRR proteins with an extended N-terminus. Mi-1.2 responds to attempted host cell manipulation by three different root-knot nematode species (*Meloidogyne* spec.). In later studies, Mi-1.2 was also found to mediate resistance against infestations of phloem-feeding pests of white-fly and aphid (Martinez de Ilarduya et al., 2003; Nombela et al., 2003; Li et al., 2006). Mi-1.2 is member of a small gene family and is located in a cluster containing a paralogue (Mi-1.1) on chromosome 6. Mi-1.1 shares 91% amino-acid identity with Mi-1.2 (Milligan et al., 1998) and, like Mi-1.2, is transcribed although no known resistance specificity has been assigned to Mi-1.1. Numerous domain swaps have been made between Mi-1.1 and Mi-1.2 to generate genetic data on regions of the gene that are important for negative and positive regulation (Hwang et al., 2000; Hwang and Williamson, 2003).

Here, we address various aspects of the function of the Mi-1.2 NB-ARC subdomains in relation to its interaction with the LRR domain. Autoactivating mutants in the NB subdomain were found to be able to trigger HR upon co-expression of the separate CC-NB-ARC and LRR parts. In contrast, autoactivating mutations in the ARC2 subdomain fail to transcomplement and induce HR. These observations suggest that the ability to transcomplement depends on the NB-ARC subdomain affected by the mutation. In all combinations of CC-NB-ARC and LRR domains analysed, the physical interactions were not abolished, indicating that no gross changes in intramolecular interactions are associated with the induction of HR signalling. These results confirm a model suggesting a distinct functional role for each of the three NB-ARC subdomains. The NB subdomain is important for nucleotide binding and for the enzymatic activity of the NB-ARC domain, the ARC1 has a general LRR interacting role, and the ARC2 subdomain plays a dual regulatory role in sensing the nucleotide and translating pathogen perception into signalling.

Results

CC-NB-ARC and LRR expressed *in trans* complement to reconstitute a signalling-competent molecule

A chimaeric protein that consists of the CC-NB-ARC part of Mi-1.1 and the LRR domain of Mi-1.2 (referred to as Mi-DS4) induces a hypersensitive response (HR) upon transient expression in *Nicotiana benthamiana* leaves when expressed from the endogenous Mi-1.1 promoter (Hwang et al., 2000). Here we show that expression of this chimera Mi-DS4, but not Mi-1.1 or Mi-1.2, driven from the strong CaMV 35S promoter induces a strong necrosis 2 days after infiltration (Figure 1, left panel). This cell death is clearly visualised upon trypan blue staining of this leaf, to stain dead cells blue. Expression of Mi-1.1 or Mi-1.2 proteins induces a background level of cell

death visualised by a light blue hue upon trypan blue staining (Figure 1, right panel). To investigate the molecular basis behind the autoactive incompatibility between the Mi 1.1 CC-NB-ARC and Mi 1.2 LRR domains in Mi-DS4, and not for example in the reciprocal domain swap (referred to as Mi-DS2), functional complementation was analysed when the CC-NB-ARC and LRR domains were expressed *in trans*. To this end, the corresponding Mi-1.1 and Mi-1.2 parts were placed behind the 35S promoter and the four combinations were expressed in overlapping circles on *N. benthamiana* leaves by agroinfiltration. In this way the effect of expression of the separate domains, and combinations of two can be compared on a single leaf. In the infiltrated leafs depicted in Figure 2, the NB-ARC domains are expressed in the upper circles whereas the LRRs are expressed in the lower circles.

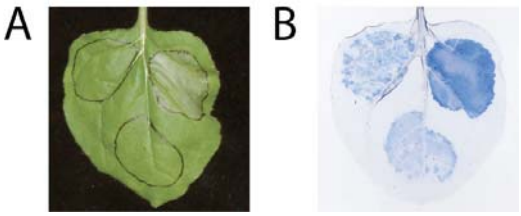

Figure 1
Mi-DS4 induces HR when expressed from the 35S promoter. *Nicotiana benthamiana* leaves were agroinfiltrated with constructs to express Mi-1.1, Mi-1.2 or Mi-DS4. A representative leaf was photographed two days after agroinfiltration (A). Cell death was visualised by trypan blue staining of the same leaf (B). Counter-clockwise, starting from top-left: Mi-1.1, Mi-1.2, and Mi-DS4.

Similar to the full-length proteins (Figure 1), HR signalling was initiated upon co-expression of Mi-1.1 CC-NB-ARC and Mi-1.2 LRR (overlapping region Figure 2B). To visualise the cell death the same leaves were stained with trypan blue (right panels in Figure 2). In contrast to Mi-DS4, the reconstituted Mi-1.1 (Figure 2A), Mi-DS2 (Figure 2C) or Mi-1.2 (Figure 2D) did not trigger HR. HR was also not observed in the non-overlapping regions, showing that expression of the separate CC-NB-ARC or LRR domain only induces a basal level of cell death. To be able to detect expression of the protein domains *in planta*, the Mi-DS4 constituents were fused to various tags at either their N- or C-terminus and analysed for functional transcomplementation. Of all combinations tested, only co-expression of non-tagged CC-NB-ARC protein and either non-tagged or N-terminally TAP-tagged LRR protein triggered HR. As the latter combination is still functional, we used it for all our transcomplementation assays (including Figure 2). These data show that we can functionally reconstitute an autoactivating Mi-1 chimaeric swap protein able to signal HR by expressing the Mi-1.1 CC-NB-ARC and Mi-1.2 LRR domains *in trans*. Because expression of the separate domains does not induce an HR, these data suggest that the two domains interact to activate defence signalling. The combination provides all positive

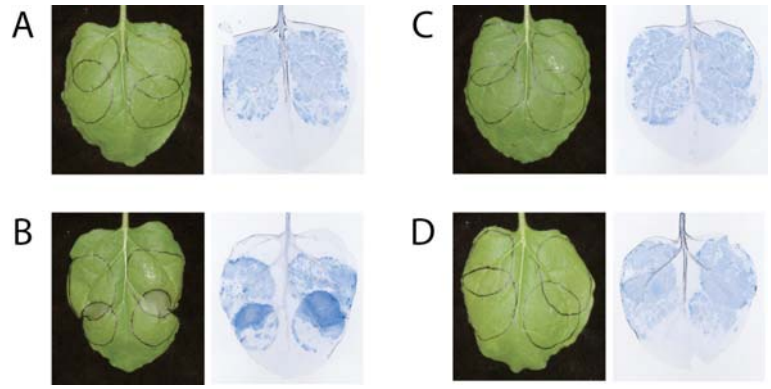

Figure 2

The Mi-DS4 phenotype can be reconstituted by co-expression of the CC-NB-ARC and LRR parts *in trans*. *N. benthamiana* leaves were agroinfiltrated with constructs to express the CC-NB-ARC or LRR domain of Mi-1.1 or Mi-1.2. Representative leaves were photographed two days after agroinfiltration. All infiltrations are performed in duplicate on the leaf halves. The top circles mark the regions of CC-NB-ARC infiltration and the bottom circles TAP-LRR infiltration. Cell death is visualised by trypan blue staining of the same leaf (right panel). **A)** Mi-1.1 CC-NB-ARC and Mi-1.1 TAP-LRR, **B)** Mi-1.1 CC-NB-ARC and Mi-1.2 TAP-LRR, **C)** Mi-1.2 CC-NB-ARC and Mi-1.1 TAP-LRR, **D)** Mi-1.2 CC-NB-ARC and Mi-1.2 TAP-LRR.

regulatory functions required to induce an HR, but lacks the negative regulation required to suppress this signalling in the absence of a pathogen.

Autoactivation in Mi-DS4 does not require dissociation of the LRR domain from the N-terminus

To analyse whether physical intramolecular interactions are responsible for the autoactivation phenotype of Mi-DS4, combinations of CC-NB-ARC and TAP-LRR constructs of Mi-1.1 and Mi-1.2 were co-expressed. On a Western blot of total protein lysates of the agroinfiltrated leaves, a band migrating at the expected size for the CC-NB-ARC protein (~100 kDa) is visualised (Figure 3, upper panel) using an Mi-1 antibody raised against the N-terminal region of Mi-1 not containing the LRR domain. The antibody also recognises the TAP-LRR fusion protein (~63 kDa) because of the general IgG-binding properties of the ProtA domain in the TAP tag.

To test physical interactions between the two protein domains, the TAP-LRR fusion protein was immunoprecipitated using agarose beads loaded with human IgG. Human IgGs were used to avoid cross-reactivity with the anti-rabbit secondary antibody needed for detection of the Mi-1 protein in subsequent immunoblots. The precipitated protein-complex was proteolytically cleaved from the beads using the specific TEV protease site in the TAP tag (Rohila et al., 2004). After pull-down, co-purification of CC-NB-ARC protein was analysed using the Mi-1 antibody (Figure 3, lower panel). Co-purification was found with all four combinations of Mi-1.1 and Mi-

1.2 domains. Apparently, the interaction of LRR domains with CC-NB-ARC is not restricted to their endogenous partners.

An interesting observation is co-precipitation of a band corresponding to the size of the TAP-LRR protein (63 kDa). As mentioned above, the Mi antibody does not recognise the cleaved non-tagged LRR domain and the ProtA epitope should remain bound to the beads. This observation suggests that either more than one LRR domain is present in one complex or that the conditions of the TEV protease cleavage are facilitating non-enzymatic dissociation of the complex from the beads. Since this phenomenon is not observed with other TAP-tagged proteins (data not shown), the latter hypothesis is unlikely. In any case, co-precipitation of CC-NB-ARC protein in the presence, and not in the absence of ,TAP-LRR protein shows that both are present in one complex and interaction is specific. This experiment clearly shows that a physical interaction is present in the transcomplementing Mi-DS4 combination. Based on the intensity of the bands the stoichiometry of the interaction is similar to that of the other combinations, implying that autoactivation does not require gross changes (i.e. dissociation) in intramolecular interactions between the N-terminus and the LRR domain.

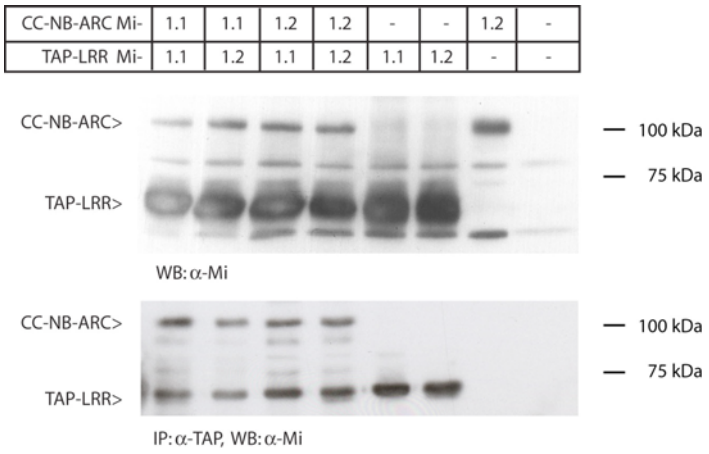

Figure 3

CC-NB-ARC and LRR domains of Mi-1.1 and Mi-1.2 physically interact when expressed *in trans. N. benthamiana* leaves were agroinfiltrated with constructs to express the domains of Mi-1.1 or Mi-1.2, as indicated in the heading. One day after agroinfiltration, protein extracts were made and subjected to immunoprecipitation using IgG-beads followed by immunoblotting and detection with αMi antibody. The upper panel represents an immunoblot of total protein extracts (input), the lower panel represents the TAP-precipitated protein complex after IP.

Identification of autoactivating mutations in the NB-ARC domain

The Mi-1.1 and Mi-1.2 proteins are 91% identical and the differences are scattered throughout the protein, making it difficult to pinpoint the residues responsible for

autoactivating incompatibilities. To be able to distinguish between positive and negative regulatory functions in the CC-NB-ARC and LRR combination, we focused on specific point mutations in the NB-ARC domain of Mi-1.2 that lead to autoactivation; T557S, H840A and D841V (Gabriëls et al., 2007; Chapter 3). Autoactivating mutants by definition represent HR signalling-competent molecules, in contrast to loss-of-function mutants that can be affected in various aspects of R protein function.

Autoactivating mutations in the NB-ARC domain map to the NB or to the ARC2 subdomain. The position of these mutations is visualised in a 3D model of the Mi-1.2 NB-ARC domain (Figure 4). This model is based on homology modelling of the Mi-1.2 NB-ARC on the crystal structure of the ADP-bound state of the NB-ARC domain of the human protein Apaf-1 (Riedl et al., 2005).

Based on this model, we selected two additional mutants. One of these represents a mutant in the NB subdomain (D630E) that maps to the Walker B motif (Fig. 4). The corresponding residue has also been shown to lead to autoactivation in I-2 (Tameling et al., 2006). The second mutant is a proposed loss-of-function mutant. In this double mutant (KT556/557AA), two highly conserved amino-acids in the nucleotide-binding P-loop are changed to alanine, thereby presumably abolishing the ability to bind nucleotides (Fig. 4). As can be clearly seen in the 3D model, all mutations used in this study cluster at the nucleotide-binding interface, showing that, although the mutations map to different regions in a linear sequence, they cluster spatially.

Mutations in the ARC2, but not in the NB subdomain, abolish transcomplementation

To compare the extend of cell death mediated by the five Mi-1.2 NB-ARC mutants, they were transiently expressed in *N. benthamiana* leaves using agroinfiltration. Figure 5 shows the infiltrated leafs two days after infiltration. At this time-point, the ARC2 mutants H840A (bottom left) and D841V (top right) induced a clear HR, whereas the NB mutants T557S (bottom right) and D630E (middle right) do not yet induce a specific cell death response. The T557S initiated HR becomes apparent after 3 days (Gabriëls et al., 2007), whereas the D630E mutation leads to visual necrosis 5 days after infiltration (data not shown). Of the four autoactivating mutants, H840A and D841V are the fastest, whereas the two NB mutants (T557S and D630E) induce a relatively slow HR, not observed with wild-type Mi-1.2 or with the KT556/557AA mutant.

To test whether transcomplementation of CC-NB-ARC and LRR domains is affected in any of these NB-ARC mutants, we co-expressed wild-type and the five mutant CC-NB-ARC proteins and wild-type TAP-LRR protein in overlapping circles in *N. benthamiana* leaves. In all leaves pictured in Figure 6, the NB-ARC domains are

infiltrated in the upper circle and the lower circle represent the region of Mi-1.2 TAP-LRR expression. As expected, the wild-type (Fig. 6A) and predicted loss-of-function KT556/557AA (Fig. 6B) NB-ARC domains did not induce HR when co-expressed with the LRR domain. The absence of HR was verified by trypan blue staining of the same leaves (right panels).

The NB mutants T557S and D630E did transcomplement and reconstituted autoactivity (overlapping zone in Fig. 6C and D). Similar as the full-length protein, the D630E mutant induced a milder response than the T557S mutant, but HR was clearly visible in the overlapping region upon trypan blue staining (Figure 6D, right panel). These results show that NB subdomain mutants are able to induce HR when the LRR domain is expressed *in trans*. The cell death response is faster than that induced by the full-length protein, presumably due to the higher expression levels observed for the separate domains (data not shown).

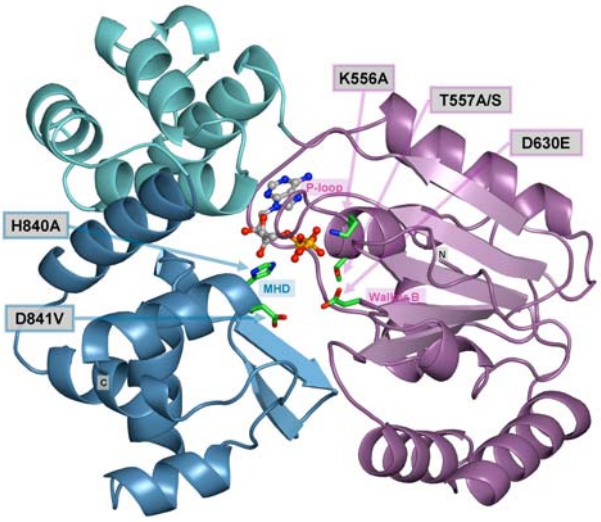

Figure 4

Structure model of the Mi-1.2 NB-ARC domain. The model was created using the ADP bound structure of human Apaf-1 (PDB code 1z6t, chain A) as structural template. The positions of the P-loop, the Walker B motif, and the MHD motif are indicated. Arrows point to the locations of Mi-1.2 mutant residues used in this study. They are represented as sticks, whereas ADP atoms are depicted as balls-and-sticks. Subdomain colouring is as follows: NB: pink, ARC1: green, ARC2: blue.

In contrast to the NB mutants, co-expression of CC-NB-ARC variants containing the strong ARC2 autoactivation mutants H840A or D841V reproducibly fails to induce HR responses (Figure 6E and F). Apparently, the mutations that result in the strongest autoactivation phenotypes *in cis* (Figure 5) cannot complement with the LRR domain to reconstitute a functional molecule when expressed *in trans* (Figure 6). These results show that functional transcomplementation of autoactivity depends on the subdomain of the NB-ARC that is affected.

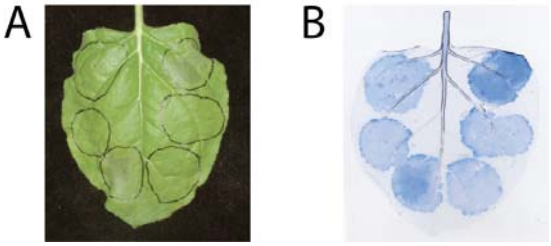

Figure 5
Specific point mutations in the Mi-1.2 NB-ARC domain result in autoactivity. *Nicotiana benthamiana* leaves were agroinfiltrated with constructs to express Mi-1.2 proteins mutated in the NB-ARC domain. A picture of a representative leaf was taken three days after agroinfiltration (A). Cell death is visualised by trypan blue staining of the same leaf (B). Counter-clockwise, starting from top-left: wild-type, KT556/557AA, H840A, T557S, D630E, D841V

Mutations in the NB-ARC domain do not lead to dissociation of the LRR domain

To investigate whether the observed differences in the transcomplementation assay can be explained by a change in physical interaction of CC-NB-ARC and LRR, combinations of mutant CC-NB-ARC and TAP-LRR proteins were co-expressed. The Western blot of the total protein lysates (Figure 7, upper panel) shows equal

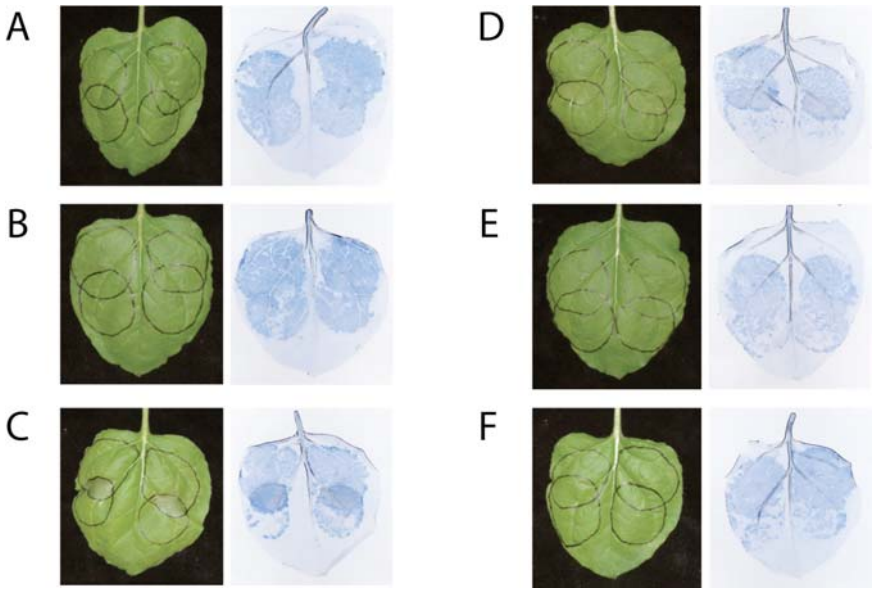

Figure 6
Transcomplementation of Mi-1.2 NB-ARC mutants depends on which subdomain is affected. *N. benthamiana* leaves were agroinfiltrated with constructs to express CC-NB-ARC (mutants) or the LRR domain of Mi-1.2. Representative leaves were photographed two days after agroinfiltration. On each leaf, duplicates are infiltrated on the leaf halves. The top circles mark the regions of (mutant) Mi-1.2 CC-NB-ARC expression and the bottom circles of Mi-1.2 TAP-LRR expression. Cell death was visualised by trypan blue staining of the same leaf (right panel). CC-NB-ARC variants: **A)** wild-type, **B)** KT556/557AA, **C)** T557S, **D)** D630E, **E)** H840A, **F)** D841A.

expression of the CC-NB-ARC variants and of the Mi-1.2 TAP-LRR proteins. Both migrate according to their predicted masses of ~100 and 63 kDa.
The Mi-1 protein-complex was precipitated using human IgG-beads and released using TEV protease. Co-precipitation of CC-NB-ARC domains with TAP-LRR was analysed on Western blots using the Mi-1 antibody. As can be seen in the lower panel of Figure 7, all CC-NB-ARC variants tested interact equally well with the Mi-1.2 LRR domain. These interactions show that even though transcomplementation of the CC-NB-ARC and LRR domains depends on the location of mutations in the NB and ARC2 subdomains, there are no detectable changes in intramolecular interactions in these mutants. Apparently, interaction of the LRR domain with its N-terminus does not depend on the functionality of the combination, and is not sufficient for autoactivation.

Discussion

We have adressed the molecular background of autoactivating domain swaps of the Mi-1.2 and Mi-1.1 proteins, and of autoactivating and loss-of-function point mutations in the NB-ARC domain of Mi-1.2, summarised in Table 1. Using an Mi-1 antibody and a tagged LRR construct, we have been able to study intramolecular interaction of the LRR domain and the CC-NB-ARC part of Mi-1 paralogues and NB-ARC mutants. The set of mutants depicted in the model in Figure 4 enabled us to investigate the effect of mutations in NB-ARC subdomains on transcomplementation and intramolecular interaction with the LRR domain. In all combinations of Mi-1 LRR and CC-NB-ARC variants, a physical interaction was observed. Apparently, autoactivation and loss-of-function mutations in NB and ARC2 studied here do not result in dissociation of the CC-NB-ARC and LRR domains. The ability to transcomplement, however, was found to be dependent on the NB-ARC subdomain affected by the autoactivating mutation.
The observed constitutive interaction between the CC-NB-ARC and LRR domain appears to contrasts with a previously proposed model based on genetic data and domain swap analyses (e.g. for Mi-DS4) that suggest dissociation of these domains upon (auto)activation (Hwang et al., 2000; Hwang and Williamson, 2003). However, it is likely that the functional interaction between these two domains is lost, even though the physical interactions remain. The observed interactions of the LRR domain with the CC-NB-ARC parts in Mi-DS4, Mi-DS2, and both wild-type proteins show that association of the LRR domain with the N-terminus is not sufficient to induce HR, nor to repress it. Since Mi-1.1 and Mi-DS2 failed to confer nematode resistance (Hwang et al., 2000), the combination of the genuine CC-NB-ARC and LRR (Mi-1.2) domains is required to perceive the nematode-derived stimulus and trigger defence.

To explain how the point mutants in the NB-ARC affect the activation state, the NB-ARC domain of Mi-1.2 was modelled on the APAF-1 template (Figure 4). The replacement of the highly conserved lysine (K556) and threonine (T557) in the P-loop of the NB subdomain to alanine is predicted to disrupt nucleotide binding. In the structure of Apaf-1, the P-loop provides 7 of the 8 direct hydrogen bonds to the bound ADP (the 8th is provided by the histidine in the MHD motif) (Riedl et al., 2005), showing the importance of this motif for nucleotide binding. Direct support for a role in nucleotide binding by the P-loop in R proteins is provided by the observation that replacement of the corresponding lysine in I-2 results in a nucleotide binding mutant with a loss-of-function phenotype (Tameling et al., 2002). The T557S mutation in the

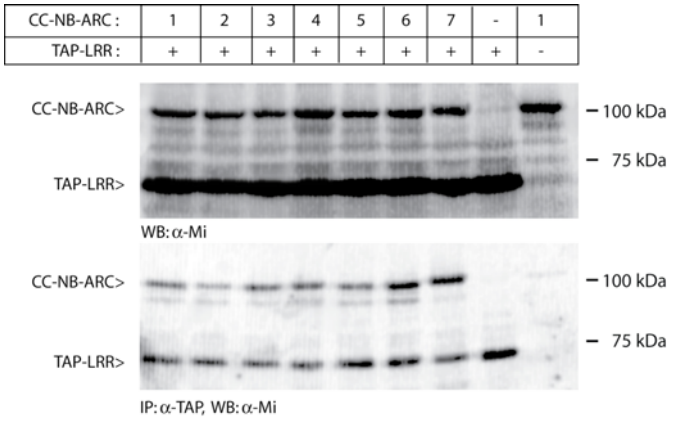

Figure 7

Mi-1.2 CC-NB-ARC mutant variants interact with the LRR domain. *N. benthamiana* leaves were agroinfiltrated with constructs to express parts of (mutant) Mi-1.2 or Mi-1.1. One day after agroinfiltration, protein extracts were made and subjected to immunoprecipitation using IgG-beads followed by immunoblotting and detection using αMi antibody. The upper panel shows an immunoblot of total protein extracts (input), the lower panel represents the precipitated protein complex after IP. In this experiment, Mi-1.2 TAP-LRR was expressed in combination with variant CC-NB-ARC constructs, as indicated in the heading. CC-NB-ARC numbering: 1: wild-type Mi-1.2, 2: KT556/557AA, 3: T557S, 4: D630E, 5: D841V, 6: H840A, 7: wild-type Mi-1.1.

P-loop of Mi-1.2 apparently does not abolish nucleotide binding, since this mutant has an autoactivation phenotype. Possibly, the orientation of the bound nucleotide is aberrant in this mutant and mimics the activated state, or, alternatively, the mutation reduces the ATPase activity. The latter hypothesis is supported by analysis of two autoactivation mutations in the NB subdomain of I-2 that were shown to have a reduced hydrolysis capacity (Tameling et al., 2006). One of them is the D283E mutation in the Walker B motif. This acidic residue is thought to be a catalytic base that is required for ATP hydrolysis by P-loop ATPases (Leipe et al., 2004). Based on the structural conservation, we therefore propose the same role for the analogous D630E mutation in Mi-1.2 and predict that it will be a hydrolysis mutant. The

autoactivating phenotypes observed upon mutation of the MHD motif in the ARC2 are likely based on a destabilised interaction between this domain and the nucleotide. A CC-NB-ARC domain harbouring an autoactivating mutation in the MHD motif is not able to induce an HR on itself (Figure 2 and 6), but requires the LRR domain *in cis* (Figure 5). When these domains are expressed *in trans*, HR signalling is not induced although their interaction is not compromised. Apparently, the positive regulatory function of the LRR on the CC-NB-ARC domain, required for the protein to activate defence signalling, is lost when presented *in trans*. We can exclude that the separated LRR domain exhibits dominant negative regulation of the MHD mutants, since co-expression of the LRR with full-length MHD mutants does not suppress HR. These observations suggest a sensory and regulatory role for the ARC2 subdomain in mediating LRR-derived signals.

In Rx, the corresponding MHD mutant D460V can still transcomplement with the LRR domain (Moffett et al., 2002). A possible basis for this difference is that Rx belongs to a different group of CC-NB-ARC-LRR proteins. It would be interesting to examine whether the ability to transcomplement the MHD mutant phenotype is NB-LRR (sub)class-specific.

To summarize, this study provides the first data on intramolecular interaction between domains of an NB-LRR R protein with an extended CC domain. The robust interaction between LRR and CC-NB-ARC domains supports the hypothesis by Rairdan et al., 2007, that the responsible interface consists of several contact points and can therefore not readily be disturbed. Our results support a distinct role for the three NB-ARC subdomains. The NB subdomain is involved in nucleotide binding and hydrolysis, and mutations that disrupt binding result in a loss of function phenotype whereas putative hydrolysis mutants are autoactivating (Figure 5). Autoactivity conferred by NB subdomain mutants is presumably caused by a shift in the equilibrium towards the ATP-bound state, which is proposed to be the active state (Tameling et al., 2006). In the NB subdomain mutants, the negative regulation exerted by the LRR is lost, but the positive regulatory functions are required and sufficient to confer the autoactivation phenotype (Figure 6). In contrast, mutation of the ARC2 also alleviates negative regulation, but the positive regulation of the LRR domain can only be provided *in cis* (Figure 5) and not *in trans* (Figure 6), suggesting that the interaction between these domains is altered even though interaction is not lost (Figure 7). Binding to the LRR is therefore likely to be mediated by the ARC1 subdomain, in accordance to the observations described for Rx (Rairdan and Moffett, 2006).

Altogether, our data support a model in which perception of a pathogen-derived factor by the LRR domain results in an alteration of the interaction interface between the LRR domain and the ARC2 subdomain, resulting in a release of the negative

regulation exerted by the LRR on the NB-ARC domain and transition to the activated state.

Further studies will be required to understand how positive and negative regulation by the LRR on the NB-ARC domain is executed. However, the analysis of intramolecular interactions aid to reveal parts of the basic mechanisms underlying activation. To fully understand the molecular dynamics of the interactions, crystal structures of full-length R proteins in the ATP- and ADP-bound state will be essential. Changes in conformation might be subtle and rather than complete association or dissociation of (sub)domains, intricate changes in binding interfaces might be sufficient to unleash the signalling potential of an R protein.

Acknowledgements

We like to thank Harold Lemereis for plant handling. We are grateful to Valerie Williamson for providing us with the Mi-DS4 construct and helpful discussions. G.v.O. is supported by the Research Council for Earth and Life Sciences (ALW) with financial aid from the Netherlands Organization for Scientific Research (NWO). G.M. and M.A. have been financially supported by the German National Genome Research Network (NGFN). The research has been conducted in the context of the BioSapiens Network of Excellence funded by the European Commission under grant number LSHG-CT-2003-503265.

Materials and methods

Construction of binary vectors

All PCR primers used in this study (marked FPxxx) were purchased from MWG (Germany), and are listed in Table 2. Construction of a binary vector expressing Mi-1.2 (pG74) was described elsewhere (Gabriëls et al., 2007). Mi-1.1 was amplified from plasmid G3 (Keygene N.V.) with primers FP764 and FP766. Gateway *att*B flanks were added by adapter PCR using primers FP872 and FP873. The PCR product was transferred via entry clone pDONR207 (Invitrogen) to binary vector CTAPi (Rohila et al., 2004) by the Gateway one-tube protocol for cloning *att*B-PCR products directly into destination vectors (Invitrogen). In the same way, Mi-DS4 was amplified from plasmid Mi-DS4 (Hwang et al., 2000) and cloned into CTAPi. Note that the endogenous stop codon remains present in these constructs, so there is no translational fusion to the TAP tag. Constructs expressing the Mi-1.2 mutants T557S, H840A and D841V have been described elsewhere (Gabriëls et al., 2007; van Ooijen et al., submitted). D630E was generated by overlap extension PCR using primer sets FP554/FP212 and FP182/FP555 on template pSE23 (Gabriëls et al., 2007). The 1330 and 260 bp pcr products were joined in a second amplification step using FP182/FP212. A 325 bp restriction fragment generated with *Age*I and *Xho*I containing the desired mutation was used to replace the wildtype sequence in pSE23 to obtain pG23. The full length Mi-1.2 D630E sequence was amplified using FP764 and FP766, Gateway *att*B sites were added with FP872 and FP873 and the resulting fragment was transferred to binary vector CTAPi as described above. The Mi-1.2 KT556/557AA

T2	Oligonucleotides used in this study
FP	Sequence
182	ggggtacccggctatttctttaccgacatc
212	catgccatggccgagctagatgaggatgaac
554	gtcttagatgaagtgtgggatac
555	gtatcccacacttcatctaagac
764	aaaaagcaggctctatggaaaaacgaaaagatatt
766	agaaagctgggttctacttaaataaggggatattctt
857	aaaaagcaggctctggtaaacacctctattctttg
859	agaaagctgggttctaagaatgccttttcttatttgaa
872	ggggacaagtttgtacaaaaaagcaggct
873	ggggaccactttgtacaagaaagctgggt
1099	gtatgccgggttcaggtgcagcaactttggcatacaaagtatac
1102	gtatactttgtatgccaaagttgctgcacctgaacccggcatac

construct was generated by circular mutagenesis (Hemsley et al., 1989) on template pG104 (van Ooijen et al., submitted) using FP1099/FP1102 to obtain pG108. An *Eco*72I/*Bsp*119I restriction fragment carrying the mutation was exchanged with that in pG74 to obtain Mi-1.2 KT556/557AA. Mi-1.1 and Mi-1.2 LRR sequences (residues 1-899) were amplified from G3 and pKG6210 (Keygene N.V.), respectively, using primers FP857 and FP766. Gateway *att*B flanks were added using FP872 and FP873 and the fragment was transferred to pDONR207 by a Gateway BP reaction (Invitrogen) and subsequently to NTAPi (Rohila et al., 2004) to obtain N-terminally TAP tagged LRR domains. All CC-NB-ARC (residues 900-1258) constructs were generated by the Gateway one-tube protocol for cloning *att*B fragments directly in destination vectors (Invitrogen). Primers FP764 and FP859 were used on PCR templates pKG6210 (Mi-1.2, Keygene N.V.) and G3 (Mi-1.1, Keygene N.V.), or the full-length clones of the Mi-1.2 mutants described above and in (Gabriëls et al., 2007; van Ooijen et al., submitted). Note that a stop codon has been incorporated in the reverse primer to prevent translational fusion to the TAP tag in these CC-NB-ARC constructs.

***Agrobacterium*-mediated transient transformation**

A. tumefaciens strain GV3101(pMP90) (Koncz and Schell, 1986) was transformed with binary constructs (Takken et al., 2000) and grown to OD_{600}=0.8 in LB-Mannitol (10g/l tryptone, 5 g/l yeast extract, 2.5 g/l NaCl, 10 g/l mannitol) medium supplemented with 20 µM acetosyringone and 10 mM MES pH 5.6. Cells were pelleted and resuspended in infiltration medium (1x MS salts, 10 mM MES pH 5.6, 2% w/v sucrose, 200 µM acetosyringone) and infiltrated at OD_{600}=0.2 (for LRR constructs) or 1 (for full-length or CC-NB-ARC constructs) into four- to five-week-old *N. benthamiana* leaves.

Protein extraction, immunoprecipitation and Western blotting

Infiltrated leaves were harvested and pooled 24 hours after agroinfiltration and frozen in liquid nitrogen. After grinding the tissue, it was allowed to thaw in 2 ml protein extraction buffer per gram of tissue (25 mM Tris pH 8, 1 mM EDTA, 150 mM NaCl, 5 mM DTT, 0,1% NP-40, 1 x Roche Complete protease inhibitor cocktail and 2% Poly-(Vinyl-Poly-Pyrolidone)). Extracts were centrifuged at 12,000 krcf at 4º C for 10 minutes and the supernatant was passed over 4 layers of Miracloth to obtain a total protein lysate. 1 ml of total protein lysate was incubated with 20 µl human IgG-agarose beads (Sigma) rotating head-over-head at 4º C for 1 hour. Beads with bound protein complexes were pelleted at 2,000 rpm for 10 seconds and washed 4 times with 1 ml ice-cold TEV cleavage buffer (10 mM Tris pH 8, 150 mM NaCl, 0.5 mM EDTA, 0.1% NP-40 and 1 mM DTT). 100 µl TEV cleavage buffer and 10 units recombinant AcTEV protease (Invitrogen) were added to the pelleted beads and the proteolytic reaction was carried out shaking vigorously for 1.5 hours at 16º C. The supernatant was mixed with Laemmli sample buffer, run on 8% SDS-PAGE gels and blotted on PVDF membranes using semi-dry blotting. 5% skimmed milk powder was used as blocking agent. As a primary antibody, a 1:4000 dilution of the Mi-1 antibody (van Ooijen et al., submitted) was used and as a secondary antibody a 1:4000 dilution of goat-anti-rabbit linked to either horseradish peroxidase (Figure 3) or alkaline phosphatase (Figure 8). The signal was visualised by

measuring either luminescence (ECL and BioMax MR film (Kodak) Figure 3) or fluorescence (ECF and detection by phospho-imager (STORM), Figure 8).

3D structure model of the Mi-1.2 NB-ARC domain

A pairwise sequence-structure alignment of tomato R protein Mi-1.2 and human Apaf-1 was constructed based on the multiple alignment of R protein NB-ARC domains described in (van Ooijen et al., submitted). The 3D-modeling server WHAT IF (Vriend, 1990) returned a full-atom structure model of the NB-ARC domain of Mi-1.2. The structure of Apaf-1 (PDB code 1z6t, chain A) comprises the residues 108-450 (UniProt sequence O14727) and is mapped onto Mi-1.2 residues 505-852 (UniProt sequence O81137). The protein structure image of the model was illustrated using PyMOL (http://www.pymol.org).

References

Ade, J., DeYoung, B.J., Golstein, C., and Innes, R.W. (2007). Indirect activation of a plant nucleotide binding site-leucine-rich repeat protein by a bacterial protease. Proc Natl Acad Sci USA **104**, 2531-2536.

Albrecht, M., and Takken, F.L.W. (2006). Update on the domain architectures of NLRs and R proteins. Biochem Biophys Res Commun **339,** 459-462.

Bendahmane, A., Farnham, G., Moffett, P., and Baulcombe, D.C. (2002). Constitutive gain-of-function mutants in a nucleotide binding site-leucine rich repeat protein encoded at the *Rx* locus of potato. Plant J **32,** 195-204.

de la Fuente van Bentem, S., Vossen, J.H., de Vries, K.J., van Wees, S., Tameling, W.I.L., Dekker, H.L., de Koster, C.G., Haring, M.A., Takken, F.L.W., and Cornelissen, B.J.C. (2005). Heat shock protein 90 and its co-chaperone protein phosphatase 5 interact with distinct regions of the tomato I-2 disease resistance protein. Plant J **43,** 284-298.

Gabriëls, S.H.E.J., Vossen, J.H., Ekengren, S.K., van Ooijen, G., Abd-El-Haliem, A.M., van den Berg, G.C.M., Rainey, D.Y., Martin, G.B., Takken, F.L.W., de Wit, P.J.G.M., and Joosten, M.H.A.J. (2007). An NB-LRR protein required for HR signalling mediated by both extra- and intracellular resistance proteins. Plant J **50,** 14-28.

Hemsley, A., Arnheim, N., Toney, M.D., Cortopassi, G., and Galas, D.J. (1989). A simple method for site-directed mutagenesis using the polymerase chain reaction. Nuc Acids Res **17,** 6545-6551.

Howles, P., Lawrence, G., Finnegan, J., McFadden, H., Ayliffe, M., Dodds, P., and Ellis, J. (2005). Autoactive alleles of the flax *L6* rust resistance gene induce non-race-specific rust resistance associated with the hypersensitive response. Mol Plant Microbe Interact **18,** 570-582.

Hwang, C.F., and Williamson, V.M. (2003). Leucine-rich repeat-mediated intramolecular interactions in nematode recognition and cell death signaling by the tomato resistance protein Mi. Plant J **34,** 585-593.

Hwang, C.F., Bhakta, A.V., Truesdell, G.M., Pudlo, W.M., and Williamson, V.M. (2000). Evidence for a role of the N terminus and leucine-rich repeat region of the *Mi* gene product in regulation of localized cell death. Plant Cell **12,** 1319-1329.

Koncz, C., and Schell, J. (1986). The promoter of Tl-DNA gene *5* controls the tissue-specific expression of chimaeric genes carried by a novel type of *Agrobacterium* binary vector. Mol Gen Genet **204,** 383-396.

Leipe, D.D., Koonin, E.V., and Aravind, L. (2004). STAND, a class of P-loop NTPases including animal and plant regulators of programmed cell death: multiple, complex domain architectures, unusual phyletic patterns, and evolution by horizontal gene transfer. J Mol Biol **343,** 1-28.

Leister, R.T., Dahlbeck, D., Day, B., Li, Y., Chesnokova, O., and Staskawicz, B.J. (2005). Molecular genetic evidence for the role of *SGT1* in the intramolecular complementation of Bs2 protein activity in *Nicotiana benthamiana*. Plant Cell **17,** 1268-1278.

Li, Q., Xie, Q.G., Smith-Becker, J., Navarre, D.A., and Kaloshian, I. (2006). Mi-1-Mediated aphid resistance involves salicylic acid and mitogen-activated protein kinase signaling cascades. Mol Plant Microbe Interact **19,** 655-664.

Martinez de Ilarduya, O., Xie, Q., and Kaloshian, I. (2003). Aphid-induced defense responses in Mi-1-mediated compatible and incompatible tomato interactions. Mol Plant Microbe Interact **16,** 699-708.

Milligan, S.B., Bodeau, J., Yaghoobi, J., Kaloshian, I., Zabel, P., and Williamson, V.M. (1998). The root knot nematode resistance gene *Mi* from tomato is a member of the leucine zipper, nucleotide binding, leucine-rich repeat family of plant genes. Plant Cell **10,** 1307-1319.

Moffett, P., Farnham, G., Peart, J., and Baulcombe, D.C. (2002). Interaction between domains of a plant NBS-LRR protein in disease resistance-related cell death. EMBO J **21,** 4511-4519.

Mucyn, T.S., Clemente, A., Andriotis, V.M.E., Balmuth, A.L., Oldroyd, G.E.D., Staskawicz, B.J., and Rathjen, J.P. (2006). The tomato NBARC-LRR protein Prf Interacts with Pto kinase in vivo to regulate specific plant immunity. Plant Cell. **18**, 2792-2808.

Nombela, G., Williamson, V.M., and Muniz, M. (2003). The root-knot nematode resistance gene Mi-1.2 of tomato is responsible for resistance against the whitefly *Bemisia tabaci*. Mol Plant Microbe Interact **16,** 645-649.

Rairdan, G., and Moffett, P. (2007). Brothers in arms? Common and contrasting themes in pathogen perception by plant NB-LRR and animal NACHT-LRR proteins. Microbes Infect **9,** 677-686.

Rairdan, G.J., and Moffett, P. (2006). Distinct domains in the ARC region of the potato resistance protein Rx mediate LRR binding and inhibition of activation. Plant Cell **18,** 2082-2093.

Rathjen, J.P., and Moffett, P. (2003). Early signal transduction events in specific plant disease resistance. Curr Opin Plant Biol **6,** 300-306.

Riedl, S.J., Li, W., Chao, Y., Schwarzenbacher, R., and Shi, Y. (2005). Structure of the apoptotic protease-activating factor 1 bound to ADP. Nature **434,** 926-933.

Rohila, J.S., Chen, M., Cerny, R., and Fromm, M.E. (2004). Improved tandem affinity purification tag and methods for isolation of protein heterocomplexes from plants. Plant J **38,** 172-181.

Shirano, Y., Kachroo, P., Shah, J., and Klessig, D.F. (2002). A gain-of-function mutation in an *Arabidopsis* Toll Interleukin1 receptor-nucleotide binding site-leucine-rich repeat type R gene triggers defense responses and results in enhanced disease resistance. Plant Cell **14,** 3149-3162.

Sun, Q., Collins, N.C., Ayliffe, M., Smith, S.M., Drake, J., Pryor, T., and Hulbert, S.H. (2001). Recombination between paralogueues at the *rp1* rust resistance locus in maize. Genetics **158,** 423-438.

Takken, F.L.W., Albrecht, M., and Tameling, W.I.L. (2006). Resistance proteins: molecular switches of plant defence. Curr Opin Plant Biol **9,** 383-390.

Takken, F.L.W., Luderer, R., Gabriëls, S.H.E.J., Westerink, N., Lu, R., de Wit, P.J.G.M., and Joosten, M.H.A.J. (2000). A functional cloning strategy, based on a binary PVX-expression vector, to isolate HR-inducing cDNAs of plant pathogens. Plant J **24,** 275-283.

Tameling, W.I.L., and Takken, F.L.W. (2007). Resistance proteins: scouts of the plant innate immune system. Eur J Plant Pathol **121,** 243-255

Tameling, W.I.L., Elzinga, S.D., Darmin, P.S., Vossen, J.H., Takken, F.L.W., Haring, M.A., and Cornelissen, B.J.C. (2002). The tomato *R* gene products I-2 and Mi-1 are functional ATP binding proteins with ATPase activity. Plant Cell **14,** 2929-2939.

Tameling, W.I.L., Vossen, J.H., Albrecht, M., Lengauer, T., Berden, J.A., Haring, M.A., Cornelissen, B.J.C., and Takken, F.L.W. (2006). Mutations in the NB-ARC domain of I-2 that impair ATP hydrolysis cause autoactivation. Plant Physiol **140,** 1233-1245.

Ueda, H., Yamaguchi, Y., and Sano, H. (2006). Direct interaction between the tobacco mosaic virus helicase domain and the ATP-bound resistance protein, N factor during the hypersensitive response in tobacco plants. Plant Mol Biol **61,** 31-45.

van Ooijen, G., van den Burg, H.A., Cornelissen, B.J.C., and Takken, F.L.W. (2007). Structure and function of resistance proteins in solanaceous plants. Annu Rev Phytopathol **45,** 43-72.

Vos, P., Simons, G., Jesse, T., Wijbrandi, J., Heinen, L., Hogers, R., Frijters, A., Groenendijk, J., Diergaarde, P., Reijans, M., Fierens Onstenk, J., De Both, M., Peleman, J., Liharska, T., Hontelez, J., and Zabeau, M. (1998). The tomato *Mi-1* gene confers resistance to both root-knot nematodes and potato aphids. Nature Biotech **16,** 1365-1369.

Vriend, G. (1990). WHAT IF: a molecular modeling and drug design program. J Mol Graph **8,** 52-56, 29.

Xing, W., Zou, Y., Liu, Q., Liu, J., Luo, X., Huang, Q., Chen, S., Zhu, L., Bi, R., Hao, Q., Wu, J.W., Zhou, J.M., and Chai, J. (2007). The structural basis for activation of plant immunity by bacterial effector protein AvrPto. Nature **449,** 243-247.

Yan, N., Chai, J., Lee, E.S., Gu, L., Liu, Q., He, J., Wu, J.W., Kokel, D., Li, H., Hao, Q., Xue, D., and Shi, Y. (2005). Structure of the CED-4-CED-9 complex provides insights into programmed cell death in *Caenorhabditis elegans*. Nature **437,** 831-837.

Chapter 5

RSI2 interacts with, and is required for function and stability of tomato resistance protein I-2

Gerben van Ooijen, Jack H. Vossen, Harrold A. van den Burg, Ben J.C. Cornelissen, Frank L.W. Takken

To be submitted

Race-specific disease resistance in plants depends on the presence of Resistance (R) genes. Most R genes encode NB-ARC-LRR proteins carrying a C-terminal Leucine-Rich Repeat (LRR). Few proteins have been identified that interact with this LRR domain, most of which have proposed (co)chaperone activity. Here, we report the identification of RSI2 (Required for Stability of I-2) as an interacting protein of the LRR domain of the tomato R protein I-2. RSI2 belongs to the family of small heat shock proteins (sHSPs). The interaction was found in a yeast two-hybrid screen and confirmed in pull-down assays. VIGS experiments revealed that RSI2 is required for the Hypersensitive Response (HR) induced by autoactive variants of I-2 and Mi-1, a second tomato R protein. Since many sHSPs have chaperone properties, involvement of RSI2 and other R protein (co)chaperones in I-2 and Mi-1 protein stability was examined. RSI2 silencing compromised the accumulation of full-length I-2 accumulation *in planta*, but did not affect Mi-1 levels. HSP90 and SGT1 silencing led to an almost complete loss of full-length I-2 accumulation and a reduction in Mi-1 protein levels. In contrast to RSI2, silencing SGT1 or HSP90 led to an accumulation of I-2 breakdown products. This difference suggests a different molecular mechanism by which RSI2 and HSP90/SGT1 chaperone I-2 protein stability. These data show that R protein function requires RSI2, for stabilizing either the R protein itself or other signalling components involved in initiation of HR.

Introduction

Resistance (R) proteins in plants mediate recognition of specific pathogen-derived factors called Avirulence (Avr) proteins. Upon Avr perception, R proteins initiate defence responses that limit further pathogen ingress. These responses often result in macroscopically visible cell death, referred to as the Hypersensitive Response (HR). The majority of R proteins are NB-ARC-LRR proteins, as they contain a central Nucleotide-Binding and -hydrolysing domain (NB-ARC) and a C-terminal Leucine-Rich Repeat (LRR) domain (Martin et al., 2003; van Ooijen et al., 2007). The LRR forms a potential protein-protein interaction surface and the LRRs of the R proteins RPM1, N, I-2 and Rx have been shown to physically interact with Heat Shock Protein 90 (HSP90) (Hubert et al., 2003; Lu et al., 2003; Liu et al., 2004; de la Fuente van Bentem et al., 2005). HSP90 is a highly conserved molecular chaperone responsible for the stability and function of a large number of proteins (Pearl and Prodromou, 2006). HSP90 consists of an N-terminal domain (NTD) containing an ATP binding and hydrolysis pocket, a central client binding domain, and a C-terminal dimerization domain. The activity of HSP90 is regulated by interactions with a number of co-chaperones that bind HSP90 and in some cases also their clients (Pearl and Prodromou, 2006). For example, the co-chaperone Protein Phosphatase 5 (PP5) interacts both with the C-terminus of HSP90, and the LRR domain of HSP90 client I-2 (de la Fuente van Bentem et al., 2005). Another HSP90-interacting co-chaperone is SGT1 (for suppressor of G2 allele of Skp1). SGT1 consists of three conserved regions: an N-terminal TPR domain, a central HSP90 interacting CS (CHORD-SGT1) domain, and a C-terminal SGT1-specific domain (Azevedo et al., 2002). Several studies have demonstrated physical interactions between HSP90, SGT1, and a third partner; RAR1 (for required for Mla12 resistance) (Hubert et al., 2003; Takahashi et al., 2003; Liu et al., 2004; Azevedo et al., 2006; Botër et al., 2007). RAR1 is composed of two zinc binding domains, CHORD I and CHORD II (Shirasu et al., 1999; Heise et al., 2007). Generally, the combined activities of RAR1, SGT1, and HSP90 are required for R protein stability and accumulation, and thereby for R protein-mediated signalling responses (Azevedo et al., 2006; Botër et al., 2007).

Another class of proteins with chaperone-associated functions are small Heat Shock Proteins (sHSPs), ranging in size from 12-43 kDa, also referred to as the HSP20 family. HSP20s are of variable sequence but are characterised by a conserved region of ~90 amino-acids forming an α-crystallin domain (Caspers et al., 1995). These proteins form large oligomers and perform their ATP independent chaperone function *in vitro* by binding to denatured proteins (Lee et al., 1995; Helm et al., 1997; Kirschner et al., 2000). *In vivo*, sHSPs are believed to confer a protective function by preventing unfolding or disassembly of other proteins (Van Montfort et al., 2001). The only HSP20 linked to disease resistance until now is tobacco HSP17 (Maimbo et al.,

2007). Expression of this gene is induced upon a range of stress treatments. In *hsp17*-silenced *N. benthamiana* plants, expression of defence-related marker genes was compromised, and disease symptoms triggered by *Ralstonia solanacearum* were enhanced, linking HSP17 to disease resistance. However, induction of HR by inoculation with pathogens or by *in planta* expression of the HR-inducing elicitor INF1 was unaffected in these silenced lines (Maimbo et al., 2007). It remains to be investigated whether this HSP17 is involved in R protein-mediated resistance.
Here, we describe identification of RSI2 (Required for Stability of I-2), an HSP20 member that specifically interacts with the tomato I-2 R protein. I-2 confers resistance to *Fusarium oxysporum* (Simons et al., 1998). Besides analysing its physical interaction, we used a virus-induced gene silencing (VIGS) approach to analyse the functional involvement of RSI2 and other known (co)chaperones in HR mediated by autoactive variants of I-2 and a second tomato R protein; Mi-1. Mi-1 belongs to a different subgroup of NB-ARC-LRR proteins (van Ooijen et al., 2007) and confers resistance to root-knot nematode (*Meloidogyne* spec.), potato top aphid and whitefly (Vos et al., 1998). Furthermore, we analysed the effect of silencing RSI2 and other (co)chaperones on I-2 and Mi-1 protein abundance and stability *in planta.*

Results

RSI2 Interacts with the I-2 LRR domain in the yeast two-hybrid system

We reported before the identification of both RSI2 (originally referred to as HSP17) and PP5 as interactors of I-2 bait LRR1-29 in a yeast two-hybrid screen (de la Fuente van Bentem et al., 2005). PP5 has indeed been found using this bait, but RSI2 was identified using a different bait; I-2 LRR12-29, corresponding to amino acid residues 823-1250 (LRR annotation described by (de la Fuente van Bentem et al., 2005)). Screening 6 x 10^6 clones of a tomato cDNA interaction library with bait LRR12-29 revealed two interacting clones. The two cDNA clones carried 733 and 742 basepair inserts (AY150040). The inserts are overlapping and differ only in the length of the 5' regions. Both cDNAs encode a full-length small heat shock protein (sHSP) with a predicted mass of 17.8 kDa. To pinpoint the region of the I-2 protein responsible for the interaction with RSI2, different N- and C-terminal truncations of the I-2 protein were analysed for their interaction in the yeast two-hybrid assay (Figure 1A). Interactions were analysed by the ability to grow on selective plates lacking auxotrophy markers histidine (-HWL) or adenine (-AWL) (Figure 1A). The minimal RSI2-interacting region of the I-2 LRR domain lies within LRRs 15-19, corresponding to amino acids 906-1015 (Figure 1A) Notably, the full-length I-2 protein and the full-length LRR domain (LRR1-29) are expressed (de la Fuente van Bentem et al., 2005), but did not interact with RSI2 in this assay system.

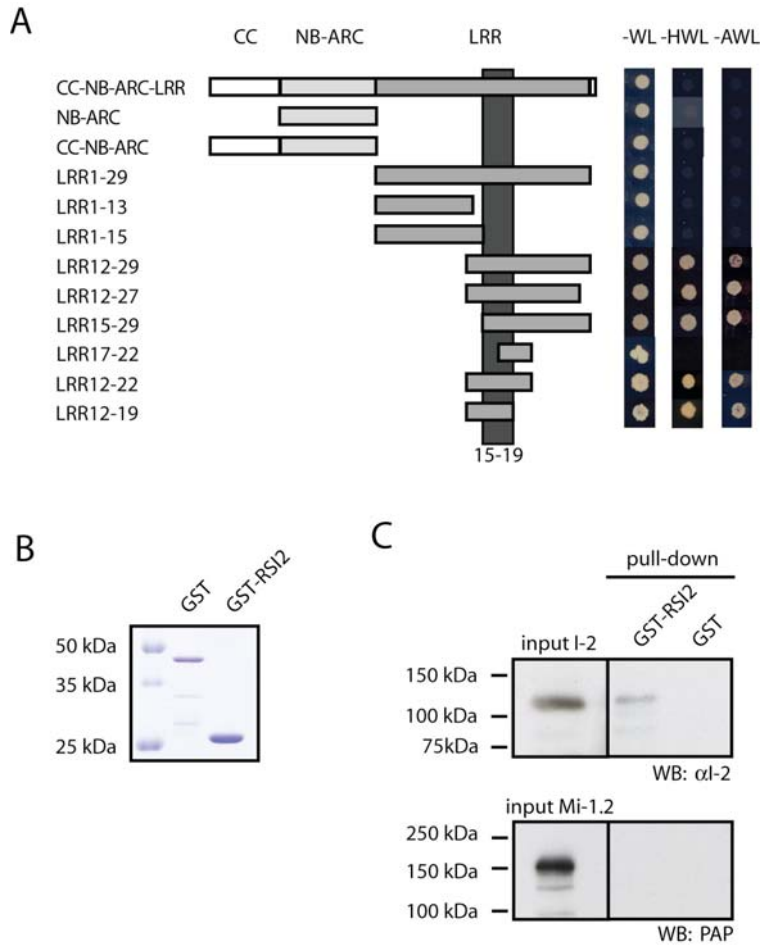

Figure 1

RSI2 interacts with I-2. A) Yeast two-hybrids show interactions between RSI2 and various I-2 baits. The presence of bath and prey plasmids is confirmed by growth on -WL plates whereas the interaction between bait and prey proteins is analyzed on -HWL and –AWL selective plates. The dark-grey area highlights the I-2 region required for RSI2-interaction. B) Coomassie-stained SDS-PAGE gel showing purified GST-RSI2 and GST proteins produced in *Escherichia coli*. C) Western blot (WB) on total protein lysates made from *N. benthamiana leaves* transiently expressing I-2, probed with I-2 antibody (upper panel), or TAP-Mi-1 (lower panel) probed with the PAP antibody. Presence of full-length R proteins in these extracts is shown in the input lanes. GST-RSI2 and GST proteins immobilized on glutathione sepharose beads were incubated with these extracts. Interacting proteins were subjected to SDS-PAGE and Western blot analysis to detect the presence of I-2 or TAP-Mi-1 (right panels).

GST-RSI2 fusion protein interacts with I-2 from plant protein extracts

To verify the interaction identified in the yeast two-hybrid assay between RSI2 and I-2, we next investigated whether RSI2 and I-2 also interact *in planta*. Because the I-2 antibody is not suitable for immunoprecipitations (data not shown), and equipping I-2 with a tag abolishes its activity (van Ooijen et al., 2008), we performed pull-down

experiments of non-tagged I-2 with *Escherichia coli*-produced GST-RSI2 and GST alone. The two GST bait proteins were affinity purified and subsequently analysed on a coomassie-stained SDS-PAGE gel. As shown in Figure 1B, the proteins migrated according to their expected molecular weights (44 and 26 kDa), and little contamination of co-purifying protein was observed.

Endogenous I-2 is expressed at very low levels in tomato and undetectable in total protein leaf extracts using our affinity purified I-2 antibody (Tameling et al., 2002; van Ooijen et al., 2008). To boost expression, we produced full-length I-2 by transient transformation of *Nicotiana benthamiana* leaves using agroinfiltration. The *N. benthamiana*-produced I-2 (Figure 1C) could readily be detected using the I-2 antibody. Total protein extracts of *N. benthamiana* plants transformed with I-2 were incubated with beads loaded with GST or GST-RSI2. A fraction of the I-2 pool was consistently co-purified with the GST-RSI2 sample, but not with the control sample containing GST alone (Figure 1C). The I-2 protein is stable during the purification procedure under the conditions employed (data not shown). The specific co-precipitation of I-2 with GST-RSI2 confirms the interaction as described above.

Interaction of GST-RSI2 with the R protein Mi-1 was also analysed. A TAP-tagged version of Mi-1 was used, as the Mi-1 antibody cross-reacts with the GST-tag (van Ooijen et al., 2008). The TAP tag does not appear to affect Mi-1 protein function, since the TAP-tagged autoactive mutant Mi-1^{H840A} (van Ooijen et al., 2008) can still induce HR similar to the non-tagged protein (Supplementary Figure 1). After agroinfiltration, the band corresponding to TAP-Mi-1 can be readily detected on western blot using a TAP antibody (Figure 1C). Although TAP-Mi-1 protein is stable throughout the pull-down procedure (data not shown), it did not co-precipitate with the GST-RSI2 fusion protein under the conditions used. Together, these results indicate that RSI2 and I-2 are present in one complex whereas no interaction between RSI2 and Mi-1 was found.

VIGS of RSI2 reveals a role in HR mediated by I-2 and Mi-1

R protein function depends on the activities of a number of chaperones or chaperone-associated proteins (de la Fuente van Bentem et al., 2005; Botër et al., 2007). Here we employed VIGS of RSI2 to analyse whether RSI2 is required for R protein function. For comparison SGT1, RAR1, PP5 and HSP90 were included in this assay. VIGS was induced using the tobacco rattle virus (TRV) silencing system, which was delivered by agroinfiltration of the viral vector constructs into the leaflets of two-week old *N. benthamiana* plants (Ratcliff et al., 2001). To analyse onset and spread of silencing in time, phytoene desaturase (PDS) was used as marker (Demmig-Adams and Adams, 1992). The nearly complete photobleaching, consistently observed three weeks after agroinfiltration, indicates extensive PDS

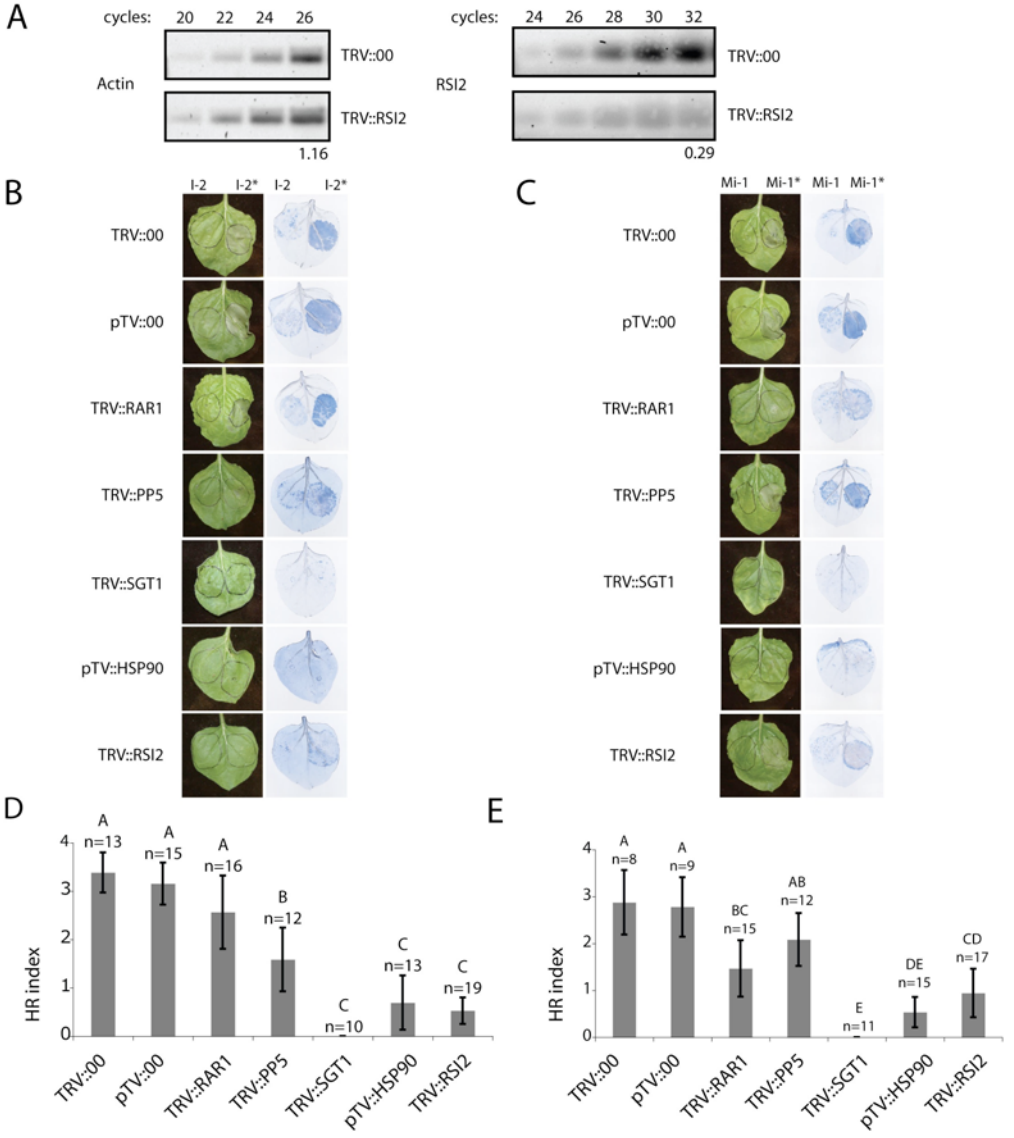

Figure 2

VIGS reveals a role for RSI2 in I-2 and Mi-1-mediated HR signaling. A) Silencing efficiency of RSI2 determined using semi-quantitative RT-PCR (right panel). Actin expression levels were measured as a control for equal cDNA quantity and quality (left panel). Number of PCR cycles are indicated at the top. The relative signal intensity is indicated below (TRV::00 sample indexed at 1). B+C) Agroinfiltration of wild-type (left side of the leaf) or constitutively active mutants (*, right side of the leaf) of I-2 (B) and Mi-1 (C) in *N. benthamiana* three weeks after induction of silencing using the indicated TRV vectors. Pictures were taken 3 days after agroinfiltration and representative leaves were stained using trypan blue to visualize cell death (right panels). D+E) Bar-representation of the severity of HR upon I-2^{D495V} (D) or Mi-1^{D841V} (E) expression in silenced plants. HR was quantified visually on a scale from 0 (no symptoms) to 4 (full necrosis). Significantly different classes can de discerned by a one-way Anova ($P<0.05$). Error bars represent a 95% confidence level.

silencing throughout these plants at this time-point (Supplementary Figure 2). To assess *RSI2* silencing levels, specific primers were designed on the closest *N. benthamiana* homolog available in the TIGR database (GenBank entry DQ275464). Although in the sequenced region, this *N. benthamiana* gene is 80% identical to *RSI2*, it is not predicted to be a silencing target (Xu et al., 2006). However, the relative expression level of this *RSI2* homolog(s) was found to be reduced to 29% in these leaves (Figure 2A). To assess I-2 function in the silenced plants, the upper fully stretched leaves were agroinfiltrated with constructs expressing wild-type I-2 (left side of the leaves) and the constitutively active I-2^{D495V} mutant (right side of the leaves) (Figure 2B). The level of cell death induced by I-2^{D495V} was scored three days after agroinfiltration, on a scale ranging from 0 (absolutely no tissue collapse) to 4 (fully developed HR in the total infiltrated region) as indicated in Supplementary Figure 3. To enhance visibility of HR, the infiltrated leaves were stained for cell death using trypan blue (Figure 2B). Leaves of plants infected with the empty virus control showed clear HR upon expression of I-2^{D495V}, but not upon expression of wild-type I-2 (Figure 2B). This result shows that induction of HR by I-2^{D495V} is not compromised by infection with TRV. In contrast, no (or only minor) tissue collapse induced by I-2^{D495V} was consistently observed in the RSI2 silenced plants (0.5±0.3) compared to the control plants (3.4±0.4), indicating that RSI2 is essential for full I-2 mediated HR. A one-way Anova showed that severity of HR symptoms on RSI2-silenced plants is reduced to similar low levels as on HSP90 and SGT1 silenced plants (Figure 2D). Silencing the established R protein (co)chaperones HSP90 or SGT1 severely suppressed HR triggered by I-2^{D495V}. Silencing of PP5 only partially compromises I-2^{D495} mediated HR, whereas RAR1 silencing did not affect HR significantly.

To analyse whether RSI2 is also involved in HR mediated by Mi-1, we analysed the induction of HR on silenced plants by the autoactivating mutant Mi-1^{D841V} (van Ooijen et al., 2008). In plants infected with the empty viruses, strong HR (2.9±0.7) was induced by this mutant (Figure 2C, right side of the leaves) and not by the wild-type Mi-1 protein (left side of the leaves). In plants silenced for RSI2, HR induced by Mi-1^{D841V} was consistently strongly compromised (Figure 2C and 2E) to 0.9±0.5. These results indicate that RSI2 is not only involved in HR mediated by I-2 but also by Mi-1. Like with I-2^{D495}, Mi-1^{D841V}-mediated HR induction is severely compromised upon SGT1 and HSP90 silencing. PP5 and RAR1 silencing also affect HR induction by Mi-1^{D841V}, although to a lesser extent. These data conclusively show that HR mediated by I-2 and Mi-1 is compromised upon RSI2 silencing.

Silencing RSI2 negatively affects I-2 protein accumulation

The suppressive effect SGT1 silencing has on *N* and *Rx* function is a result of compromised R protein stability due to reduced chaperone activity (Azevedo et al.,

2006; Mestre and Baulcombe, 2006; Botër et al., 2007). HSP20s are also associated with chaperone functions *in vitro* (Nover and Scharf, 1997; Kirschner et al., 2000). To analyse whether the observed effects on HR by silencing RSI2, SGT1, HSP90, PP5 or RAR1 can be attributed to reduced R protein stability, protein accumulation of I-2 and Mi-1 was analysed in the silenced plants. To exclude the possibility that silencing any of these genes adversely influences transgene expression via agroinfiltration *per se*, we agroinfiltrated a construct expressing TAP-tagged GUS protein. Expression levels of this control protein are not altered by silencing the indicated genes (Figure 3C), as shown by a western blot using an antibody against the TAP tag.

R protein accumulation in the silenced plants was assessed in *N. benthamiana* leaves agroinfiltrated with I-2 and Mi-1 constructs. Compared to the vector controls, silencing of RAR1 and PP5 was found to reduce I-2 protein accumulation (Figure 3A). No full-length I-2 protein could be detected in plants silenced for SGT1 and HSP90. However, an accumulation of smaller proteins that cross-react with the I-2

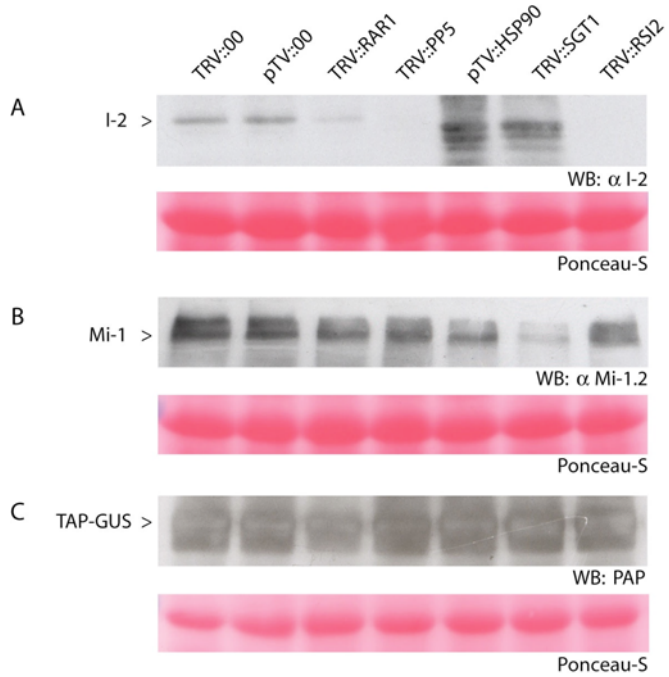

Figure 3

Expression levels of I-2, Mi-1 and GUS protein in silenced *Nicotiana benthamiana* leaves. *N. benthamiana* plants were silenced using the indicated TRV-based silencing construct. Three weeks after induction of silencing, the upper leaves were agroinfiltrated with constructs expressing either I-2, Mi-1 or TAP-tagged GUS. One day after agroinfiltration, leaves were harvested and protein was extracted. 50 µg (I-2 and Mi-1) or 10 µg (TAP-GUS) of total protein was loaded on SDS-page gels. Expression of I-2 (A) Mi-1 (B) or TAP-GUS (C) was analysed on Western blots with the antibody indicated. Equal loading of these blots was confirmed by Ponceau-S staining of Rubisco (lower panels).

antibody was found, suggestive for I-2 derived degradation products. Silencing of RSI2 also led to loss of full-length I-2 accumulation. However, this elimination was not associated with the accumulation of lower molecular weight products.Mi-1 protein abundances in RAR1- or PP5-silenced plants was similar to those observed in the empty virus controls (Figure 3B). Silencing SGT1 led to a clear reduction of Mi-1 protein abundance, whereas HSP90 silencing only slightly affected Mi-1 protein accumulation. In neither case, an increase in lower molecular weight products cross-reacting with the Mi-1 antibody was detected. Hence, although RSI2 is necessary for HR induction by autoactive Mi-1, silencing of RSI2 does not directly affect accumulation of the Mi-1 protein.

To conclude, our data indicate that HSP90 and SGT1 are required for maintaining full-length I-2 and Mi-1 integrity and stability. The functional involvement of RSI2 in I-2 mediated HR is linked to I-2 protein stabilisation, whereas no effect on Mi-1 stability was observed.

Discussion

RSI2 interacts with the I-2 disease resistance protein

In this study we describe the identification of RSI2 as component of the I-2 multiprotein complex. It is unclear whether the RSI2/I-2 interaction is direct, or requires a bridging protein that is functionally conserved in yeast. The RSI2 interacting region was mapped to LRR15-19 of I-2 (Figure 1). This patch differs from that required for the interaction with HSP90 (LRR1-11), but overlaps with the PP5 interacting region (LRR12-22) (de la Fuente van Bentem et al., 2005) suggesting that both proteins might compete for binding. LRR1-29 and full-length I-2 contain the RSI2 interaction patch, however no interaction was observed with these baits in the yeast two-hybrid assay. Likewise a PP5/I-2 interaction in yeast was also found only with truncated versions of I-2 and not with the full-length protein (de la Fuente van Bentem et al., 2005). Possibly folding of extended LRR domains in yeast shields the interaction surface.

The RSI2/I-2 interaction was confirmed in pull-down experiments (Figure 1). Crucial for this experiment was the ability to detect expression of full-length I-2 protein in homogenates of agroinfiltrated *N. benthamiana* leaves. Previous attempts to express I-2 protein using agroinfiltration in a greenhouse or growth chamber did not yield detectable amounts of protein (van Ooijen et al., 2008). Possibly the different conditions used here (lower temperature, light and humidity) enhance the efficiency of *Agrobacterium*-mediated transformations as also reported by (Fu et al., 2006). The enhanced expression under these conditions does not seem to be gene-specific as

enhanced expression was also found with other transgenes tested, such as Mi-1, GUS, PP5 and HSP90 (data not shown).
We do not observe an interaction between RSI2 and Mi-1 in pull-down assays (Figure 1), and accumulation of Mi-1 expression *in planta* was not affected upon RSI2 silencing (Figure 3). However, Mi-1-mediated HR was compromised by silencing RSI2 (Figure 2). Possibly, RSI2 is required for the function of a protein downstream of Mi-1. A possible candidate is the NB-ARC-LRR protein NRC1, that is involved in signalling mediated by many resistance proteins including Mi-1 (Gabriëls et al., 2007). Further studies could reveal whether NRC1 is indeed an RSI2 client.

Silencing experiments reveal a role for RSI2 in HR signalling
RSI2 is, like SGT1, HSP90 and PP5, required for HR triggered by autoactivating mutants of I-2 and Mi-1 (Figure 2). The relative expression of the closest *N. benthamiana* RSI2 homolog is reduced to 29% upon VIGS using the tomato *RSI2* sequence. The presence of other, possibly even closer related, unknown *RSI2* genes in the *N. benthamiana* genome can not be excluded, and silencing might therefore also target other RSI2 homologs. Nevertheless, silencing using the heterologous tomato RSI2 sequence is apparently sufficient to suppress I-2 and Mi-1 mediated HR signalling.
That silencing of SGT1, HSP90 or RAR1 reduces I-2 mediated HR is in line with an earlier study (de la Fuente van Bentem et al., 2005). In that study PP5 was shown to interact with the I-2 LRR domain, however, no effect on I-2 mediated HR was observed upon VIGS of PP5 (de la Fuente van Bentem et al., 2005). Here, we find a relatively small but statistically significant effect on I-2 mediated HR. The difference between these studies might be due to the enhanced efficiency of the *Agrobacterium*-mediated transformation and hence silencing levels (Fu et al., 2006). Support for enhanced silencing efficiency is the more extensive bleaching observed upon PDS silencing in our study as compared to (de la Fuente van Bentem et al., 2005).
We found that HR mediated by a constitutively active variant of Mi-1 is dependent on SGT1 and HSP90, consistent with the involvement of these genes in Mi-1 mediated resistance towards whitefly in tomato (Bhattarai *et al.*, 2007). RAR1 was found not to be involved in Mi-1 mediated resistance to whitefly (Bhattarai *et al.*, 2007), whereas we show that this protein is required for full HR induction by Mi-1. This difference might suggest that HR is not involved or not required for whitefly resistance. The observation that PP5 silencing reduces Mi-1^{D841V}-mediated HR is consistent with the reported yeast two-hybrid interaction between the two (de la Fuente van Bentem et al., 2005).

Chaperones involved in R protein stability

We describe that silencing of RSI2 severely reduces I-2 protein accumulation *in planta* (Figure 3), pointing out a role for RSI2 in chaperoning I-2. Silencing of HSP90 and SGT1 also leads to a reduction in the abundance of full-length I-2 and Mi-1. The interaction between SGT1 and HSP90 has been shown to be necessary for SGT1 to fulfil its functions in resistance mediated by the R protein Rx (Botër et al., 2007). Interestingly, SGT1 is also linked to protein degradation by the ubiquitin/26S proteasome pathway, as it is important for the function of several SCF (for SKP1/CULLIN1/F-box protein) complexes (Kitagawa et al., 1999; Azevedo et al., 2002; Gray et al., 2003). Since SGT1 is also involved in maintaining protein stability, it is thought to be an important regulator determining the fate of a client protein. Silencing SGT1 or interaction partner HSP90 might thus destabilise the full-length I-2 protein by reduced chaperoning activity, but at the same time, the cell might not be able to degrade the resulting unstable, incorrectly folded I-2 products because the link to the proteasome is broken by SGT1 silencing. This link could explain the accumulation of degradation products that cross-react with the I-2 antibody (Figure 3). Upon RSI2 silencing this accumulation is not observed, indicating that this protein is involved in stabilizing I-2, but not in its elimination by the 26S proteasome.

HSP20s have been shown to prevent aggregation of client proteins in an HSP90 and ATP independent manner, RSI2 might function in a similar fashion. Alternatively, RSI2 might function in conjunction with HSP90. HSP20s are characterised by a HSP20/α-crystalline fold, forming a beta-sandwich of two parallel β-sheets. The crystal structure of wheat HSP20 (van Montfort et al., 2001) reveals that this fold closely resembles that of the CS domain (Finn et al., 2006), as found in SGT1 and in p23, where it is required for their binding to HSP90 (Boter et al., 2007). P23 regulates human HSP90 activity by a direct interaction with the ATP-bound active form of HSP90 (Johnson et al., 1994). *In vitro*, p23 has been shown to interact with partially folded proteins and to prevent these from aggregation (Bose et al., 1996). The related fold of HSP20s and p23, together with the experimentally verified chaperoning activities of both, could indicate a similar biochemical function as chaperones and co-regulators of HSP90 activity. The absence of the I-2 breakdown products in RSI2 silenced plants (that was observed in SGT1 and HSP90 silenced plants), might indicate that RSI2 is mainly involved in the chaperoning functions (possibly together with the HSP90/SGT1 machinery) and is not involved (or redundant) in the process of targeted protein degradation via SGT1. Efforts to test this hypothesis and show an interaction between RSI2 and HSP90 in yeast two-hybrid where not successful (results not shown). Likewise, we where unable to establish the presence of a ternary complex of I-2, RSI2 and HSP90 in our RSI2 pull-downs (Figure 2) after probing the blot with an HSP90 antibody (data not shown).

Future studies should reveal whether RSI2 functions as a p23-like regulator of the HSP90/SGT1 machinery, or that it performs it chaperone functions independent of HSP90.

To summarize, we report an HSP20 that engages in the I-2 protein complex and positively contributes towards a full HR mediated by autoactive I-2 and Mi-1 mutants. We observe a significant effect of RSI2, SGT1 and HSP90 silencing on I-2 protein accumulation, showing that these proteins are required for I-2 accumulation. Mi-1 protein abundance was also reduced upon silencing of HSP90 and SGT1 but not by RSI2. Possibly another RSI2 client protein required for Mi-1 mediated HR is affected in these plants. These results add RSI2 to the list of chaperones that are required for R protein function.

Acknowledgements

Jesse van de Hove is thanked for his help with the yeast two-hybrid library screen. Harold Lemereis, Thijs Hendrix and Ludek Tikovsky are acknowledged for plant care. We thank Patrick Mak for construction of the RSI2 silencing vector, Wendy Roels and Klaas Jan de Vries for help with the yeast two-hybrid analyses and construction of the GST-HSP17 clone. Martijn Rep is thanked for critical review of the manuscript. David Baulcombe and Savithramma Dinesh-Kumar are acknowledged for sharing the TRV silencing constructs. GvO is supported by the Research Council for Earth and Life Sciences (ALW) with financial aid from the Netherlands Organization for Scientific Research (NWO), and by the Centre for BioSystems Genomics, the Netherlands. HvdB is supported by the Netherlands Organization for Scientific Research (NWO VENI grant 863.04.018).

Materials and methods

Yeast two-hybrid

The PJ69-4a host strain was grown on Minimal Medium (MM: 2% glucose, 0.17% yeast nitrogen base, 0,5% $(NH_4)_2SO_4$) supplemented with 0.002% Uracil, 0.004% D/L-Methionine, 0.01% L-Leucine (L), 0.002% L-Tryptophane (W), 0.002% Adeninesulfate (A) and 0.002% L-Histidine (H). PJ69-4a harbors three reporter genes that can be transcriptionally activated upon reconstitution of the Gal4 transcription factor. These genes are the *E. coli LacZ* gene, whose expression can be detected by X-gal staining of the yeast colony, and the yeast *ADE2* and *HIS3* genes, which can be selected for by adenine and histidine prototrophy, respectively. If selection for an auxotrophy marker was desired, one or more of the components was omitted from the medium (MM-W, L, A, H). PJ69-4a was transformed with plasmids that contain bait (pAS2-1) and prey (pACT2) constructs (Clontech). Tryptophane and leucine prototrophic transformants were selected on MM-WL plates. Droplets of a cell dilution corresponding to 10^4 cells were spotted on MM-WL, MM-HWL and MM-AWL plates. The I-2 baits used in this study have been described before (de la Fuente van Bentem *et al.*, 2005).

***Agrobacterium*-mediated transformation and silencing**

Agrobacterium tumefaciens strain GV3101(pMP90) (Koncz and Schell, 1986) was transformed with the indicated vectors and grown to OD_{600}=0.8 in LB-Mannitol (10 g/l tryptone, 5 g/l yeast extract, 2.5 g/l NaCl, 10 g/l mannitol) medium supplemented with 20 µM acetosyringone and 10 mM MES pH 5.6. Cells were pelleted and resuspended in infiltration medium (1x MS salts, 10 mM MES pH 5.6, 2% w/v sucrose, 200 µM acetosyringone) and infiltrated at OD_{600}=1. Importantly, all *Agrobacterium* infiltrations were performed in a laboratory (no direct sunlight, 20º C) rather than a growthchamber or a greenhouse. Two week-old *N. benthamiana* leaves were used for infiltration with TRV-based silencing constructs. Subsequently, the plants were kept in the laboratory for 3 days and then transferred to the greenhouse to allow spread of the TRV virus. *Agrobacterium*-mediated expression of the R proteins was performed in the laboratory 2.5 weeks after silencing. Trypan blue staining was performed as described before (van Ooijen *et al.*, 2008).
RSI2 silencing was performed with the tobacco rattle virus (TRV) system by cloning an *Eco*RI/*Xho*I fragment from the cDNA pACTII library clone (de la Fuente van Bentem *et al.*, 2005) into pYL156 (Liu *et al.*, 2002). An *Eco*RI/*Sal*I fragment from the tomato PP5 TPR domain pAS2-1 bait vector (de la Fuente van Bentem *et al.*, 2005) was ligated into pYL156 digested with *Eco*RI/*Xho*I. An *Bam*HI/*Sal*I fragment from the SGT1 silencing vector used by (Peart *et al.*, 2002) is ligated into pYL156 digested with *Bam*HI/*Xho*I. RAR1 was silenced using the silencing vector described by (Liu *et al.*, 2002). HSP90 silencing is performed using the TRV silencing vector described by (Ratcliff *et al.*, 2001) and the RNA2 clone used in (de la Fuente van Bentem *et al.*, 2005). Silencing was performed with the corresponding RNA1 construct (Ratcliff et al., 2001; Liu et al., 2002). Empty RNA2 vectors were used as negative controls.

RT-PCR

RNA was extracted with Trizol. cDNA was amplified from 1 ug RNA using SupersrciptIII (invitrogen, according to manufacterer). RSI2 fragments were amplified using the primer set (ctgaagcacatgtgtttaaggcc and cttgacatcaggcttcttcac). Agarose gel was stained for 12 hrs using SYBR Green (Invitrogen) and scanned using a STORM phosphoimager (Amersham Bioscience). The signal intensities were measured using ImageQuant and corrected for background levels.

Binary vector construction

The binary vectors for wild-type I-2, I-2 D495V, wild-type Mi-1 and Mi-1 D841V have been described by (van Ooijen *et al.*, 2008). The TAP tagged wild-type Mi-1 construct was generated by PCR on pSE23 (Gabriëls *et al.*, 2007) using (aaaaagcaggctctatggaaaaacgaaaagatatt) and agaaagctgggttcttaaataaggggatattcttctg). Gateway *att*B sequences were added by adapter PCR using the primer set (ggggacaagtttgtacaaaaaagcaggct) and (ggggaccactttgtacaagaaagctgggt). The PCR products were transferred to binary vector CTAPi (Rohila *et al.*, 2004) by the Gateway one-tube protocol for cloning *att*B-PCR products directly into destination vectors (Invitrogen). To obtain a TAP-tagged autoactive mutant, a *Bsp*119I/*Bcu*I fragment was exchanged between the non-tagged Mi-1 H840A construct described in (van Ooijen *et al.*, 2008) and the wild-type clone. This removes the stop codon in the original mutant construct and allows a translational fusion to the tag. The TAP-GUS control was generated by a Gateway LR reaction from the GUS control plasmid included in the LR kit (Invitrogen) to the binary vector NTAPi (Rohila *et al.*, 2004). Clones were sequenced to verify the correct insert sequence.

One-way Anova

For the statistical analysis of HR induction by autoactive R protein mutants on silenced plants, HR was visually scored three (I-2) or four (Mi-1) days after agroinfiltration. Data sets from three independent silencing experiments on 5 to 8 plants per silenced gene were scored, adding up to 30 (SGT1) to 47 (RSI2) independent scores. On these data, a one-way Anova was performed with StatView using a significance interval of 95%. Error bars in charts represent a 95% confidence level calculated using Microsoft Excel.

Protein extraction and Western blotting

For the analysis of R protein expression level in silenced plants, 3 leaves from 3 independent silenced plants (9 total) were harvested and pooled 24 hours after agroinfiltration with GUS, I-2 or Mi-1 and frozen in liquid nitrogen. After grinding the tissue, it was allowed to thaw in 1 ml protein extraction buffer per 500 mg of tissue (25 mM Tris pH 8, 1 mM EDTA, 150 mM NaCl, 5 mM DTT, 0,1% NP-40, 1 x Roche Complete protease inhibitor cocktail and 2% poly-(vinyl-poly-pyrolidone) (PVPP)). Extracts were cleared by centrifugation at 12,000 *g* for 10 minutes at 4º C and the supernatant was passed over 4 layers of Miracloth. Protein concentrations were measured using a Bradford assay (Bradford, 1976) and standardised with extraction buffer without PVPP. The extract was mixed with Laemmli sample buffer. 50µg of total plant protein was separated on 8% SDS-PAGE gels and blotted on PVDF membranes using the semi-dry blotting system TE77 (GE Healthcare). Equal loading was verified by staining the membrane using Ponceau S. 5% skimmed milk powder was used as a blocking agent. As a primary antibody, a 1:4000 dilution of the I-2 or Mi-1 antibody (van Ooijen *et al*., 2008) was used and as a secondary antibody a 1:4000 dilution of goat-anti-rabbit linked to horseradish peroxidase. For TAP-GUS detection, a 1:10,000 dilution was used of the PAP antibody (Sigma). Luminescence was visualised with ECL Plus (GE healthcare) and BioMax MR film (Kodak).

GST-RSI2 production and pull-down

E. coli strain BL21 (DE3) was transformed with empty pGEX-KG and with pGEX-KG containing full-length RSI2. The latter was generated by cloning the full-length RSI2 sequence from the pACTII interaction clone into pGEX-KG digested with *Nco*I/*Xho*I. 5 ml LB overnight culture supplemented with 50 µg/ml carbenicillin was diluted 10 times. After 2 hours of incubation at 37º C, protein expression was induced by incubation at room-temperature for 5 hours in the presence of 1.5 mM IPTG. Pelleted cells were frozen at -20º C and thawed by resuspending in 10 ml ice-cold PBS pH 7.4, supplemented with 1x protein inhibitor cocktail (Roche). Lysozyme was added to a final concentration of 1mg/ml and the suspension was rotated gently at 4º C for 30 min. After adding Triton X-100 (0.5%) the mixture was rotated for an additional 30 minutes at 4º C. The cell mixture was sonicated on ice 2 times for 2 minutes. Cell debris was removed by two centrifugation steps of 20 minutes at 18000 *g* at 4º C. The supernatant was 1x diluted in PBS pH 7.4 and aliquots were frozen. To 1 ml of extract, 200 µl 50% GST beads slurry (GE Healthcare) was added and the capture was performed rotating at 4º C for 1.5 hour. Pelleted beads were washed 4 times with 0.5 ml ice-cold PBS pH 7.4 supplemented with Roche Complete protease inhibitors. I-2 or Mi-1-TAP protein was extracted from *N. benthamiana* tissue in which I-2 or Mi-1-TAP was expressed by *Agrobacterium* transformation. 10 mg of total protein lysate was supplemented with an additional 0.1% NP40 to obtain the interaction buffer and added to 10 µg of immobilised GST-RSI2 or GST protein. The final interaction buffer conditions were 25 mM Tris pH 8, 1 mM EDTA, 150 mM NaCl, 5 mM DTT, 0.2% NP-40, 1 x Roche Complete protease inhibitor cocktail. This mixture was incubated overnight at 4º C to allow the interaction to take place. The beads were pelleted and washed for 5 times with interaction buffer. Proteins were eluted by addition of Laemmli sample buffer to the pelleted beads and samples were run on an 8% SDS-PAGE gel. Blotting and detection procedures as described above.

The sequence of RSI2 was deposited in genbank under accession number AY150040.

Supplementary data

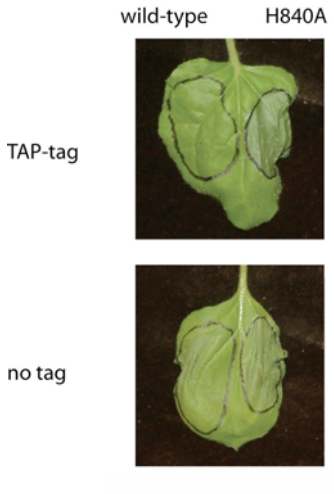

Supplementary Figure 1
C-terminally TAP tagged Mi-1 H840 induces HR. Agroinfiltrated *N. benthamiana* leaves expressing wild-type Mi-1 or constitutively active mutant Mi-1 H840A, either C-terminally TAP-tagged (top leaf) or non-tagged (bottom leaf).

Supplementary Figure 2
Nicotiana benthamiana plants were silenced for phytoene desaturase to visualise the efficiency of silencing. Due to a disturbed carotenoid biosynthesis, the plants become susceptible to photobleaching. Pictures were taken three weeks after agroinfiltration with TRV::PDS.

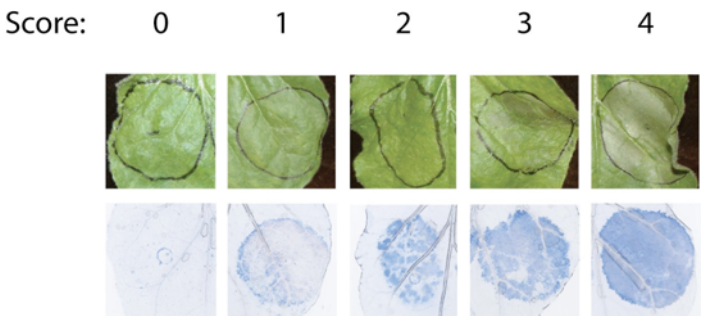

Supplementary Figure 3
The visual range of HR intensity scores. HR initiated by agroinfiltration of the autoactive mutants I-2^{D495V} and Mi-1^{D841V} on silenced plants was scored on a visual range from 0 to 4. Representative leafs of all 5 classes are depicted (top panels) and cell death is visualised by Trypan blue staining (lower panels). 0: no visible cell death, 1: first symptoms (a grey shade) of tissue collapse in the infiltrated region on the lower side of the leaf, but no symptoms on the top side of the leaf, 2: clearly developing tissue collapse on the lower side of the leaf and first symptoms of HR on the upper side of the leaf, 3: clear HR visible on the upper side of the leaf, but not in the total infiltrated zone, 4: total infiltrated region shows cell death.

References

Azevedo, C., Sadanandom, A., Kitagawa, K., Freialdenhoven, A., Shirasu, K., and Schulze-Lefert, P. (2002). The RAR1 interactor SGT1, an essential component of *R* gene-triggered disease resistance. Science **295,** 2073-2076.

Azevedo, C., Betsuyaku, S., Peart, J., Takahashi, A., Noel, L., Sadanandom, A., Casais, C., Parker, J., and Shirasu, K. (2006). Role of SGT1 in resistance protein accumulation in plant immunity. EMBO J **25,** 2007-2016.

Bose, S., Weikl, T., Bugl, H., and Buchner, J. (1996). Chaperone function of Hsp90-associated proteins. Science **274,** 1715-1717.

Boter, M., Amigues, B., Peart, J., Breuer, C., Kadota, Y., Casais, C., Moore, G., Kleanthous, C., Ochsenbein, F., Shirasu, K., and Guerois, R. (2007). Structural and functional analysis of SGT1 reveals that its interaction with HSP90 is required for the accumulation of Rx, an R protein involved in plant immunity. Plant Cell **19,** 3791-3804.

Botër, M., Amigues, B., Peart, J., Breuer, C., Kadota, Y., Casais, C., Moore, G., Kleanthous, C., Ochsenbein, F., Shirasu, K., and Guerois, R. (2007). Structural and functional analysis of SGT1 reveals that its interaction with HSP90 is required for the accumulation of Rx, an R protein involved in plant immunity. Plant Cell **19,** 3791-3804.

Caspers, G.J., Leunissen, J.A., and de Jong, W.W. (1995). The expanding small heat-shock protein family, and structure predictions of the conserved "alpha-crystallin domain". J Mol Evol **40,** 238-248.

de la Fuente van Bentem, S., Vossen, J.H., de Vries, K.J., van Wees, S., Tameling, W.I.L., Dekker, H.L., de Koster, C.G., Haring, M.A., Takken, F.L.W., and Cornelissen, B.J.C. (2005). Heat shock protein 90 and its co-chaperone protein phosphatase 5 interact with distinct regions of the tomato I-2 disease resistance protein. Plant J **43,** 284-298.

Demmig-Adams, B., and Adams, W.W. (1992). Photoprotection and other responses of plants to high light stress. Annu Rev Plant Physiol Plant Mol Biol **43,** 599-626.

Finn, R.D., Mistry, J., Schuster-Bockler, B., Griffiths-Jones, S., Hollich, V., Lassmann, T., Moxon, S., Marshall, M., Khanna, A., Durbin, R., Eddy, S.R., Sonnhammer, E.L., and Bateman, A. (2006). Pfam: clans, web tools and services. Nucleic Acids Res **34,** D247-251.

Fu, D.Q., Zhu, B.Z., Zhu, H.L., Zhang, H.X., Xie, Y.H., Jiang, W.B., Zhao, X.D., and Luo, K.B. (2006). Enhancement of virus-induced gene silencing in tomato by low temperature and low humidity. Mol Cells **21,** 153-160.

Gabriëls, S.H.E.J., Vossen, J.H., Ekengren, S.K., van Ooijen, G., Abd-El-Haliem, A.M., van den Berg, G.C., Rainey, D.Y., Martin, G.B., Takken, F.L.W., de Wit, P.J.G.M., and Joosten, M.H.A.J. (2007). An NB-LRR protein required for HR signalling mediated by both extra- and intracellular resistance proteins. Plant J **50,** 14-28.

Gray, W.M., Muskett, P.R., Chuang, H.W., and Parker, J.E. (2003). Arabidopsis SGT1b is required for SCF(TIR1)-mediated auxin response. Plant Cell **15,** 1310-1319.

Heise, C.T., Le Duff, C.S., Boter, M., Casais, C., Airey, J.E., Leech, A.P., Amigues, B., Guerois, R., Moore, G.R., Shirasu, K., and Kleanthous, C. (2007). Biochemical characterization of RAR1 cysteine- and histidine-rich domains (CHORDs): a novel class of zinc-dependent protein-protein interaction modules. Biochem **46,** 1612-1623.

Helm, K.W., Lee, G.J., and Vierling, E. (1997). Expression and native structure of cytosolic class II small heat-shock proteins. Plant Physiol **114,** 1477-1485.

Hubert, D.A., Tornero, P., Belkhadir, Y., Krishna, P., Takahashi, A., Shirasu, K., and Dangl, J.L. (2003). Cytosolic HSP90 associates with and modulates the Arabidopsis RPM1 disease resistance protein. EMBO J **22,** 5679-5689.

Johnson, J.L., Beito, T.G., Krco, C.J., and Toft, D.O. (1994). Characterization of a novel 23-kilodalton protein of unactive progesterone receptor complexes. Mol Cell Biol **14,** 1956-1963.

Kirschner, M., Winkelhaus, S., Thierfelder, J.M., and Nover, L. (2000). Transient expression and heat-stress-induced co-aggregation of endogenous and heterologous small heat-stress proteins in tobacco protoplasts. Plant J **24,** 397-411.

Kitagawa, K., Skowyra, D., Elledge, S.J., Harper, J.W., and Hieter, P. (1999). *SGT1* encodes an essential component of the yeast kinetochore assembly pathway and a novel subunit of the SCF ubiquitin ligase complex. Mol Cell **4,** 21-33.

Koncz, C., and Schell, J. (1986). The promoter of Tl-DNA gene *5* controls the tissue-specific expression of chimaeric genes carried by a novel type of *Agrobacterium* binary vector. Mol Gen Genet **204,** 383-396.

Lee, G.J., Pokala, N., and Vierling, E. (1995). Structure and in vitro molecular chaperone activity of cytosolic small heat shock proteins from pea. J Biol Chem **270,** 10432-10438.

Liu, Y., Schiff, M., Serino, G., Deng, X.W., and Dinesh-Kumar, S.P. (2002). Role of SCF ubiquitin-ligase and the COP9 signalosome in the *N* gene-mediated resistance response to *Tobacco mosaic virus*. Plant Cell **14,** 1483-1496.

Liu, Y., Burch-Smith, T., Schiff, M., Feng, S., and Dinesh-Kumar, S.P. (2004). Molecular chaperone Hsp90 associates with resistance protein N and its signaling proteins SGT1 and Rar1 to modulate an innate immune response in plants. J Biol Chem **279,** 2101-2108.

Lu, R., Malcuit, I., Moffett, P., Ruiz, M.T., Peart, J., Wu, A.J., Rathjen, J.P., Bendahmane, A., Day, L., and Baulcombe, D.C. (2003). High throughput virus-induced gene silencing implicates heat shock protein 90 in plant disease resistance. EMBO J **22,** 5690-5699.

Maimbo, M., Ohnishi, K., Hikichi, Y., Yoshioka, H., and Kiba, A. (2007). Induction of a small heat shock protein and its functional roles in Nicotiana plants in the defense response against Ralstonia solanacearum. Plant Physiol **145,** 1588-1599.

Martin, G.B., Bogdanove, A.J., and Sessa, G. (2003). Understanding the functions of plant disease resistance proteins. Annu Rev Plant Biol **54,** 23-61.

Mestre, P., and Baulcombe, D.C. (2006). Elicitor-mediated oligomerization of the tobacco N disease resistance protein. Plant Cell **18,** 491-501.

Nover, L., and Scharf, K.D. (1997). Heat stress proteins and transcription factors. Cell Mol Life Sci **53,** 80-103.

Pearl, L.H., and Prodromou, C. (2006). Structure and mechanism of the Hsp90 molecular chaperone machinery. Annu Rev Biochem **75,** 271-294.

Ratcliff, F., Martin-Hernandez, A.M., and Baulcombe, D.C. (2001). Technical Advance. Tobacco rattle virus as a vector for analysis of gene function by silencing. Plant J **25,** 237-245.

Shirasu, K., Lahaye, T., Tan, M.W., Zhou, F., Azevedo, C., and Schulze-Lefert, P. (1999). A novel class of eukaryotic zinc-binding proteins is required for disease resistance signaling in barley and development in C. elegans. Cell **99,** 355-366.

Simons, G., Groenendijk, J., Wijbrandi, J., Reijans, M., Groenen, J., Diergaarde, P., Van der Lee, T., Bleeker, M., Onstenk, J., De Both, M., Haring, M., Mes, J., Cornelissen, B., Zabeau, M., and Vos, P. (1998). Dissection of the fusarium *I2* gene cluster in tomato reveals six homologs and one active gene copy. Plant Cell **10,** 1055-1068.

Takahashi, A., Casais, C., Ichimura, K., and Shirasu, K. (2003). HSP90 interacts with RAR1 and SGT1 and is essential for RPS2-mediated disease resistance in *Arabidopsis*. Proc Natl Acad Sci USA **100,** 11777-11782.

Tameling, W.I.L., Elzinga, S.D., Darmin, P.S., Vossen, J.H., Takken, F.L.W., Haring, M.A., and Cornelissen, B.J.C. (2002). The tomato *R* gene products I-2 and Mi-1 are functional ATP binding proteins with ATPase activity. Plant Cell **14,** 2929-2939.

Van Montfort, R., Slingsby, C., and Vierling, E. (2001). Structure and function of the small heat shock protein/alpha-crystallin family of molecular chaperones. Adv Protein Chem **59,** 105-156.

van Montfort, R.L., Basha, E., Friedrich, K.L., Slingsby, C., and Vierling, E. (2001). Crystal structure and assembly of a eukaryotic small heat shock protein. Nat Struct Biol **8,** 1025-1030.

van Ooijen, G., van den Burg, H.A., Cornelissen, B.J.C., and Takken, F.L.W. (2007). Structure and function of resistance proteins in solanaceous plants. Annu Rev Phytopathol **45,** 43-72.

van Ooijen, G., Mayr, G., Kasiem, M.M.A., Albrecht, M., Cornelissen, B.J.C., and Takken, F.L.W. (2008). Structure-function analysis of the NB-ARC domain of plant disease resistance proteins. J Exp Bot **59,** 1383-1397

Vos, P., Simons, G., Jesse, T., Wijbrandi, J., Heinen, L., Hogers, R., Frijters, A., Groenendijk, J., Diergaarde, P., Reijans, M., Fierens Onstenk, J., De Both, M., Peleman, J., Liharska, T., Hontelez, J., and Zabeau, M. (1998). The tomato *Mi-1* gene confers resistance to both root-knot nematodes and potato aphids. Nature Biotechnol **16,** 1365-1369.

Xu, P., Zhang, Y., Kang, L., Roossinck, M.J., and Mysore, K.S. (2006). Computational estimation and experimental verification of off-target silencing during posttranscriptional gene silencing in plants. Plant Physiol **142,** 429-440.

Chapter 6

General Discussion

The research described in this thesis has been aimed at gaining knowledge on plant Resistance (R) protein structure and function. Resistance mediated by R proteins is dependent on the presence of a cognate Avirulence (AVR) protein in the pathogen. Because of this genetic interaction, this type of resistance was called gene-for-gene resistance (Flor, 1942). The mechanism underlying this gene-for-gene resistance is still not conclusively known. The main questions that have intrigued scientists around the world for decades (and will continue to do so) involve the process of R proteinactivation and the function that the different (sub)domains and conserved sequence elements play in these processes. Additionally, we know little about which other proteins are involved in orchestrating the plant R protein-mediated disease resistance mechanism. In this chapter, the results described in this thesis will be highlighted. Possible future directions and opportunities for research are presented that could help us writing the remaining blank pages in the textbook on R protein-mediated disease resistance pathways.

A functional role for the MHD motif as sensor to transduce nucleotide-dependent conformational changes

As discussed in Chapter 2, most R proteins consist of three domains (CC/TIR, NB-ARC, and LRR (Figure 1A)). The central domain is called the NB-ARC domain (van der Biezen and Jones, 1998), because of its proposed Nucleotide-Binding properties, and its presence in the human protein APAF-1 (apoptotic protease-activating factor-1), R proteins and CED-4 (*Caenorhabditis elegans* death-4 protein). Domains structurally related to the NB-ARC can be found in animal proteins of the NLR (nucleotide-binding domain, LRR containing) family (Ting et al., 2008). Many of these proteins act as receptors sensing intracellular perturbations.

No crystal structure has been solved for any plant NB-ARC domain, but it has been for APAF-1 (Riedl et al., 2005) and CED-4 (Yan et al., 2005). The APAF-1 NB-ARC domain consists of the nucleotide-binding (NB) subdomain and three other subdomains called ARC1, -2, and -3. In CED-4 and plant R proteins, the ARC3 subdomain is absent but the ARC1 and ARC2 subdomains are conserved (Albrecht and Takken, 2006). Specific ADP-binding by APAF-1 is achieved through interactions with various conserved residues present in the NB, ARC1, and ARC2 subdomains (Riedl et al., 2005). Because only the ADP-bound structure has been solved for APAF-1, it is not known how it senses the γ-phosphate of ATP. In CED-4, a conserved arginine in the NB subdomain sensor I region directly interacts with the γ-phosphate (Yan et al., 2005).

Numerous motifs have been identified throughout the R protein NB-ARC domain (Meyers et al., 1999; Pan et al., 2000) (Figure 1A). The functional importance of these motifs is exemplified by the many mutations of motif residues that were demonstrated to result in either loss-of-function or autoactivation of the NB-ARC-LRR protein (Chapters 3, 4, and reviewed in (Takken et al., 2006)). The MHD motif is one of the most conserved regions in R proteins (Chapter 3 and (Howles et al., 2005)). This MHD motif is located in the NB-ARC domain, at the C-terminus of the ARC2 subdomain (Figure 1A). By constructing a 3D model of the I-2 NB-ARC domain, the structural position of the MHD residues have been visualised (Chapters 3, 4, and Figure 1). As can be seen in Figure 1B, the position of the MHD histidine (H494) suggests that it directly interacts with, and positions the β-phosphate of the ADP, like it does in APAF-1 (Riedl et al., 2005; Albrecht and Takken, 2006). A direct interaction of the ARC2 subdomain with the nucleotide via this histidine is not found in related AAA+ ATPases. These proteins contain a so-called sensor II motif in the ARC1 subdomain, surrounding a conserved arginine residue that coordinates the bound nucleotide and controls intersubunit interactions (Ogura et al., 2004). APAF-1 and R proteins do not appear to share this sensor II motif, and its function might be taken

over by the MHD motif. The interaction of the MHD histidine with the ADP molecule is proposed to stabilize the ADP-bound conformation and participate in the interaction between the NB and the ARC2 subdomains. The MHD aspartate (D495) likely directly interacts with an arginine (R313) in the NB subdomain sensor I motif (Figure 1B). Mutation of this arginine in I-2 leads to a strong loss-of-function phenotype (Chapter 3).

Mutation of the 100% conserved MHD histidine or the 83% conserved aspartate would weaken interactions between the NB-ARC subdomains and between the ADP molecule and the protein. This perturbation is likely to result in destabilization of the inactive conformation, allowing transition to the active state (Chapter 3). In the cases that the MHD aspartate is not conserved, it is always replaced by another polar hydrophilic amino acid (except for the atypical rice R protein Pita), that probably does not affect the inactive conformation. Based on these observations, we propose that the MHD motif takes over both AAA+ protein sensor II functions; notably coordination of the bound nucleotide and control of intersubunit interactions.

Although the model of the planrt NB-ARC domain presented in Chapter 3 has been validated by mutational analysis, it remains a model. Ultimately, to solve the R protein NB-ARC structure and dynamic changes upon activation of the defence response, crystal structures of both the ADP- and ATP-bound pockets would be essential. Although modelling leads to a good view of the inactive ADP-bound conformation, we know little about the activated, ATP-bound state. Although many people in the plant disease resistance research community seem to be convinced that these structures would be a big leap towards understanding R protein function, this goal is still not achieved. The main reason for this is probably the difficulty of obtaining sufficient amounts of properly folded R protein. Besides the opportunity to crystallize the R protein, the production of full-length R protein would also open ways to analyse the nucleotide binding and hydrolysis characteristics of (mutant) R proteins. Thus far, we have only been able to show ATPase activity for truncated I-2 and Mi-1 versions (Tameling et al., 2002) produced in *E. coli*, but we have been unable to produce sufficient amounts of properly folded full-length protein up to date (data not shown). Hopefully these experiments will be possible in the near future, and encouraging results are obtained using the yeast *Pichia pastoris* as a heterologous expression system for the production of full-length flax R protein M (Schmidt et al., 2007). Alternatively, R protein could be produced in *N. benthamiana* plants by agroinfiltration. For the subsequent purification, tandem affinity tagged R protein variants might be useful, such as the TAP-tagged Mi-1 described in Chapter 5. To boost the protein expression levels, co-infiltration with silencing suppressors could be helpful, although we observe a rapid cell death response upon expression of wild-type Mi-1 in the presence of silencing suppressors (data not shown). This might be

overcome by using a system in which HR is not induced, like a mutant background or a plant species irresponsive to the R protein. Otherwise, R protein might be produced in animal cells. Encouragingly, we have been able to detect a small amount of full-length I-2 protein produced in human cells (K.J. de Vries, unpublished data).
Anyhow, at least until crystal structures of R proteins become available, the models presented in Chapters 3 and 4 will be a useful source of information to study the function of the NB-ARC domain as a molecular switch regulating R protein activity.

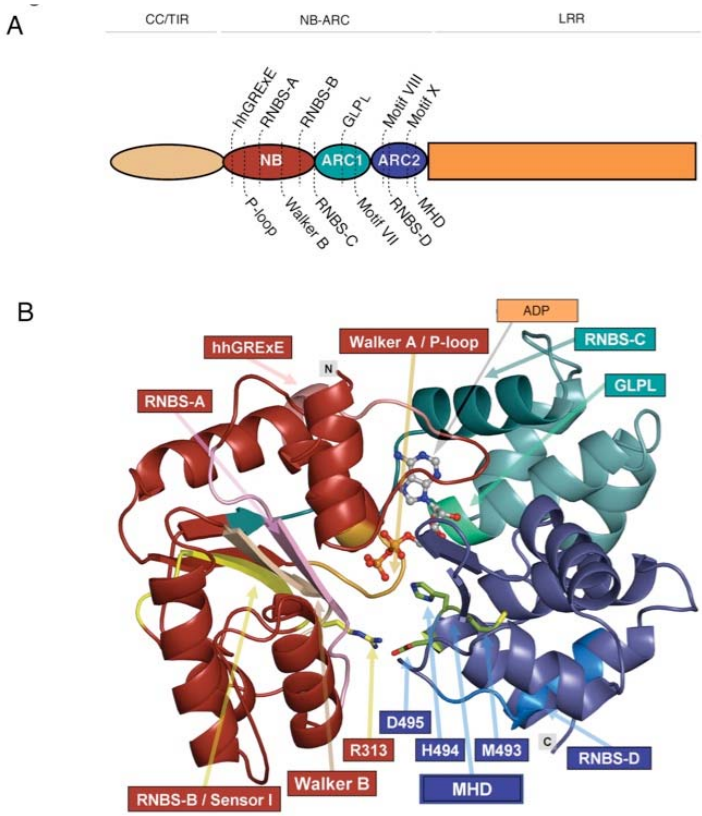

Figure 1
Proposed protein topology of the NB-ARC domain. (A) The position of conserved motifs in the NB, ARC1, and ARC2 subdomains is indicated in the schematic representation of a typical NB-LRR R protein. Picture adapted from Chapter 2. (B) Computationally derived 3D structure model of the NB-ARC domain of the resistance protein I-2. The model was created using the ADP bound structure of human APAF-1 (PDB code 1z6t, chain A) as structural template for I-2. The locations of R protein motifs are marked with arrows. Amino acids of the MHD motif as well as the sensor I arginine are shown in stick representation. ADP atoms are depicted as balls-and-sticks. Subdomain colouring is: NB: red, ARC1: green, ARC2: blue. Picture adapted from Chapter 3.

Intramolecular association with the LRR domain is not compromised upon activation

Domain swaps between Mi-1 (also referred to as Mi-1.2) and its paralogue Mi-1.1, lead to chimaeric proteins with different characteristics. For example, incorporation of the Mi-1.2 LRR domain in a Mi-1.1 context, leads to a chimaeric protein (DS4) that strongly autoactivates (Hwang et al., 2000). These experiments initially led to a model proposing that in the repressed state, the LRR domain interacts with the N-terminus. In case of autoactivation by Mi-DS4, this interaction would be released, leading to an autoactive molecule (Hwang et al., 2000; Hwang and Williamson, 2003). The observed constitutive interaction between the CC-NB-ARC and LRR domain described in Chapter 4 shows that the initial model is oversimplified. Not only did we observe physical interactions between both autoactive (Mi-DS4) and inactive (Mi-DS2) domain combinations of Mi-1 paralogues, but also autoactivation and loss-of-function mutations in NB and ARC2 did not result in dissociation of the CC-NB-ARC and LRR domains. The ability to transcomplement and reconstitute an HR signalling-competent molecule was compromised in autoactivating MHD mutants, but not in NB autoactivation mutants or autoactive domain swaps.

Likely, in the Mi-1 variants mentioned above, the functional interaction between parts of the protein is lost, even though the physical interaction between the LRR domain and its N-terminus remains. In Rx, MHD mutant D460V can still transcomplement with the LRR domain (Moffett et al., 2002). A possible reason for this difference is that Rx belongs to a different group of CC-NB-ARC-LRR proteins (Chapter 2). Further pull-down experiments with domains of different R proteins would be helpful to reveal whether subclass-specific differences are involved. Another consideration is that the effect of a given mutation might be similar, but has a different outcome in a different protein. A mutation that leads to a change in the conformation of an R protein could cause an autoactivation phenotype, whereas the analogous mutation in a different R protein could lead to inactivation (Figure 5 in Chapter 3). This could be due to a slightly more pronounced outcome of the same structural effect, leading to inactivation rather than autoactivation. Based on the modelling in Chapter 3, it is possible to point out structurally important residues, but it remains difficult to predict whether mutation would lead to loss- or to gain-of-function.

To provide more detailed information on intramolecular interactions and their dynamic changes in response to activation of Mi-1, more extensive pull-down experiments with transcomplementing protein domain combinations should be performed. Ideally, interaction between Mi-1 domains would be studied in the presence and absence of the nematode-derived stimulus that activates Mi-1 in the natural defence response. The first putative Mi-1 activating protein from nematodes was about protein MAP-1 (Semblat et al., 2001). However, co-expression of MAP-1

with Mi-1 did not induce HR, and the proteins do not interact in yeast two-hybrid analysis (S. Elzinga, unpublished data). Very recently it was reported that upon silencing of a sequence called Cg-1, virulence on Mi-1 plants was acquired in normally avirulent nematodes (Gleason et al., 2008), indicating that Cg-1 might be the factor that is recognised by Mi-1. Unfortunately, Cg-1 does not show any similarity to sequences in databases, except for a histone stem loop near the 3' end of the transcript. There are several presumptive ORFs present in this transcript, and so far it is not clear what the gene product is. Another possibility is that the Cg-1 transcript itself is somehow responsible for the avirulence (Gleason et al., 2008). Further analyses of the Cg-1 region could contribute to reveal the basis of Mi-1 mediated nematode recognition.

RSI2 as a new member of the R protein complex

R proteins have been shown to participate in protein complexes with chaperones and chaperone-associated proteins (Chapter 5, and references herein). The LRR domain of the R proteins RPM1, N, I-2 and Rx physically interacts with Heat Shock Protein 90 (HSP90) and silencing HSP90 compromises function of a large number of NB-ARC-LRR proteins (Hubert et al., 2003; Lu et al., 2003; Takahashi et al., 2003; Liu et al., 2004; de la Fuente van Bentem et al., 2005; Gabriëls et al., 2007). HSP90 is a highly conserved molecular chaperone responsible for the stability and activation of a large number of signalling proteins, and is regulated by interaction with several co-chaperones (Pearl and Prodromou, 2006). HSP90-interacting co-chaparones include Protein Phosphatase 5 (PP5) (de la Fuente van Bentem *et al.*, 2005) and SGT1, whose crystal structure was recently identified (Boter *et al.*, 2007). Several studies have demonstrated physical interaction between HSP90, SGT1, and a protein called RAR1 (Hubert et al., 2003; Takahashi et al., 2003; Liu et al., 2004; Azevedo et al., 2006; Boter et al., 2007). Accumulation of the R proteins N and Rx depends on SGT1 and its interaction with HSP90 (Azevedo et al., 2006; Mestre and Baulcombe, 2006; Boter et al., 2007). Generally, the R protein complex members RAR1, SGT1, and HSP90 are required for R protein accumulation and signalling competence (Boter *et al.*, 2007).

In Chapter 5 we have demonstrated physical interaction of the I-2 disease resistance gene product with RSI2, a member of the family of small heat shock proteins (sHSPs). RSI2 is also highly important in maintaining I-2 protein stability, and thereby also in initiation of HR by I-2. These results strongly establish RSI2 as a new type protein involved in R protein function. sHSPs share the three-dimensional structure fold of p23, an important regulator of HSP90 in mammals. In humans, p23 participates in the folding of a plethora of proteins (Bose *et al.*, 1996). At its N-terminus, HSP90 has an ATP binding- and hydrolysis domain. P23 regulates HSP90

activity by direct interaction with the ATP-bound active form of HSP90 (Johnson *et al.*, 1994), inhibiting ATPase activity. This system appears to be important for tight regulation of HSP90 functions. The central CS domain in SGT1 shows structural similarity to p23 (Boter *et al.*, 2007). Despite this structural similarity, their mode of interacting with HSP90 is probably distinct since the CS domain of SGT1 does not share the strand of p23 that has been shown to interact with HSP90 (Boter *et al.*, 2007). Furthermore, SGT1 has been shown not to affect HSP90 ATPase activity, unlike p23 and most other HSP90 co-chaperones.

The observation that loss of RSI2 adversely affects I-2 stability (Chapter 5), could possibly be due to reduced chaperoning activity by the HSP90/SGT1 machinery. The presumed common phylogenetic origin of p23 and HSP20 proteins (Garcia-Ranea *et al.*, 2002), and the experimentally verified chaperoning activities of both proteins points towards a related functional behaviour as a co-chaperone of HSP90 and regulator of its activity. Since HSP90 is present both in plants and in yeast, the interaction we observe between RSI2 and I-2 could be mediated by HSP90. However, the interaction surface of HSP90 in the I-2 LRR maps to LRR1-11 and the interaction with RSI2 is mediated by LRR15-19. Possibly, RSI2 interacts with both its client I-2 and with HSP90, similar to HSP90 co-chaperone and I-2 interacting PP5 (de la Fuente van Bentem et al., 2005). Further experimentation into this specific class of small heat shock proteins could reveal whether they indeed act as ATP-dependent regulators of HSP90 chaperone activity in analogy to P23. Members of this class of proteins could be conserved factors maintaining integrity and signalling competence of the plant NB-ARC-LRR immune receptors.

How do R proteins recognise pathogens?

The molecular mechanism by which R proteins recognise pathogen attack is not conclusively known. The most simple interpretation of the gene-for-gene interaction would be a receptor-ligand interaction between the R and AVR proteins. This idea is supported by the fact that most R-AVR couples co-localize in the plant cell and that R proteins have an LRR domain that functions as an interaction interface in several receptors. Indeed, a number of cases are known in which the AVR protein directly interacts with the R protein. A canonical example is the direct interaction underlying flax rust resistance (Dodds et al., 2006; Ellis et al., 2007). Direct interaction has also been shown between Pita/AvrPita in rice (Jia et al., 2000) and PopP2/RRS-1 in *Arabidopsis* (Deslandes et al., 2003).

In contrast to the examples of direct interaction between R proteins and their cognate AVR proteins described above, direct interaction was not observed in a lot of other cases (Chapter 2). An additional mechanism has been proposed to be responsible for initiation of R protein-mediated responses to the invading pathogen. Most AVR

proteins probably act as effector proteins that target host cell components, and R proteins have been reported to sense the presence of a pathogen by monitoring the state of host targets attacked by AVR proteins. This model is referred to as the guard hypothesis (Van der Biezen and Jones, 1998). Examples in which the AVR protein does not directly interact with the R protein, include the following. (1) Phosphorylation or cleavage of *Arabidopsis* RIN4 protein by AvrB, AvrRpm1, and AvrRpt2 is monitored by, and activates R proteins Rpm1, Rps2, and Tao1 (Mackey et al., 2002; Kim et al., 2005; Eitas et al., 2008); (2) The *Arabidopsis* PBS1 kinase is inactivated by the avrPphB protease, which in turn activates RPS5 (Shao et al., 2003; Ade et al., 2007); (3) The interaction between the *Pseudomonas syringae* AvrPto or AvrPtoB effectors and the tomato kinase Pto is sensed and responded to by NB-ARC-LRR protein Prf (Kim et al., 2002; Mucyn et al., 2006; Xing et al., 2007); (4) Tomato cysteine protease Rcr3 is inhibited by interaction with AVR2 from *Cladosporium fulvum*. Tomato transmembrane R protein Cf-2 is triggered by the Rcr3-AVR2 complex (Rooney et al., 2005); (5) The helicase domain (p50) of Tobacco mosaic virus (Burch-Smith et al., 2007) interacts with the tobacco protein NRIP1. This protein is normally localized to the chloroplasts, but upon interaction with p50 it localizes to the cytoplasm and nucleus (Caplan et al., 2008), where it is recognised by the R protein N; (6) Resistance to *Xanthomonas campestris* in pepper, conferred by the *Bs3* gene, is based on binding of AvrBs3 to the *Bs3* promoter region. The AVR protein probably activates this promoter (Römer et al., 2007).

Originally, the general assumption was that the R protein waits until its guardee is attacked and inactivated by pathogen effectors. In the absence of the corresponding R protein, this inactivation of a host protein would be beneficial to the pathogens virulence. Alternatively, rather than being virulence targets, the proteins that are guarded by R proteins evolved especially to be attacked by pathogen effectors and initiate defence signalling. This would for example explain the fact that Pto is not necessary for the contribution of AvrPto towards virulence, and neither is RIN4 for AvrRpt2 and AvrRpm1 virulence functions. This idea would also solve the problem of opposing evolutionary selection on the guardee; without the cognate R protein, the guardee would evolve to avoid interaction with the effector to decrease virulence, whereas on the other hand the plant would benefit from a strong interaction in the presence of the R protein (R.A.L. van der Hoorn and S. Kamoun, personal communication).

For the R proteins I-2 and Mi-1, used as model proteins for the studies described in this thesis, we do not know much about the mechanism in which they recognise pathogen attack. In the near future, more detailed studies will be possible since very recently, candidate AVR proteins have been identified both for Mi-1 (Gleason et al., 2008) and for I-2 (P.H. Houterman and M. Rep, unpublished data). Identification of

targets for these effectors in plants (whether it is the R protein or a different plant protein) will open doors to investigate the molecular mechanism underpinning I-2 and Mi-1 mediated resistance. The emerging picture is that there is a large diversity in the way that R proteins recognise pathogen attack, since R protein recognition specificities likely evolve at random. In all cases, an important clue is to identify the plant protein(s) targeted by the cognate AVR protein, since this interaction is the frontline of the race-specific battle between the plant and the pathogen.

References

Ade, J., DeYoung, B.J., Golstein, C., and Innes, R.W. (2007). Indirect activation of a plant nucleotide binding site-leucine-rich repeat protein by a bacterial protease. Proc Natl Acad Sci USA **104,** 2531-2536.

Albrecht, M., and Takken, F.L.W. (2006). Update on the domain architectures of NLRs and R proteins. Biochem Biophys Res Commun **339,** 459-462.

Azevedo, C., Betsuyaku, S., Peart, J., Takahashi, A., Noel, L., Sadanandom, A., Casais, C., Parker, J., and Shirasu, K. (2006). Role of SGT1 in resistance protein accumulation in plant immunity. EMBO J **25,** 2007-2016.

Bose, S., Weikl, T., Bugl, H., and Buchner, J. (1996). Chaperone function of Hsp90-associated proteins. Science **274,** 1715-1717.

Boter, M., Amigues, B., Peart, J., Breuer, C., Kadota, Y., Casais, C., Moore, G., Kleanthous, C., Ochsenbein, F., Shirasu, K., and Guerois, R. (2007). Structural and functional analysis of SGT1 reveals that its interaction with HSP90 is required for the accumulation of Rx, an R protein involved in plant immunity. Plant Cell **19,** 3791-3804.

Burch-Smith, T.M., Schiff, M., Caplan, J.L., Tsao, J., Czymmek, K., and Dinesh-Kumar, S.P. (2007). A novel role for the TIR domain in association with pathogen-derived elicitors. PLoS Biol **5,** e68.

Caplan, J.L., Mamillapalli, P., Burch-Smith, T.M., Czymmek, K., and Dinesh-Kumar, S.P. (2008). Chloroplastic protein NRIP1 mediates innate immune receptor recognition of a viral effector. Cell **132,** 449-462.

de la Fuente van Bentem, S., Vossen, J.H., de Vries, K.J., van Wees, S., Tameling, W.I.L., Dekker, H.L., de Koster, C.G., Haring, M.A., Takken, F.L.W., and Cornelissen, B.J.C. (2005). Heat shock protein 90 and its co-chaperone protein phosphatase 5 interact with distinct regions of the tomato I-2 disease resistance protein. Plant J **43,** 284-298.

Deslandes, L., Olivier, J., Peeters, N., Feng, D.X., Khounlotham, M., Boucher, C., Somssich, I., Genin, S., and Marco, Y. (2003). Physical interaction between RRS1-R, a protein conferring resistance to bacterial wilt, and PopP2, a type III effector targeted to the plant nucleus. Proc Natl Acad Sci USA **100,** 8024-8029.

Dodds, P.N., Lawrence, G.J., Catanzariti, A.M., Teh, T., Wang, C.I.A., Ayliffe, M.A., Kobe, B., and Ellis, J.G. (2006). Direct protein interaction underlies gene-for-gene specificity and coevolution of the flax resistance genes and flax rust avirulence genes. Proc Natl Acad Sci USA **103,** 8888-8893.

Eitas, T.K., Nimchuk, Z.L., and Dangl, J.L. (2008). Arabidopsis TAO1 is a TIR-NB-LRR protein that contributes to disease resistance induced by the Pseudomonas syringae effector AvrB. Proc Natl Acad Sci USA **105,** 6475-6480.

Ellis, J.G., Dodds, P.N., and Lawrence, G.J. (2007). Flax rust resistance gene specificity is based on direct resistance-avirulence protein interactions. Annu Rev Phytopathol **45,** 289-306.

Flor, H. (1942). Inheritance of pathogenicity in a cross between physiologic races 22 and 24 of *Melampsora lini*. Phytopathol **32**.

Gabriëls, S.H.E.J., Vossen, J.H., Ekengren, S.K., van Ooijen, G., Abd-El-Haliem, A.M., van den Berg, G.C., Rainey, D.Y., Martin, G.B., Takken, F.L.W., de Wit, P.J.G.M., and Joosten, M.H.A.J. (2007). An NB-LRR protein required for HR signalling mediated by both extra- and intracellular resistance proteins. Plant J **50,** 14-28.

Garcia-Ranea, J.A., Mirey, G., Camonis, J., and Valencia, A. (2002). p23 and HSP20/alpha-crystallin proteins define a conserved sequence domain present in other eukaryotic protein families. FEBS Lett **529,** 162-167.

Gleason, C.A., Liu, Q.L., and Williamson, V.M. (2008). Silencing a candidate nematode effector gene corresponding to the tomato resistance gene MI-1 leads to acquisition of virulence. Mol Plant Microbe Interact **21,** 576-585.

Howles, P., Lawrence, G., Finnegan, J., McFadden, H., Ayliffe, M., Dodds, P., and Ellis, J. (2005). Autoactive alleles of the flax *L6* rust resistance gene induce non-race-specific rust resistance associated with the hypersensitive response. Mol Plant Microbe Interact **18,** 570-582.

Hubert, D.A., Tornero, P., Belkhadir, Y., Krishna, P., Takahashi, A., Shirasu, K., and Dangl, J.L. (2003). Cytosolic HSP90 associates with and modulates the Arabidopsis RPM1 disease resistance protein. EMBO J **22,** 5679-5689.

Hwang, C.F., Bhakta, A.V., Truesdell, G.M., Pudlo, W.M., and Williamson, V.M. (2000). Evidence for a role of the N terminus and leucine-rich repeat region of the *Mi* gene product in regulation of localized cell death. Plant Cell **12,** 1319-1329.

Jia, Y., McAdams, S.A., Bryan, G.T., Hershey, H.P., and Valent, B. (2000). Direct interaction of resistance gene and avirulence gene products confers rice blast resistance. EMBO J **19,** 4004-4014.

Johnson, J.L., Beito, T.G., Krco, C.J., and Toft, D.O. (1994). Characterization of a novel 23-kilodalton protein of unactive progesterone receptor complexes. Mol Cell Biol **14,** 1956-1963.

Kim, H.S., Desveaux, D., Singer, A.U., Patel, P., Sondek, J., and Dangl, J.L. (2005). The *Pseudomonas syringae* effector AvrRpt2 cleaves its C-terminally acylated target, RIN4, from *Arabidopsis* membranes to block RPM1 activation. Proc Natl Acad Sci USA **102,** 6496-6501.

Kim, Y.J., Lin, N.C., and Martin, G.B. (2002). Two distinct *Pseudomonas* effector proteins interact with the Pto kinase and activate plant immunity. Cell **109,** 589-598.

Liu, Y., Burch-Smith, T., Schiff, M., Feng, S., and Dinesh-Kumar, S.P. (2004). Molecular chaperone Hsp90 associates with resistance protein N and its signaling proteins SGT1 and Rar1 to modulate an innate immune response in plants. J Biol Chem **279,** 2101-2108.

Lu, R., Malcuit, I., Moffett, P., Ruiz, M.T., Peart, J., Wu, A.J., Rathjen, J.P., Bendahmane, A., Day, L., and Baulcombe, D.C. (2003). High throughput virus-induced gene silencing implicates heat shock protein 90 in plant disease resistance. EMBO J **22,** 5690-5699.

Mackey, D., Holt, B.F., Wiig, A., and Dangl, J.L. (2002). RIN4 interacts with *Pseudomonas syringae* type III effector molecules and is required for RPM1-mediated resistance in *Arabidopsis*. Cell **108,** 743-754.

Mestre, P., and Baulcombe, D.C. (2006). Elicitor-mediated oligomerization of the tobacco N disease resistance protein. Plant Cell **18,** 491-501.

Meyers, B.C., Dickerman, A.W., Michelmore, R.W., Sivaramakrishnan, S., Sobral, B.W., and Young, N.D. (1999). Plant disease resistance genes encode members of an ancient and diverse protein family within the nucleotide-binding superfamily. Plant J **20,** 317-332.

Mucyn, T.S., Clemente, A., Andriotis, V.M.E., Balmuth, A.L., Oldroyd, G.E.D., Staskawicz, B.J., and Rathjen, J.P. (2006). The tomato NBARC-LRR protein Prf Interacts with Pto kinase in vivo to regulate specific plant immunity. Plant Cell **18,** 2792-806.

Ogura, T., Whiteheart, S.W., and Wilkinson, A.J. (2004). Conserved arginine residues implicated in ATP hydrolysis, nucleotide-sensing, and inter-subunit interactions in AAA and AAA+ ATPases. J Struct Biol **146,** 106-112.

Pan, Q., Liu, Y.S., Budai Hadrian, O., Sela, M., Carmel Goren, L., Zamir, D., and Fluhr, R. (2000). Comparative genetics of nucleotide binding site-leucine rich repeat resistance gene homologues in the genomes of two dicotyledons: tomato and *Arabidopsis*. Genet **155,** 309-322.

Pearl, L.H., and Prodromou, C. (2006). Structure and mechanism of the Hsp90 molecular chaperone machinery. Annu Rev Biochem **75,** 271-294.

Riedl, S.J., Li, W., Chao, Y., Schwarzenbacher, R., and Shi, Y. (2005). Structure of the apoptotic protease-activating factor 1 bound to ADP. Nature **434,** 926-933.

Römer, P., Hahn, S., Jordan, T., Strauss, T., Bonas, U., and Lahaye, T. (2007). Plant pathogen recognition mediated by promoter activation of the pepper Bs3 resistance gene. Science **318,** 645-648.

Rooney, H.C.E., Van't Klooster, J.W., van der Hoorn, R.A.L., Joosten, M.H.A.J., Jones, J.D.G., and De Wit, P.J.G.M. (2005). Cladosporium Avr2 inhibits tomato Rcr3 protease required for *Cf-2*-dependent disease resistance. Science **308,** 1783-1786.

Schmidt, S.A., Williams, S.J., Wang, C.I., Sornaraj, P., James, B., Kobe, B., Dodds, P.N., Ellis, J.G., and Anderson, P.A. (2007). Purification of the M flax-rust resistance protein expressed in Pichia pastoris. Plant J **50,** 1107-1117.

Semblat, J.P., Rosso, M.N., Hussey, R.S., Abad, P., and Castagnone-Sereno, P. (2001). Molecular cloning of a cDNA encoding an amphid-secreted putative avirulence protein from the root-knot nematode Meloidogyne incognita. Mol Plant Microbe Interact **14,** 72-79.

Shao, F., Golstein, C., Ade, J., Stoutemyer, M., Dixon, J.E., and Innes, R.W. (2003). Cleavage of *Arabidopsis* PBS1 by a bacterial type III effector. Science **301,** 1230-1233.

Takahashi, A., Casais, C., Ichimura, K., and Shirasu, K. (2003). HSP90 interacts with RAR1 and SGT1 and is essential for RPS2-mediated disease resistance in *Arabidopsis*. Proc Natl Acad Sci USA **100,** 11777-11782.

Takken, F.L.W., Albrecht, M., and Tameling, W.I.L. (2006). Resistance proteins: molecular switches of plant defence. Curr Opin Plant Biol **9,** 383-390.

Tameling, W.I.L., Elzinga, S.D., Darmin, P.S., Vossen, J.H., Takken, F.L.W., Haring, M.A., and Cornelissen, B.J.C. (2002). The tomato *R* gene products I-2 and Mi-1 are functional ATP binding proteins with ATPase activity. Plant Cell **14,** 2929-2939.

Ting, J.P., Willingham, S.B., and Bergstralh, D.T. (2008). NLRs at the intersection of cell death and immunity. Nat Rev Immunol **8,** 372-379

Van der Biezen, E.A., and Jones, J.D.G. (1998). Plant disease-resistance proteins and the gene-for-gene concept. Trends Biochem Sci **23,** 454-456.

van der Biezen, E.A., and Jones, J.D.G. (1998). The NB-ARC domain: a novel signalling motif shared by plant resistance gene products and regulators of cell death in animals. Curr Biol **8,** R226-228.

van Ooijen, G., van den Burg, H.A., Cornelissen, B.J.C., and Takken, F.L.W. (2007). Structure and function of resistance proteins in solanaceous plants. Annu Rev Phytopathol **45,** 43-72.

van Ooijen, G., Mayr, G., Kasiem, M.M.A., Albrecht, M., Cornelissen, B.J.C., and Takken, F.L.W. (2008). Structure-function analysis of the NB-ARC domain of plant disease resistance proteins. J Exp Bot **59**: 1383-1397

Xing, W., Zou, Y., Liu, Q., Liu, J., Luo, X., Huang, Q., Chen, S., Zhu, L., Bi, R., Hao, Q., Wu, J.W., Zhou, J.M., and Chai, J. (2007). The structural basis for activation of plant immunity by bacterial effector protein AvrPto. Nature **449,** 243-247.

Yan, N., Chai, J., Lee, E.S., Gu, L., Liu, Q., He, J., Wu, J.W., Kokel, D., Li, H., Hao, Q., Xue, D., and Shi, Y. (2005). Structure of the CED-4-CED-9 complex provides insights into programmed cell death in *Caenorhabditis elegans*. Nature **437,** 831-837.

Summary

Race-specific disease resistance in plants is mediated by Resistance (R) proteins that recognise pathogen-derived molecules and subsequently initiate defence responses such as the Hypersensitive Response (HR). The results presented in this thesis pivot on the tomato R proteins I-2 and Mi-1, that mediate resistance against *Fusarium* wilt and root-knot nematodes, respectively.

Most R proteins contain a central nucleotide-binding NB-ARC domain and a C-terminal leucine-rich repeat (LRR) domain (Chapter 2). The NB-ARC domain is a functional ATPase module, and its nucleotide-binding state has been proposed to control the R protein activation state (Takken *et al.*, 2006; Tameling *et al.*, 2006). In this model, the ATP-bound state represents the activated conformation that initiates HR, whereas the ADP-bound state corresponds to the resting state. Three subdomains can be discerned in the NB-ARC domain: NB, ARC1 and ARC2. Each of them carries between three and five conserved sequence motifs (Albrecht and Takken, 2006). One very highly conserved motif at the carboxy-terminus of the ARC2 subdomain is the methionine-histidine-aspartate (MHD) motif (Chapter 3). We have performed an extensive mutational analysis of this MHD motif in the R proteins I-2 and Mi-1. Mutation of the histidine and aspartate residues resulted in several novel autoactivating and loss-of-function mutations. Autoactivation is defined as induction of HR in the absence of the pathogen-derived stimulus. Combination of these MHD mutations with existing autoactivating hydrolysis mutants in the NB subdomain revealed that the autoactivation phenotypes are neither additive, nor synergetic. This result indicates that the MHD motif represents an important element negatively regulating R protein activity.

To reveal the structural basis underlying the function of the MHD motif, a three-dimensional model of the NB-ARC domain of I-2 was built using the structurally related human protein APAF-1 as a template. Based on this model, we propose that in the inactive state, the MHD motif coordinates the bound ADP molecule and thereby controls the physical interactions between the NB and ARC2 subdomains. In this way, the MHD motif fulfils both functions of the sensor II motif, that is found in the related AAA+ protein family, but is absent in R proteins and APAF-1. The 3D model was additionally applied as a framework for the formulation of hypotheses on how previously identified mutations in the NB-ARC exert their effects, and to identify residues that are important for I-2 structure and function.

Next, the effect of specific point mutations in the Mi-1 NB and ARC2 subdomains on intramolecular interactions between the LRR domain and its N-terminus was investigated (Chapter 4). Autoactivating mutations in the NB subdomain trans-complemented and triggered HR upon co-expression of the N-terminus and the LRR domain of Mi-1. These data show that these parts of the R protein can functionally

complement when expressed *in trans*. Likewise, known autoactivating chimaeric LRR domain swaps using an Mi-1 paralogue were found to induce HR upon expression *in trans*. However, point mutations in the MHD motif that induced strong autoactivation in the full-length Mi-1 protein did not lead to HR upon co-expression. All analysed combinations of Mi-1 CC-NB-ARC and LRR domains physically engage in the same protein complex, indicating that total dissociation of the LRR is not required for activation of Mi-1.

According to the general assumption, R proteins function in protein complexes. To discern constituents of such a complex we applied yeast two-hybrid analyses, and identified RSI2 as part of the I-2 protein complex (Chapter 5). This protein is a member of the HSP20/α-crystallin small heat-shock proteins. Small heat shock proteins are evolutionary conserved across kingdoms and are involved in establishing proper protein folding and stability. The yeast two-hybrid interaction was confirmed by pull-down experiments from plant protein lysates. HR signalling by autoactivating variants of I-2 and Mi-1 was strongly compromised upon silencing of RSI2, indicating its functional involvement in R protein-mediated HR signalling. Furthermore, the accumulation of I-2 protein *in planta* was heavily reduced in RSI2-silenced plants, indicating its role in maintaining I-2 protein stability.

Albrecht, M., and Takken, F.L.W. (2006). Update on the domain architectures of NLRs and R proteins. Biochem Biophys Res Commun **339,** 459-462.

Takken, F.L.W., Albrecht, M., and Tameling, W.I.L. (2006). Resistance proteins: molecular switches of plant defence. Curr Opin Plant Biol **9,** 383-390.

Tameling, W.I.L., Vossen, J.H., Albrecht, M., Lengauer, T., Berden, J.A., Haring, M.A., Cornelissen, B.J.C., and Takken, F.L.W. (2006). Mutations in the NB-ARC domain of I-2 that impair ATP hydrolysis cause autoactivation. Plant Physiol **140,** 1233-1245.

Samenvatting

Planten zijn in de natuur constant blootgesteld aan mogelijke ziekteverwekkers. Ze hebben niet de keuze om het een tijdje rustiger aan te doen of op bed fruit te gaan liggen eten. Ze zijn volledig aangewezen op hun fysieke ondoordringbaarheid en op hun afweersysteem. Gelukkig doen ze dit met verve en aanschouwt men in het veld meestal gezonde planten. De vraag *hoe* planten in staat zijn zich ziekteverwekkende organismen van het lijf te houden, is mede vanwege het belang in de land- en tuinbouw één van de grotere onderzoeksvelden binnen de plantenwetenschappen. Het onderzoek dat is beschreven in dit proefschrift, is gericht op één van de manieren waarop een plant zich kan beschermen. Dit mechanisme noemen we fysio-specifieke resistentie, of gen-om-gen resistentie. Dit principe is gebaseerd op de aanwezigheid van een eiwit in het pathogeen, dat word herkend door een eiwit in de plant. Twee van deze plant eiwitten zijn in het hier beschreven onderzoek nader bestudeerd; de eiwitten I-2 and Mi-1 uit tomaat. I-2 biedt resistentie tegen de wortel infecterende schimmel *Fusarium oxysporum*, die groeit in de vaten van de plant en deze daardoor doet verwelken. Mi-1 biedt bescherming tegen wortelknobbelaaltjes; zoals de naam al aangeeft zijn dit aaltjes die zich nestelen in de wortels en daar gezwollen knobbels veroorzaken waaruit ze voedsel opnemen. Een groot aantal R (voor Resistentie) eiwitten is in de plant aanwezig en deze herkennen allemaal een pathogeen gerelateerd eiwit (Hoofdstuk 2). Zodra de plant via deze R eiwitten het gevaar bespeurt dat op de loer ligt, wordt een rigoureuze beslissing genomen. In het deel van de plant waarin infectie is waargenomen, plegen de cellen collectieve zelfmoord. Met het bewonderenswaardige doel voor ogen de rest van de plant te redden, kiest het R eiwit aldus de minder nobele “tactiek van de verschroeide aarde”. Dit zelfmoordmechanisme noemen we de overgevoeligheidsreactie, of Hypersensitieve Respons (HR). Ook zonder dat pathogenen in de buurt zijn, kan HR geactiveerd worden door specifieke mutaties te maken in het R eiwit. Een mutatie kan leiden tot een verkeerde regulatie van het R eiwit, waardoor deze de cel doet sterven zonder dat er acute dreiging is. De conformatie van een eiwit laat zich, simplistisch gezien, vergelijken met een kluwen touw. De resultaten die we hebben verkregen bleken grotendeels te verklaren te zijn door te kijken welk effect bepaalde mutaties uitoefenen op hoe het R eiwit “opgerold” is. Door het effect van mutaties op de activatiestaat te onderzoeken, hebben we aangetoond dat een geconserveerd stukje R eiwit sequentie (methionine-histidine-aspartaat) optreed als sensor voor de stimulus en deze omzet tot activatie van HR (Hoofdstuk 3). Een andere eigenschap van een eiwit (of een stuk touw) is dat sommige delen tegen elkaar aan liggen en aan elkaar gebonden zijn. Zodra zo’n binding verbroken word kan dat leiden tot het aannemen van een hele andere vorm. In hoofdstuk 4 hebben we gekeken naar bindingen tussen twee helften van het R eiwit Mi-1. We ontdekten dat wanneer deze

twee stukken apart van elkaar gesynthetiseerd worden, er genoeg bindingsplaatsen zijn om ze fysiek met elkaar te laten interacteren. In veel gevallen leidde dit tot reconstitutie van een actief R eiwit, dat haar functies (zoals HR stimuleren) nog kon verrichten (Hoofdstuk 4). Hoewel het R eiwit de belangrijkste rol speelt in dit type resistentie, kan het dit klusje niet in zijn eentje klaren. Het eiwit is ingebed in een complex van meerdere eiwitten die tezamen één of enkele functies uitoefenen in de cel. Van een klein aantal eiwitten is bekend dat deze nodig zijn om te zorgen dat het R eiwit stabiel blijft, en de juiste vouwing blijft aannemen. Deze eiwitten noemen we chaperones. In hoofdstuk 5 beschrijven we hoe we een nieuw eiwit hebben gevonden, genaamd RSI2, dat een deel van deze rol voor zich lijkt op te eisen in het toezicht op, en de regulatie van het I-2 eiwit.